AN INVESTIGATION OF CARBONYL INSERTION INTO M-CF_3 BONDS

JAYANTHI JACOB, M.Sc.

AN INVESTIGATION OF CARBONYL INSERTION INTO M-CF_3 BONDS

By

©JAYANTHI JACOB, M.Sc.

A thesis submitted to the School of Graduate Studies
in partial fulfillment of the
requirements for the degree of
Master of Science

Department of Chemistry
Faculty of Science
Memorial University of Newfoundland
July 1990

St. John's Newfoundland Canada

ISBN 0-315-61847-7

Abstract

Carbonyl insertion continues to be of current interest as it plays a vital role in many industrial preparations like hydroformylation, Reppe synthesis, Fischer-Tropsch process, etc. Carbonyl insertion has not been observed in M-CF_3 bonds (M = transition metals) and the first report of apparent carbonyl insertion in a Fe-CF_3 bond stands in open conflict with both experimental and theoretical results. An investigation of the above report is presented in this thesis.

$Fe(CO)_3$(diars) (diars = o-phenylenebis(dimethylarsine)) reacts with excess CF_3I to form the perfluoroacyl $Fe(CO)_2$(diars)($C(O)CF_3$)I and the perfluoroalkyl $Fe(CO)_2$(diars)(CF_3)I compounds in varying yields, depending on the reaction conditions. A high concentration ratio of CF_3I to $Fe(CO)_3$(diars) favours the perfluoroalkyl while a dilute solution favours the perfluoroacyl compound. Concentration vs. time profiles of the reaction monitored by ^{19}F NMR, indicate that the perfluoroalkyl and perfluoroacyl compounds are formed by two independent reaction pathways. The perfluoroalkyl is formed by oxidative addition of CF_3I to $Fe(CO)_3$(diars) by a nonchain, free radical mechanism while the perfluoroacyl is formed by an intermolecular insertion mechanism via an ionic intermediate. The higher analogues of CF_3I form only the perfluoroalkyl owing to the greater stability of the R_f radical which enhances the rate of the free radical reaction.

Two isomers of the perfluoroalkyl compound were isolated and spectroscopically identified by ^1H, ^{13}C, ^{19}F NMR, IR and Mass spectra as cis,cis and cis,trans isomers. Similarly, four isomers of the perfluoroacyl compound were isolated and identified. The structures of one perfluoroacyl and one perfluoromethyl isomer were confirmed by single crystal X-ray data.

Contents

List of Figures

List of Tables

List of Abbreviations

CNDO	complete neglect of differential overlap
Cp	η^5–cyclopentadienyl
diars	o-phenylenebis (dimethylarsine)
Et	ethyl
HFS	Hartree-Fock-Slater
HOMO	highest occupied molecular orbital
MO	molecular orbital
Ph	phenyl
PPh_3	triphenylphosphine
Pr	propyl
PRDDO	partial retention of diatomic differential method
TLC	thin layer chromatography

ACKNOWLEDGEMENTS

I am deeply indebted to my supervisor, Dr. Chet Jablonski, for his invaluable direction and technical advice during the course of this investigation. His continuous guidance and encouragement has helped me immensely.

I would like to extend my sincere gratitude to the Dean of Graduate Studies and to the Head, Department of Chemistry for providing the financial support during the course of this work.

I would like to thank my husband and my dear children, who put up with my swinging moods and extended full support.

O LORD, OUR LORD!
HOW MAJESTIC IS YOUR NAME IN ALL THE EARTH!
WHEN I CONSIDER YOUR HEAVENS,
THE WORK OF YOUR FINGERS,
THE MOON AND THE STARS,
WHICH YOU HAVE SET IN PLACE,
WHAT IS MAN THAT YOU ARE MINDFUL OF HIM,
THE SON OF MAN THAT YOU CARE FOR HIM?
O LORD, OUR LORD,
HOW MAJESTIC IS YOUR NAME IN ALL THE EARTH!

[King David's Psalms in The Bible]

Chapter 1

Introduction

1.1 Insertion Reactions

The term "insertion reaction" is often used in a very broad context without mechanistic significance. It simply reflects the overall structural change wherein an unsaturated ligand Y interposes into a metal-element, M-X bond (cf. Eq.1.1).

$$M - X \; + \; Y \; \rightarrow \; M - Y - X \tag{1.1}$$

The reverse reaction is referred to as elimination or extrusion and unlike oxidative addition, insertion reactions do not alter the coordination or the oxidation number of the metal. Two different types of insertion reactions have been identified in the literature, namely, intramolecular and intermolecular insertion reactions [53].

1.1.1 Intramolecular Insertion Reactions

Intramolecular insertion, also known as "migratory insertion", occurs when both X and Y are coordinated to the same metal center (cf. Eq.1.2).

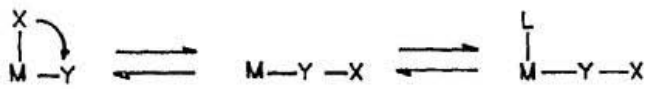

(1.2)

An external ligand L in a subsequent step often occupies the site vacated by X, where L = CO, R_3P, amine, halide or a basic metal center. Depending on the nature of Y, these insertion reactions are further classified into two groups. The first group in which M and X add to the same atom of the unsaturated ligand (Y=CO, isonitriles, carbenes, etc.) is classified as a 1,1 insertion reaction.

(1.3)

The second group in which M and X add to different atoms of the unsaturated ligand (Y=olefins, acetylenes, etc.) is classified as a 1,2 insertion reaction.

(1.4)

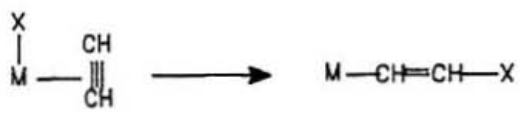

1,4 Insertion reactions, though less frequently observed, have been reported for $(CN)_2C=C(CN)_2$ [125].

Migratory insertion reactions are diverse. The migrating ligand, X, can be H, halogen, alkyl, S, N, P or other metals, and the unsaturated ligand Y can be CS, CO, CHO, SO_2, SO_3, dienes, acetylene, acetylene, carbenes, isonitriles, nitrosyls, carbenes, olefins or organic isocyanides. The metal centers are shown by the shaded portion of Table 1.1 [38, 117, 125].

Li	Be											B	C
Na	Mg											Al	Si
K	Ca	Sc	Ti	V	Cr	Mn	Fe	Co	Ni	Cu	Zn	Ga	Ge
Rb	Sr	Y	Zr	Nb	Mo	Te	Ru	Rh	Pd	Ag	Cd	In	Sn
Cs	Ba	La	Hf	Ta	W	Re	Os	Ir	Pt	Au	Hg	Tl	Pb

Table 1.1: Metal Centers for Migratory Insertion

1.1.2 Intermolecular Insertion Reaction

Intermolecular insertion reactions involve a direct nucleophilic attack on the unsaturated ligand attached to the metal by an external nucleophilic reagent.

(1.5)

These reactions occur typically when X = Grignard reagent, organolithium, hydride, aqueous hydroxide, amines, amino N-oxides, azide ion, etc., and Y is the same as that described for the intramolecular insertion reactions. Several factors favoring nucleophilic addition reactions have been identified, such as the nucleophilicity of X, a net positive charge on the metal complex, and the coordinative saturation of the metal complex [53, 61].

1.2 Carbonyl Insertion Reactions

When the inserting molecule Y = CO for the reaction in Eq. (1.3), the 1,1 insertion is also known as carbonyl insertion reaction. A great deal of work has been focussed on $RMn(CO)_5$ systems and CO insertion is found to be intramolecular with the alkyl group migrating to the cis carbonyl group; it is stereospecific with respect to the migrating alkyl group. The entering ligand, solvent and the Lewis acid added all have a profound effect on the rate of the carbonyl insertion reaction. These features are discussed below.

Carbonylation of **1** with ^{13}CO gives **2** with ^{13}CO cis to the acyl group [137]. ^{13}CO, therefore serves as an external ligand and the inserted CO originates from

the already coordinated CO groups thereby showing that the CO insertion is intramolecular (cf. Eq.1.6)

(1.6)

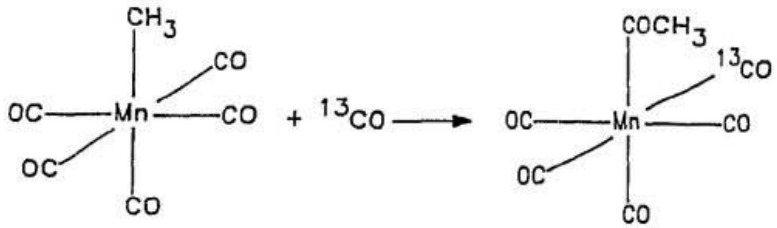

[1] [2]

A more intriguing question concerning the above system is whether the alkyl group migrates to a carbonyl group or the CO group inserts into the Mn-CH_3 bond to form the acyl group. One extensively quoted set of experiments is the decarbonylation of 2 [137]. Product ratio studies by IR indicate alkyl migration in the $Mn(CO)_5(CH_3)$ system and not CO migration. However, studies by Flood et al. [75] demonstrate that even though insertion takes place by alkyl migration in the $Mn(CO)_5(CH_3)$ system, CO migration is also possible for $FeCp(C(O)CH_2CH_3)L$ (L = CO, isocyanides) depending on the solvent and the incoming ligand (cf. Eq.1.7) [74].

(1.7)

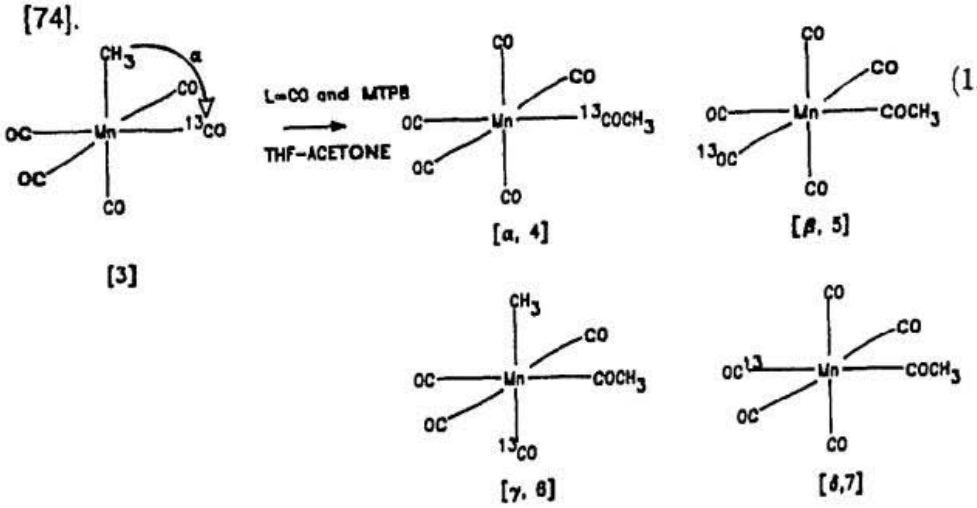

[3] [α, 4] [β, 5]

[γ, 6] [δ,7]

Insertion in **3** was induced by two ligands, CO and $P(OCH_2)_3CCH_3$. The position of the CO label in the reaction products could be α, β, γ or δ as shown in Eq. 1.7. Any of the structural possibilities shown in Table 1.2 is feasible depending on the structure of the intermediate and the type of migration. ^{13}C NMR analysis of the isotopic label in the products was consistent only with methyl migration proceeding through a square pyramid with a basal acyl group.

Structure of the Intermediate	L	
	CO $(\beta + \gamma) / \delta$	$P(OCH_2)_3CCH_3$ $(\beta + \gamma) / \delta$
Alkyl Migration:		
square pyramid	2/1	2/0/1
trigonal bipyramid (axial acyl)	2/1	2/1/1.5
trigonal bipyramid (radial acyl)	5/1	2/0.5/0.5
CO Migration:		
square pyramid	all/0	2/1/0
trigonal bipyramid (axial acyl)	all/0	2/1/0
trigonal bipyramid (radial acyl)	5/1	2/0.5/0.5
stereo-random intermediate	3/1	2/1/1

Table 1.2: Position of ^{13}CO Label in Products of the Reaction in Eq. 1.7 After Flood et al.

In the $FeCp(CO)(PPh_3)Et$ system shown in Eq.1.8, the configuration of the product corresponds to >95% formal alkyl migration in nitroethane as the solvent while in hexamethyl phosphoramide (HMPA), the configuration of the product corresponds to 73% formal CO migration [74].

$$FeCp(CO)(PPh_3)Et \xrightarrow{CO} FeCp(CO)(PPh_3)(C(O)Et) \qquad (1.8)$$

However, the cyclohexylisocyanide induced reaction forms products corresponding to alkyl migration in both nitroethane and HMPA solvents. Pankowski [141] has proposed a similar CO migration instead of alkyl migration.

The requirement of a cis coordination site has been elegantly demonstrated by Herlinger and Brown [91]. $[(CH_3)(CO)Co(DH)_2]_2$ (DH = dimethyl glyoxymate) reacts with

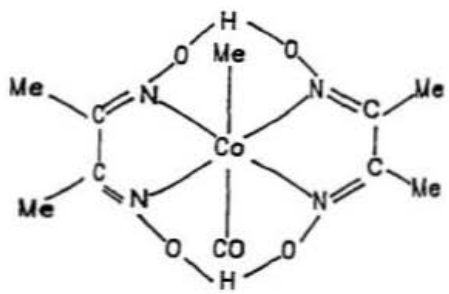

[8]

CO to give compound 8 which on further treatment with CO does not give the acyl complex owing to the unfavourable disposition of the alkyl and the CO groups. Decarbonylation of the labelled acyl compound 9 prepared by treating $NaMn(CO)_5$ with $^{13}CH_3C(O)Cl$ gives the cis alkyl compound 10 exclusively [136]. Using the principle of microscopic reversibility, the R group and the inserting CO must be

mutually cis to each other (cf. Eq.1.9).

(1.9)

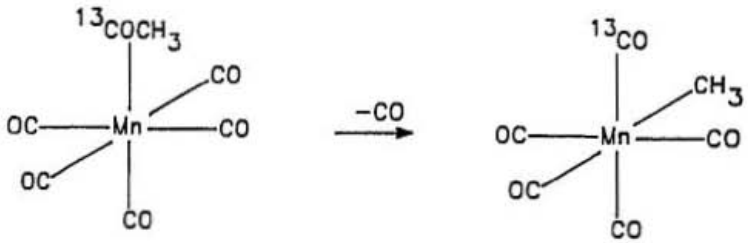

[9] [10]

Insertion is stereospecific at the migrating alkyl group [5, 29, 33, 73, 136, 151]. This is shown in Eq. 1.10 where the optically active Fe compound **11**, undergoes CO insertion with retention of configuration [29].

(1.10)

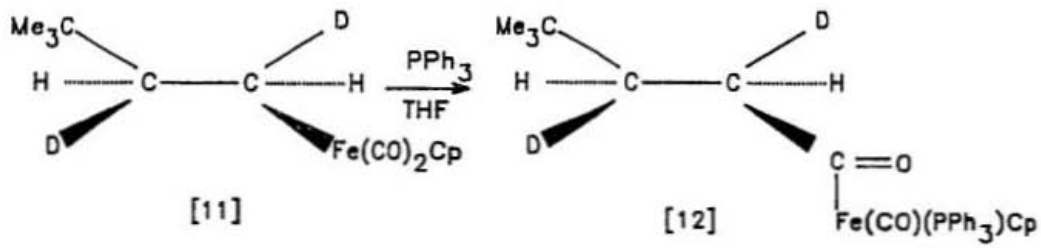

[11] [12]

This result suggests a concerted mechanism involving the transition state **13** [6].

(1.11)

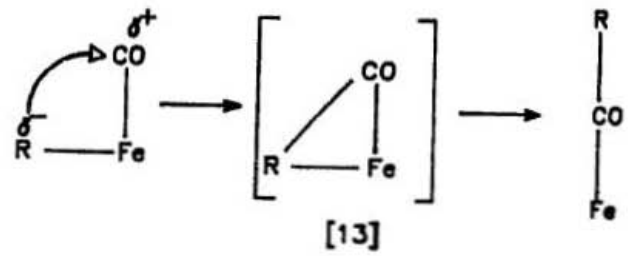

[13]

The migrating R group and the entering ligand L have a profound effect on the rate of CO insertion in 1. The rate decreases with increasing electron withdrawing ability of the R group, and increases with increasing nucleophilicity of the entering ligand. However, this dependence of the rate on the nucleophilicity is not as large as would be expected for a direct nucleophilic attack [47].

As seen in the reactions of $FeCp(CO)(PPh_3)Et$, solvent plays a key role in CO insertion reactions [74]. Coordinating solvents accelerate carbonyl insertion suggesting solvent co-ordination to the metal complex during the course of the reaction [37, 42, 47, 59, 128, 134, 165, 166]. A series of methyl substituted tetrahydrofurans with constant dielectric constant but varying donor ability reveals that the rate of CO insertion in $CpMo(CH_3)(CO)_3$ increases with the donor ability of the solvent [165]. Hence, it is the donor ability of the solvent which affects the rate of the reaction and not the bulk polarity effect. The effect of solvent nucleophilicity appears to be sensitive to the system investigated since the rate of CO insertion of $[Fe(CO)_3(diars)(CH_3)]^+$ is independent of solvent [100]. Other results indicate that the role of nucleophilic solvent is to catalyze the formation of the coordinatively unsaturated acyl intermediate and not necessarily to stabilize it [42, 134]. Lewis acids accelerate CO insertion and the most probable mechanism involves Lewis acid coordination to the oxygen of a CO ligand followed by alkyl migration [93].

1.2.1 Kinetics and Rate Law

Extensive kinetic studies [27, 40, 41, 62, 63, 82, 83, 84, 114, 136] have suggested a mechanism involving the reversible formation of an unsaturated 16 electron

intermediate which reacts with the external ligand L in a subsequent step:

(1.12)

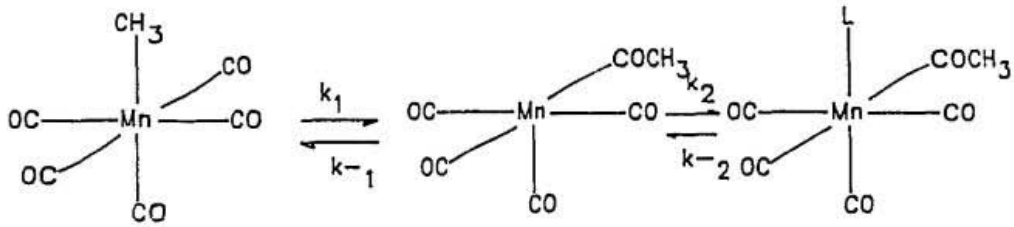

[1] [14] [15]

The nature of the intermediate is still unclear. Matrix isolation and other studies indicate a trigonal bipyramid intermediate with the acyl group in the equatorial plane [44, 98, 129]. However, ^{13}C NMR studies by Flood and Jensen favour a square pyramidal intermediate with the acyl group in the basal plane [45, 46, 71, 81, 137, 167]. There is also some speculation of an η^2- acyl structure [33, 34, 43, 72, 74, 97, 155, 162]. Also the intermediate may be solvent coordinated, since highly coordinating solvents increase the rate of the reaction [21, 43].

Most of the CO insertion studies have been performed under conditions where the second step is irreversible i.e. k_{-2} is insignificant (cf. Eq. 1.12). Applying the steady state approximation to the above mechanism, the rate of reaction becomes

$$\begin{aligned} \text{Rate} &= \frac{k_1 k_2 [L][Mn(CO)_5(CH_3)]}{k_1 + k_2[L]} \\ &= k_{obs}[Mn(CO)_5(CH_3)] \end{aligned} \tag{1.13}$$

where,

$$k_{obs} = \frac{k_1 k_2 [L]}{k_1 + k_2[L]} \tag{1.14}$$

When $k_2[L]$ is very large, k_1 becomes insignificant and the equation reduces to

$$Rate = k_1[Mn(CO)_5(CH_3)] \tag{1.15}$$

However at low [L], the rate equation is dependent on the ligand concentration and thus reduces to

$$Rate = \frac{k_1 k_2[L]}{k_1}[Mn(CO)_5(CH_3)] \tag{1.16}$$

1.2.2 Carbonyl Insertion in Industry

Carbonyl insertion has gained the attention of many researchers due to its extensive application in industrial synthesis as outlined below.

Hydroformylation

The hydroformylation reaction, also known as the Oxo or Roelen reaction, converts olefins to aldehydes or alcohols (cf. Fig.1.1) [68, 149]. Six plants currently use this process which involves insertion of olefins into a metal hydride bond, followed by carbonyl insertion (step 3), hydrogenation (step 4) to form the aldehyde, and further hydrogenation (step 5) to form the alcohol.

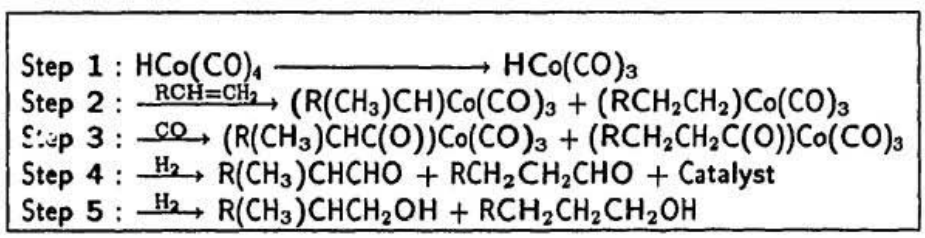

Figure 1.1: Hydroformylation

Reppe Reactions

In the Reppe synthesis, an addend, HX, with a labile hydrogen can be added to an olefinic or acetylenic C-C bond with simultaneous insertion of CO as shown in Fig.1.2 [23, 48, 68, 90]. Insertion of CO into the C-OH bond of alcohols is also possible. Monsanto uses this method to synthesize acetic acid from methanol [76].

Catalyst : $HCo(CO)_4$, $Ni(CO)_4$, $Fe(CO)_5$

X : -OH, -O-alkyl, -O-acyl, $-NR_2$, etc.

$$HC{=}CH + HX \xrightarrow{\text{catalyst/CO}} HCH{=}CH\text{-}C(O)X$$

$$H_2C{=}CH_2 + HX \xrightarrow{\text{catalyst/CO}} HCH_2\text{-}CH_2\text{-}C(O)X$$

$$CH_3X \xrightarrow{\text{catalyst/CO}} H_3C\text{-}C(O)X$$

Figure 1.2: Reppe Reactions

In the Monsanto acetic acid synthesis shown in Fig.1.3, methanol is made from synthesis gas (step 1). This is converted to methyl iodide (step 2) which oxidatively adds to the rhodium catalyst (step 3). A rapid CO insertion occurs (step 3). followed by the release of acetyl iodide which undergoes hydrolysis to form acetic acid (step 4).

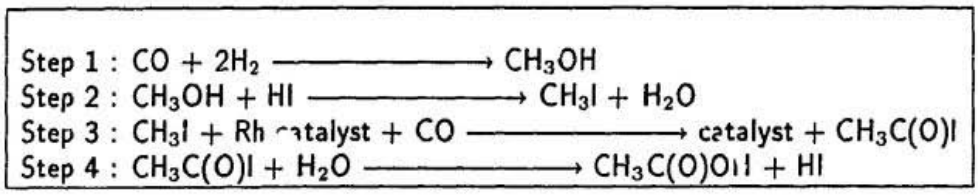

Figure 1.3: Monsanto Acetic Acid Synthesis

Fischer-Tropsch Synthesis

This is a heterogeneously catalyzed reaction where the reductive polymerization of CO in the presence of hydrogen affords a plethora of products like, α olefins, alkanes, alcohols, aldehydes, carboxylic acids, esters and arenes [86]. The product selectivity depends on many factors such as the CO/H_2 ratio, pressure, temperature, catalyst, and the promoters. Thus far, a consensus has not been reached regarding the mechanism of the reaction , however, carbonyl insertion has been proposed to account for the C-C bond formation during the course of the catalytic reaction.

Ethylene Glycol Synthesis

Although there are many possible ways to obtain ethylene glycol, a direct synthesis from synthesis gas is economically attractive. The Union Carbide mechanism is presented in Fig. 1.4 [66].

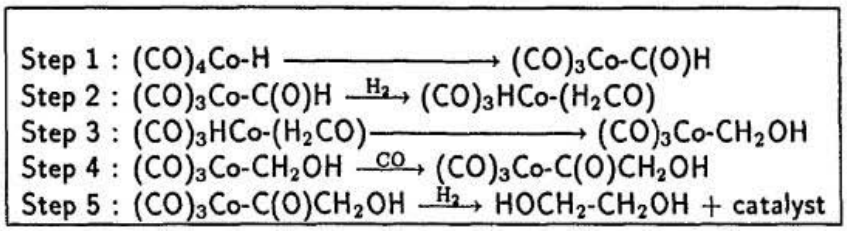

Figure 1.4: Ethylene Glycol Synthesis

The major organometallic species present under the reaction conditions is $HCo(CO)_4$. The reaction proceeds by intramolecular migration of the hydride ion from the metal to a carbonyl ligand (step 1) to form the formyl ligand. Analogous migration of alkyl groups to a CO ligand is observed but the hydride migration is rare under normal conditions apparently because of the thermodynamic instability of most metal formyl complexes. Step 2 is the conversion of the formyl ligand to formaldehyde by hydrogenation. The formaldehyde complex is a highly reactive species and further reactions are similar to those of hydroformylation. Formaldehyde inserts into the metal-hydrogen bond to form the hydroxymethyl ligand (step 3) which undergoes subsequent CO insertion (step 4) and hydrogenation (step 5) in the presence of CO and H_2 respectively to form ethylene glycol. Glycerol is often formed as a side product.

1.2.3 Molecular Orbital Studies of CO Insertion

Five different molecular orbital (MO) theories have been employed to explore the reaction path of carbonyl insertion. They are briefly outlined in the following sections.

Extended Hückel Theory

The carbonyl insertion of $Mn(CO)_5(CH_3)$ was computed along a reaction coordinate involving five arbitrary steps by Hoffman [20], using the extended Hückel method. Full optimization of all degrees of freedom was not carried out and the bond breaking and making are on the border line of what can be reliably treated by this method. The computational results are therefore supported by qualitative arguments.

As the reaction proceeds through the five steps, C_s symmetry of the complex is maintained and the change in bond angles is optimized. The reaction begins with the migration of the methyl group to the cis carbonyl group and the orbitals of the methyl group overlap with that of the carbonyl group. The reaction then proceeds through a transition state (Step 3) to the intermediate complex (Step 5), where the acyl anion is fully formed. Simultaneous formation of an empty donor orbital, mainly d_{z^2} in character, results in a drastic decrease in energy and hence stabilization of the system.

According to these calculations, the five coordinate intermediate is a distorted square pyramid and lacks low energy pathways to other square pyramidal, trigonal bipyramidal or η^2-acyl octahedral isomers. Since the main energy change is due to the metal-alkyl bond, as the electronegativity of the R group increases, the orbital energy level decreases and the R group becomes a poorer σ donor. This then raises the activation energy for the alkyl migration. Alkyl migration therefore becomes difficult as the electronegativity of the alkyl group increases. The greater ease of migration with increasing chainlength is explained as partly due to the electronegativity effect and partly due to the decreasing bond strength of the initial reactant. The results also show that alkyl migration is favoured energetically

compared to carbonyl insertion.

Complete Neglect of Differential Overlap (CNDO) Method

Saddei et al. used CNDO formalism to study CO insertion. The reaction path was followed by computing the changes in charge density and bond order [153]. Since all reaction mechanisms are explained in terms of nucleophilic and electrophilic processes the authors claim that any theoretical method should involve computation of charge densities and bond orders.

The charge on the carbon of methyl group is negative while the carbon of the equatorial CO group is positive. Thus, a polar attack of the CH_3 group on the equatorial CO group is favoured as shown in Fig.1.5. It is therefore alkyl migration and not CO migration which is preferred in the $Mn(CO)_5(CH_3)$ reaction. The charge at the equatorial CO is nearly independant of the alkyl group. The negative charge at the α carbon atom of the substituent decreases in the order: $C_2H_5 > CH_3 > CFH_2 > CF_3$. Hence the polar attack should become increasingly difficult. The calculations predict a trigonal bipyramid intermediate.

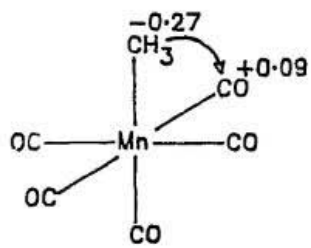

Figure 1.5: Polar attack of CH_3 on CO group

Ruiz et al. [152] also used CNDO method, treating the problem in terms of bond order arguments. The methyl migration coordinate was studied by allow-

ing the methyl group to leave its octrahedral site and approach a cis coordinated group, which finally results in a trigonal bipyramid intermediate. The course of the reaction was divided into six arbitary stages and a sequence of six calculations representing the corresponding structural changes during these six stages are worked out using CNDO methods. Both the concerted and nonconcerted mechanisms were considered and the energy barrier for the concerted mechanism was found to be higher than that for the two step nonconcerted mechanism.

Ab initio Hartree Fock Method

This method was used to investigate carbonyl insertion in $Pt(CH_3)F(CO)PH_3$ and it was concluded that both methyl migration and concerted mechanisms are energetically favoured while CO insertion is not [154].

Hartree-Fock-Slater (HFS) Transition State Method

Ziegler's HFS calculations show that the highest occupied molecular orbital (HOMO) of the reactant $Mn(CO)_5(CH_3)$ is the metal d_{z^2} orbital. Orbital interactions are considered between the σ donor orbital of CH_3 and the orbitals of the $Mn(CO)_5$ system. As the intermediate forms, the σ-CH_3 orbital interacts with the π^* orbital of the cis CO of $Mn(CO)_5$. This brings considerable stabilization in energy and Zeigler therefore proposed that methyl migration is energetically favourable [168].

Various conformations of the intermediate have been suggested and their relative energies calculated. An η^2-intermediate structure is favoured by about 80 $kJmol^{-1}$ compared to the η^1-acyl at equilibrium.

Partial Retention of Diatomic Differential Overlap (PRDDO) Method

Axe and Marynick used the PRDDO method [7] to obtain the geometry of the complexes involved while their energetics were evaluated by the ab initio Hartree Fock theory. This is the first ab initio study of the complete alkyl migration pathway with the first optimized geometry of the transition state. Six important equilibrium structures were computed.

Initially, the lone pair in the Mn-CH_3 orbital is donated to the vacant π anti-bonding orbital of the interacting CO group. As the methyl group migrates the orbital energy rises and the MO evolves into what is predominantly an acyl oxygen π type lone pair orbital. A Mullikan population analysis of the HOMO indicates a gradual depopulation of the Mn-CH_3 orbital, which is accompanied by a build-up of electron density on the carbon acyl and oxygen acyl atoms. A dramatic switch in the orbital character takes place in the neighbourhood of the estimated transition state geometry. Lewis acids accelerate the reaction since they coordinate at the acyl oxyen and lower the energy of the transition state. A vacant site is created in the transition state due to the leaving methyl group. The solvent can bind to the metal at this point. Any kind of stabilisation of the transition state should increase the rate of the reaction. Hence the rate of the reaction increases in polar coordinating solvents.

The kinetic intermediate product resembles a square pyramid with the acyl group in the basal position. In the absence of solvent coordination, the dihapto structure is the lowest energy product.

1.3 Absence of CO Insertion Into M-CF_3 Bonds

The absence of CO insertion into M-CF_3 bonds has been indicated by kinetic studies, thermodynamic data, and molecular orbital studies. In 1962, Calderazzo and Cotton reported that the rate of carbonylation of $RMn(CO)_5$ with CO in 2,2'-diethoxydiethyl ether at 30°C decreases in the order:

$$n-Pr > Et > Ph > CH_3 >> CH_2Ph \ and \ CF_3$$

No kinetic data was reported for CH_2Ph and CF_3 as the reaction is extremely slow [40]. Later in 1964, Calderazzo and Noack reported the following reactivity order:

$$(CH_3)Mn(CO)_5 > (FCH_2)Mn(CO)_5 >> (CF_3)Mn(CO)_5$$

Insertion is found to be much slower for R = CFH_2 than CH_3, while no insertion is observed for R = CF_3 [41]. In 1969, King, Kapoor and Pannell demonstrated a similar trend in the $Cp(CO)_3Fe$-R system [106]. Recently it has been shown that the insertion of CO into a preformed M-R_f bond is not a viable approach [104].

The enthalpy of carbonylation at 288 K for Eq. 1.17

$$RMn(CO)_5 \ + \ CO \ \rightarrow \ Mn(CO)_5COR, \qquad R = C_6H_5, CH_3, CF_3 \quad (1.17)$$

was determined and the following trend was observed:

$$R = C_6H_5(-63 \pm 8 kJmol^{-1}) < R = CH_3(-54 \pm 8 kJmol^{-1}) < R = CF_3(-12 \pm 7 kJmol^{-1})$$

Also, the Gibbs free energy change, $\Delta G°$, remains negative for R = C_6H_5 and CH_3 while it is positive for R = CF_3 [55]. The positive $\Delta G°$ indicates that the reaction is not favourable. Thermodynamic calculations on other systems also indicate a similar conclusion [26, 138].

MO studies support the above kinetic and thermodynamic data. Extended Hückel calculations attribute the lack of insertion reactivity to the strength of the M-CF_3 bond [20] while CNDO caiculations focus on the decreased negative charge on the α–carbon atom of the CF_3 group [153].

Axe and Marynick used PRDDO and ab initio Hartree-Fock calculations to study the effects of a large set of different substituents upon the kinetic and thermodynamic behaviour of the group migration reaction in the $Mn(CO)_5R$ system where R = CH_3, CH_2CH_3, $CH_2CH_2CH_3$, $CH(CH_3)_2$, H, $CH_2C_6H_5$, C_6H_5, CH_2F, CF_2H and CF_3 [8]. This study argues in terms of the Lewis acid-base character of alkyl substitutents. More basic alkyl groups tend to interact more favourably with the CO $2\pi^*$ orbitals while less basic alkyl groups interact to a lesser extent. This leads to a reduced tendency for electron withdrawing alkyls to migrate relative to electron releasing alkyls. This acid-base picture is supported by calculations of the overlap populations, degrees of bonding, group charges, optimized metal-alkyl bond lengths and localized molecular orbitals. Hence electron withdrawing substituents retard the migration while electron donating substitutents favour it.

1.4 Overview of the Research Work

Not many years ago, the first case of apparent CO insertion into the Fe-CF_3 bond was reported [95].

$$Fe(CO)_3(diars) + CF_3I \longrightarrow Fe(CO)_2(diars)(C(O)CF_3)I \qquad (1.18)$$

Even though the reaction was reported to be unaffected by radical scavengers, the presumed CO insertion into a transition metal perfluoroalkyl (M-R_f) bond stands in open conflict with both experimental and theoretical results. The prime objective of this research work was to reinvestigate the report.

$Fe(CO)_3$(diars) was treated with a large excess of CF_3I at -78 °C in CH_2Cl_2 solution. Variable yields of the perfluoroalkyl $Fe(diars)(CO)_2(CF_3)I$, the perfluoroacyl $Fe(CO)_2(diars)(C(O)CF_3)I$, along with the di-iodo compound $Fe(CO)_2(diars)I_2$ were isolated and identified. The product ratios were determined to be a function of the reaction conditions. The perfluoroalkyl was the major product in solutions with high concentrations of CF_3I, while in dilute solutions the perfluoroacyl was the major product. Intermediate concentrations gave both the perfluoroalkyl and the perfluoroacyl products. Concentration vs. time profiles monitored at low temperature by ^{19}F NMR provided evidence suggesting that the apparent CO insertion observed in Eq. 1.18 occurs by intermolecular insertion and not by the intramolecular insertion mechanism. The formation of the perfluoroalkyl compound was found to be a free radical reaction. With higher analogues of CF_3I, i.e. C_2F_5I, n-C_3F_7I, n-$C_6F_{13}I$, n-$C_7F_{15}I$ as well as CF_3CH_2I, only the perfluoroalkyl complex was isolated [96].

Chapter 2

Reaction of CF_3I with $Fe(CO)_3$(diars)

2.1 Introduction

CF_3I is known to react with transition metals to afford the product of simple oxidative addition as shown in Table 2.1. The general mechanism is however not yet established. The oxidative addition may occur via a concerted or free radical mechanism [133]. In keeping with theoretical results which predict that CO insertion into M-R_f bond is unlikely, carbonyl insertion has not been observed in the above reactions. However, reaction of excess of CF_3I gas with $Fe(CO)_3$(diars) at 0 °C has been reported to form a perfluoroacyl product instead of the expected simple oxidative addition product [95]. The research presented here attempts to rationalize this apparent contradiction.

2.2 Experimental

All the experiments were performed in an atmosphere of dinitrogen using standard Schlenk techniques [157]. Nitrogen gas was purified by passing through a series of columns containing heated 'De-ox' catalyst (Alpha), activated (4Å) molecular sieves, and P_4O_{10}. CF_3I gas was used as purchased from Aldrich Chemical Co.

Reagent	Product	% Yield	Reference
$(PhP(CH_3)_2)_2Fe(CO)_3$	$(PhP(CH_3)_2)_2(CO)_2Fe(CF_3)I$	-	[36]
$Fe(CO)_5$	$(CF_3)Fe(CO)_4I$	6	[107]
$(EtC(CH_2O)_3P)_2Ru(CO)_3$	$(EtC(CH_2O)_3P)_2Ru(CO)_2(CF_3)I$	-	[36]
$(Cp)Co(CO)_2$	$(Cp)Co(CO)(CF_3)I$	8	[110]
$(Cp)Rh(CO)_2$	$(Cp)Rh(CO)(CF_3)I$	60	[130]
$(P(CH_3)_2Ph)_2RhCl(CO)$	$(P(CH_3)_2Ph)_2RhCl(CO)(CF_3)I$	73	[51]
$(P(CH_3)_2Ph)_2RhBr(CO)$	$(P(CH_3)_2Ph)_2RhBr(CO)(CF_3)I$	70	[51]
$(Cp)Ir(CO)_2$	$(Cp)Ir(CO)(CF_3)I$	40	[79]
$(\eta^5\text{-}(CH_3)_5C_5)Ir(CO)_2$	$(\eta^5\text{-}(CH_3)_5C_5)Ir(CO)(CF_3)I$	78	[108]
$IrCl(CO)(PPh_3)_2$	$IrCl(CO)(PPh_3)_2(CF_3)I$	57	[28]
$IrCl(CO)(P(CH_3)Ph_2)_2$	$IrCl(CO)(P(CH_3)Ph_2)_2(CF_3)I$	49	[54]

Table 2.1: Reaction of CF_3I with Transition Metals

Methylene chloride was freshly distilled from P_4O_{10} under a nitrogen atmosphere. Toluene was distilled from sodium/benzophenone ketyl under nitrogen.The samples were prepared in degassed solvents. Solution infrared spectra in CH_2Cl_2 were recorded on a Perkin-Elmer model-283 spectrophotometer. NMR spectra were recorded on GE300NB or Bruker WP80 instruments. Mass spectra were recorded on VG7070HS mass spectrometer. Melting points were taken in a Thomas-Hoover apparatus using sealed, nitrogen-filled capillary tubes and are uncorrected. Elemental analyses were performed by the Canadian Microanalytical Service Ltd., Vancouver B.C. All chromatography was done on a Chromatron Model 7924T, using Silica gel adsorbent. Element analysis and spectral data are recorded in Tables 2.6 to 2.10.

2.2.1 Preparation of $Fe(CO)_3$(diars)

$Fe(CO)_3$(diars) was prepared in four steps. CH_3AsI_2 and $(CH_3)_2AsI$ were prepared following the method of Miller et al. [131]. Diars was prepared from $(CH_3)_2AsI$ following the method of Nyholm et al. [139] and $Fe(CO)_3$(diars) was prepared from the above compound using a modification of the literature procedure [95]. A high yield of the product was obtained when the reaction mixture was heated in a Carius tube at 180 °C for seven hours. Decreasing the temperature or time of the reaction resulted in decreased yield. The crude product was washed in hexane two or three times until a pure lemon yellow substance was obtained.

2.2.2 Reaction of $Fe(CO)_3$(diars) with CF_3I

4.5 g (0.01 moles) of $Fe(CO)_3$(diars) was dissolved in 5 mL of distilled, degassed CH_2Cl_2 and treated with excess of CF_3I gas (10 g or 0.05 moles) at -78 °C. The lemon yellow solution instantly turned brown and then deep pur-

ple. After 2-3 hours, an IR spectrum of the solution showed a dominant peak around 1620 cm^{-1} peak indicating the formation of the perfluoroacyl compound as reported earlier. On warming the solution to room temperature the solution turned from purple to brown. The reaction flask was kept in the freezer at –15 °C for two days. Removal of solvent and other volatiles followed by preparative thin layer chromatography (TLC) under nitrogen with toluene as the eluant separated four products. The first band (yellow) was identified spectroscopically as cis,trans-(diars)Fe($C(O)CF_3$)$(CO)_2I$ (**16**), the second band (dark yellow) as cis,cis-(diars)Fe($C(O)CF_3$)$(CO)_2I$ (**17**), the third band (brown) as another cis,cis-(diars)Fe($C(O)CF_3$)$(CO)_2I$ (**18**), and the fourth band (pink) as the di-iodo compound, cis,cis-(diars)Fe$(CO)_2I_2$ (**22**). The first two major products were identical with those reported earlier [95]. Isomerization of the two major acyl products occured when kept in solution in the freezer for two days and the fourth isomer, trans,cis (diars)Fe($C(O)CF_3$)$(CO)_2I$ (**19**), was isolated subsequently. Crystals for X-ray structure analysis were grown by a slow diffusion of hexane into a solution of the product in dichloromethane.

The above experiment was repeated by adding excess CF_3I (120 mL, 20 °C, 1 atm) at –78 °C to a solution of 1 g (0.002 moles) of $Fe(CO)_3$(diars) dissolved in 10 mL of CH_2Cl_2. The solution was stirred for 2 to 3 hours. The 1620 cm^{-1} peak, diagnostic of the perfluoroacyl formation, was not observed in the IR spectrum. Prolonged reaction in the freezer for 24 to 48 hours did not result in the formation of a compund showing the 1620 cm^{-1} peak. Preparative TLC under nitrogen with toluene as the eluant separated two products, which were identified spectroscopically as the perfluoroalkyl compound, cis,cis-Fe$(CO)_2$(diars)$(CF_3)I$ and the di-iodo compound, Fe$(CO)_2$(diars)I_2. A clean separation could not be obtained and there was always a tailing of bands. TLC analysis of the above crude sample after stir-

ring overnight at room temperature showed a new TLC spot, which was isolated and identified as cis,trans-$Fe(CO)_2(diars)(CF_3)I$ (**22**).

To identify the conditions which determined the product distribution, a series of small scale preparations was performed. The reaction was followed by IR spectroscopy and the presence of the perfluoroacyl and the perfluoroalkyl compounds was confirmed by their peaks at about 1600 and 1000 cm^{-1} respectively. The results are presented in Table 2.2.

Concentration of $Fe(CO)_3(diars)$ (mol/L)	Volume of CH_2Cl_2 (mL)	Products Obtained
1.17×10^{-1}	5.00	M-CF_3
2.35×10^{-1}	2.50	M-CF_3
5.87×10^{-1}	1.00	M-CF_3 and M-$C(O)CF_3$
1.17×10^{-2}	0.50	M-CF_3 and M-$C(O)CF_3$
2.35×10^{-2}	0.25	M-CF_3 and M-$C(O)CF_3$
5.87×10^{-2}	0.10	only M-$C(O)CF_3$
-	No solvent	M-CF_3 and M-$C(O)CF_3$

M-CF_3 = $Fe(CO)_2(diars)(CF_3)I$; M-$C(O)CF_3$ = $Fe(CO)_2(diars)(C(O)CF_3)I$
$Fe(CO)_3(diars)$ = 250mg (5.87×10^{-4} moles)
CF_3I = 20 mL at 20°C/1 atm. (8.93×10^{-4} moles)

Table 2.2: Reaction of $Fe(CO)_3(diars)$ and CF_3I with Change in Volume of the Solvent

2.3 Results and Discussion

Four geometrical isomers are possible for an octahedral compound of the type Ma_2b_2cd. All have been isolated and characte.ized for the perfluoroacyl compound while only two isomers were characterized for the perfluoroalkyl compound. These are shown in Fig. 2.1.

Perfluoroacyl Isomers

Isomer **16** has a vertical plane of symmetry and hence ^{1}H NMR shows two As-CH_3 resonances (Table 2.7). Carbon-13 NMR shows six resonances attributable to two As-CH_3, three As-C_6H_4, and one CO. The two carbon atoms in $C(O)CF_3$ are coupled to fluorine and hence two quartets are observed. The quartet at 256ppm ($^2J = 29.5$Hz) is assigned to $\underline{C}(O)CF_3$ and the quartet at 113ppm ($^1J = 303$Hz) to $C(O)\underline{C}F_3$. The ^{19}F spectrum shows a singlet due to the CF_3 group. The IR spectrum shows two strong CO peaks due to mutually cis CO groups and another CO peak due to the perfluoroacyl group. Strong C-F stretches are seen at 1230, 1180, 1125 cm^{-1} (see Fig. 2.2).

Isomers **17** and **18** lack symmetry planes and show spectral features as explained below. The ^{1}H NMR spectrum shows four As-CH_3 lines. The ^{13}C NMR spectrum of **17**, shown in Fig. 2.3, shows four As-CH_3, five As-C_6H_4 (one of which is degenerate), two CO resonances and two quartets due to the two carbon atoms of the $C(O)CF_3$ group which are coupled with fluorine. One of the two terminal CO resonances shows further unresolved couplings which may be due to a four bond coupling with the ^{19}F nuclei of the acyl group ($^4J_{CF} = 4$ Hz). The ^{19}F NMR spectrum shows a singlet due to the CF_3 group. The IR spectrum shows two terminal carbonyl peaks and one CO peak due to $C(O)CF_3$ along with strong C-F

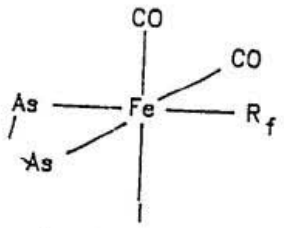

cis,cis $Fe(CO)_2(diars)R_fI$
R_f=CF_3[21],$COCF_3$[17]
R_f=I=$Fe(CO)_2(diars)I_2$[22]

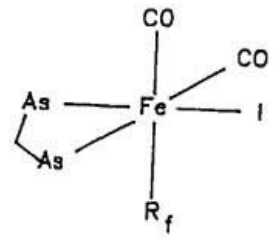

cis,cis $Fe(CO)_2(diars)R_fI$
R_f=$COCF_3$[18]

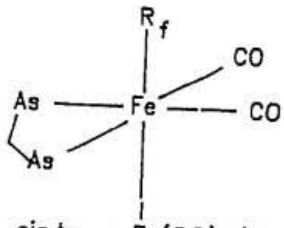

cis,trans $Fe(CO)_2(diars)R_fI$
R_f=CF_3[20],$COCF_3$[16]

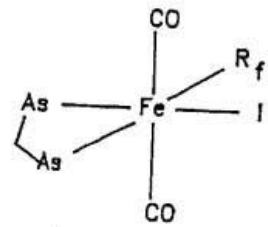

trans,cis $Fe(CO)_2(diars)R_fI$
R_f=$COCF_3$[19]

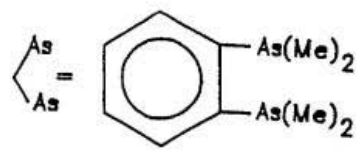

Figure 2.1: Perfluoroalkyl and Perfluoroacyl Isomers

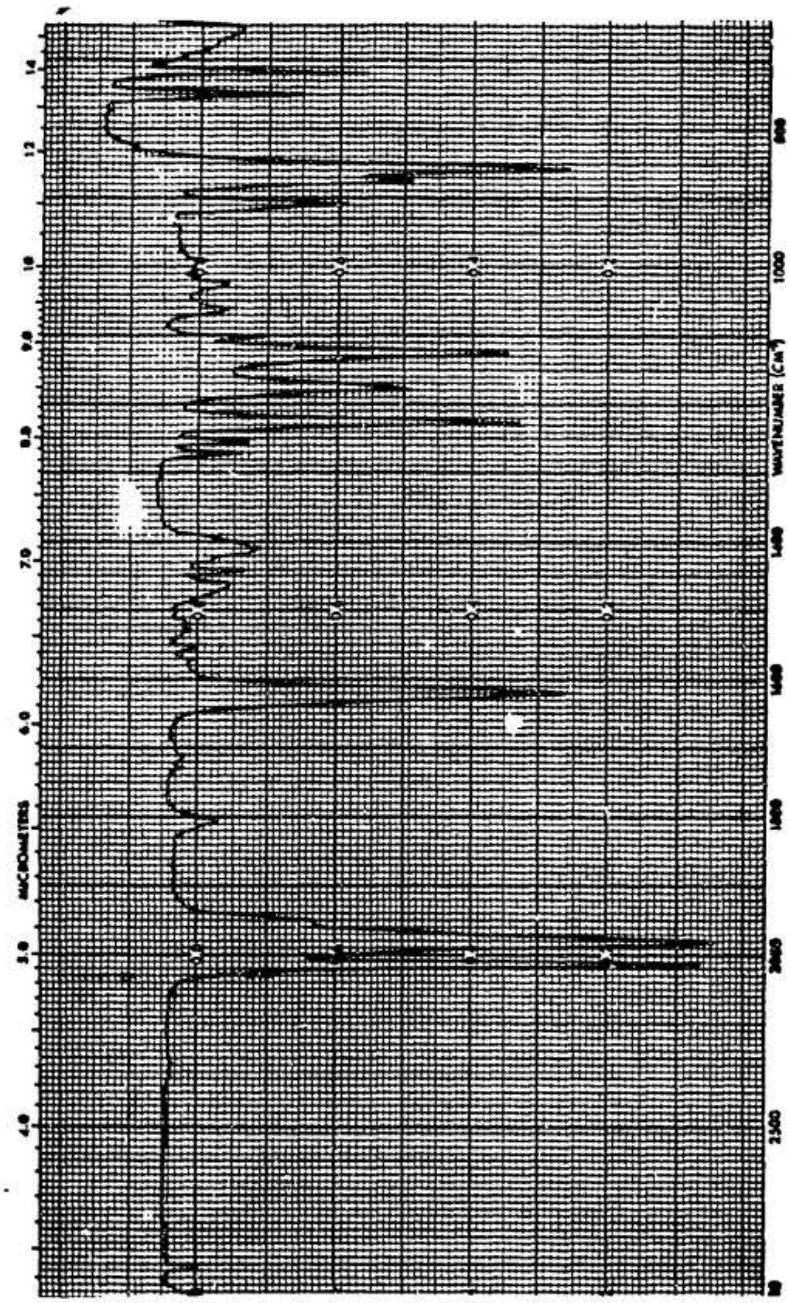

Figure 2.2: IR Spectrum of **16** in CH_2Cl_2

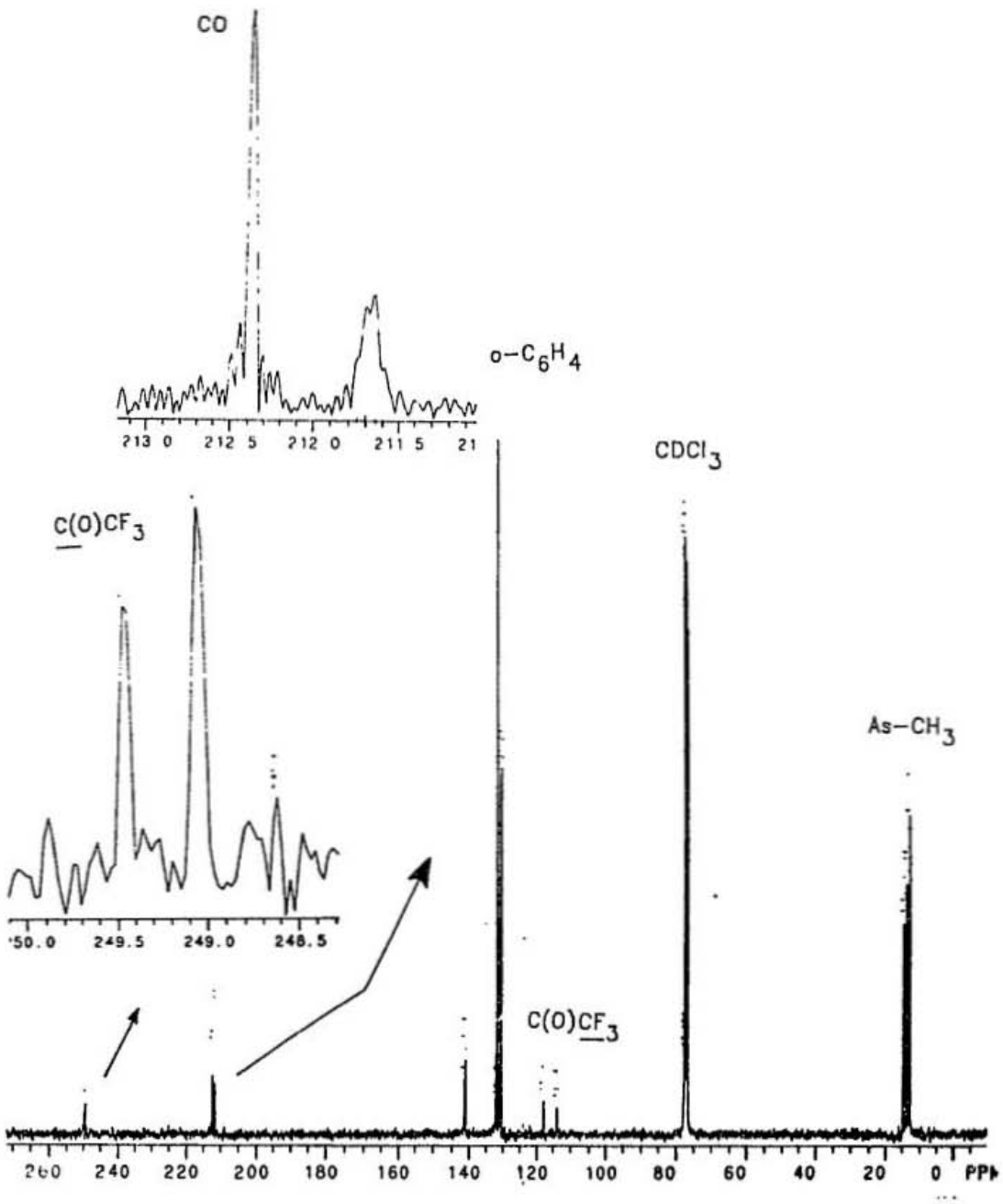

Figure 2.3: ^{13}C NMR of **17** in $CDCl_3$

stretches. Isomers **17** and **18** show similar spectral features. X-ray crystallography was used to distinguish the isomers and to confirm the structure of **17**. Isomer **19** has a horizontal plane of symmetry and and its ^{1}H NMR spectrum shows only two As-CH_3 lines. The IR spectrum shows one strong and one weak absorption consistent with mutually trans CO groups, and another CO peak due to $C(O)CF_3$.

The mass spectral fragmentation pattern of compounds **16** and **17** is given in Table 2.9. In general, the mass spectra of fluorocarbon derivatives of transition metals display sequential loss of carbonyls present followed by elimination of neutral metal fluorides, HF, CF_2, CF, CF_3, and F atoms [121]. Compounds **16** and **17** show extrusion of $CF_3^{\cdot}$ followed by sequential loss of the three carbonyls (cf. Fig. 2.4). The peak height of $M^{+\cdot}$-CF_3 for **16** is 39.08% of the base height while that of $M^{+\cdot}$-CO is only 0.88% of the base height. However, the peak at 488 which is due to the rearrangement of a fluorine atom from the CF_3 ligand to the metal ion is abundant (39.05% base height). This suggests that sequential loss of carbonyls which must be in competition with the process leading to elimination of the $CF_3^{\cdot}$ fragment has also occured.

Perfluoroalkyl Isomers

Isomer **21**, like **17** and **18** lacks a symmetry plane and shows the same spectral pattern as the acyl isomers. Isomer **20** has symmetry elements similar to the perfluoroacyl isomer **16** and shows a similar spectral pattern (cf. Tables 2.6 to 2.9). However, the fragmentation pattern in the mass spectrum is different. Sequential loss of carbonyls is not seen and instead two CO groups are lost simultaneously followed by the rearrangement of a fluorine atom from the CF_3 ligand to the metal ion. Hence the CF_2 group is eliminated giving the 488 peak which then loses a fluorine atom giving the 469 peak (cf. Fig. 2.5). Such a rearrangement has been

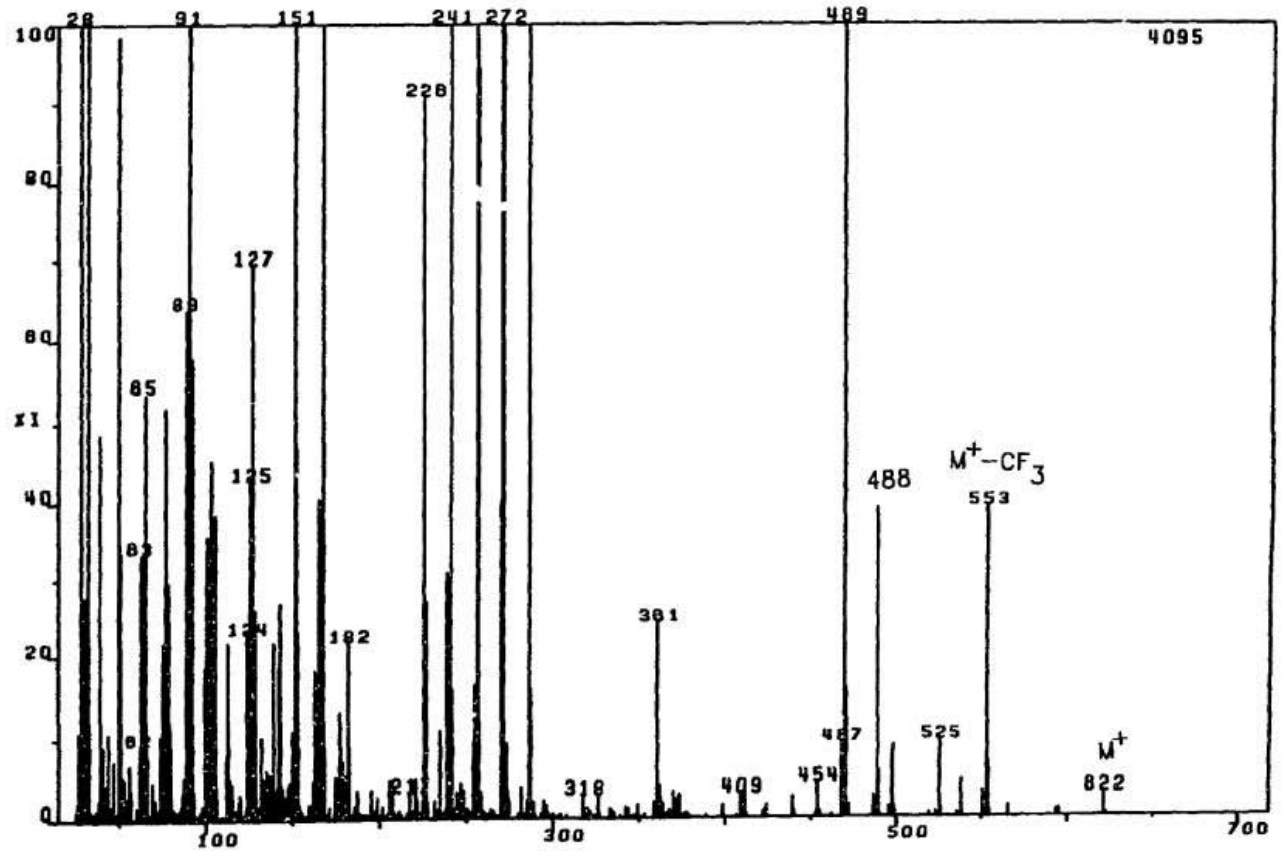

Figure 2.4: Mass Spectrum of **16**

reported in a wide range of fluorocarbons [121].

$Fe(CO)_2(diars)I_2$

The di-iodo compound [135] **22** is formed along with the perfluoroalkyl and the perfluoroacyl compounds. Its NMR and IR spectra show a spectral pattern similar to those of the perfluoroacyl isomers **17** and **18** and hence cis,cis geometry was assigned (see Tables 2.6 to 2.9).

The small scale experiments done to identify the conditions which favour the acyl and the alkyl products indicated that when the quantities of the reactants $Fe(CO)_3(diars)$ and CF_3I are constant, a highly concentrated solution favours the perfluoroacyl as the major product while a dilute solution favours the perfluoroalkyl as the major product. Intermediate concentrations resulted in the formation of both the acyl and alkyl products. Reaction in the solid state also afforded both the alkyl and the acyl products.

2.4 Solid State Structure

Crystal structures were obtained for several products in order to confirm their structures and geometries. ORTEP drawings of cis,cis-$Fe(CO)_2(diars)(C(O)CF_3)I$ **17** and cis,cis-$Fe(CO)_2(diars)(CF_3)I$ **21** are shown in Figs. 2.6 and 2.7 respectively. A summary of crystal data for **17** and **21** is given in Table 2.3. Selected bond lengths and bond angles are listed in Table 2.4.[1] Intensity data was collected on a Nonius diffractometer at 295 K using the $\theta/2\theta$ scan technique with profile analysis at a scan speed of 4°/min. Three standards were measured after every 100 reflections and no significant crystal decay was detected. Space groups were

[1] The final atomic positional parameters and the equivalent isotropic temperature factors are listed in Appendix C.

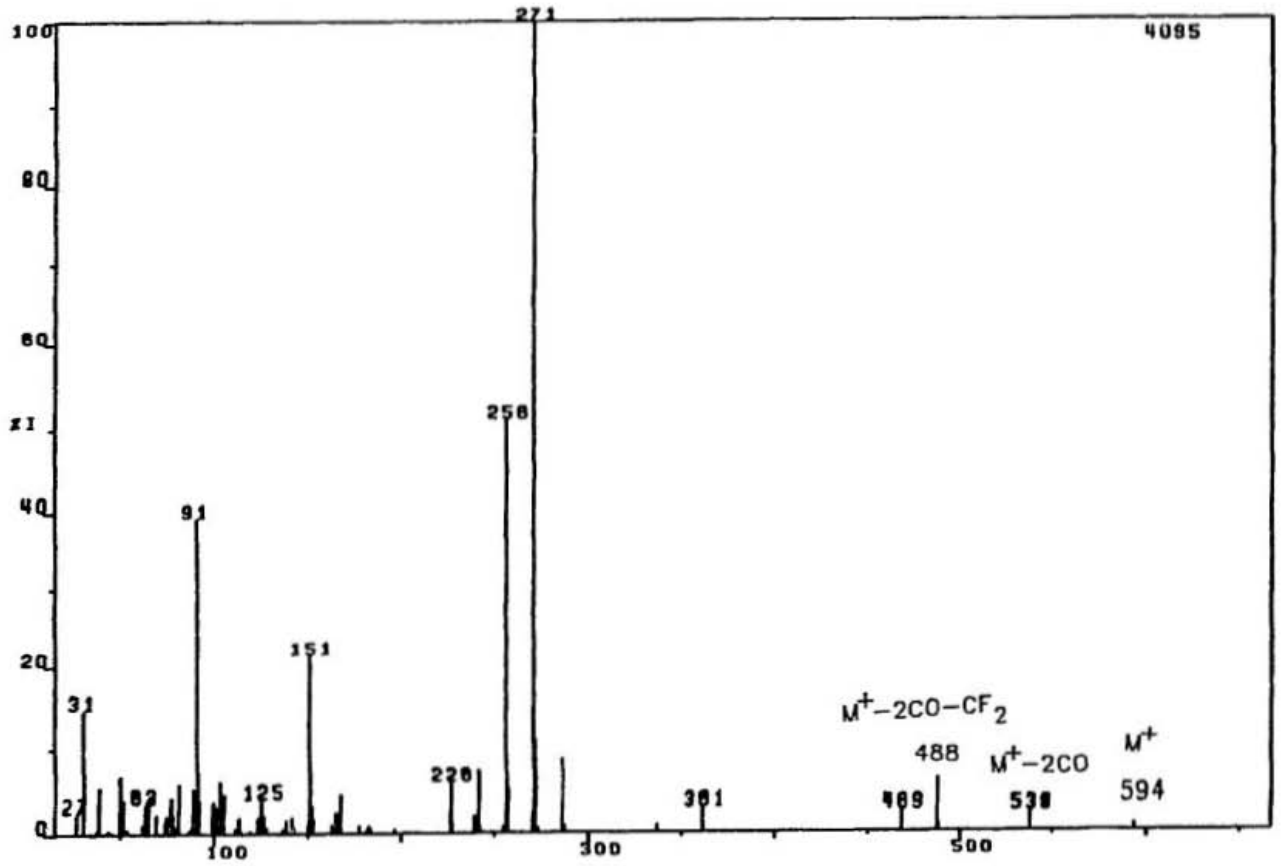

Figure 2.5: Mass Spectrum of **21**

determined by systematic absences. Unit cell parameters for **17** were obtained by least squares refinement of the setting angles for 22 reflections ($40^\circ \leq 2\theta \leq 44.8^\circ$) and for **21**, 30 reflections ($40^\circ \leq 2\theta \leq 45^\circ$). Corrections were made for absorption.

The structures were solved using direct methods (MULTAN) plus a difference Fourier map and refined by full matrix least-squares with counting statistics weights. H-atom positions were calculated but their parameters were not refined. The C-H default distance was set at 1.08 Å. All heavier atoms were refined anisotropically for **17**, and for **21**, only I, As, and F were done. The C2 and C9 carbon atoms of **21** are therefore seen as distorted ellipsoids. The refinement of **21** is not satisfactory as suggested by the difference between R and R_w, unusual C-F distances, and the residual electron density. The structure is being resolved using a disordered model for the CF_3 group[1] All calculations were performed with the NRCVAX Crystal Structure programs [78]. Scattering factors were taken from the International tables for X-ray crystallography [94].

The structures of both **17** and **21** describe a slightly distorted octahedron with a cis,cis geometry thereby confirming the assignment made by spectroscopy. In both these compounds, anomalously large thermal factors were found around Fe-C(2)-O(2) (**17**) and Fe-CF_3 (**21**) and reliable bond distances/angles could not be made for these groups. In **17**, the Fe-C(O) bond is 2.05 Å, which is in agreement with the reported value of 2.00 Å [104]. The average C-F bond distance is 1.375 Å and agrees well with the literature value shown in Table 2.5. The Fe-C(1)O bond length is 1.73 Å as expected.

[1] E.Gabe, NRC Chemistry Division, Ottawa, Ontario.

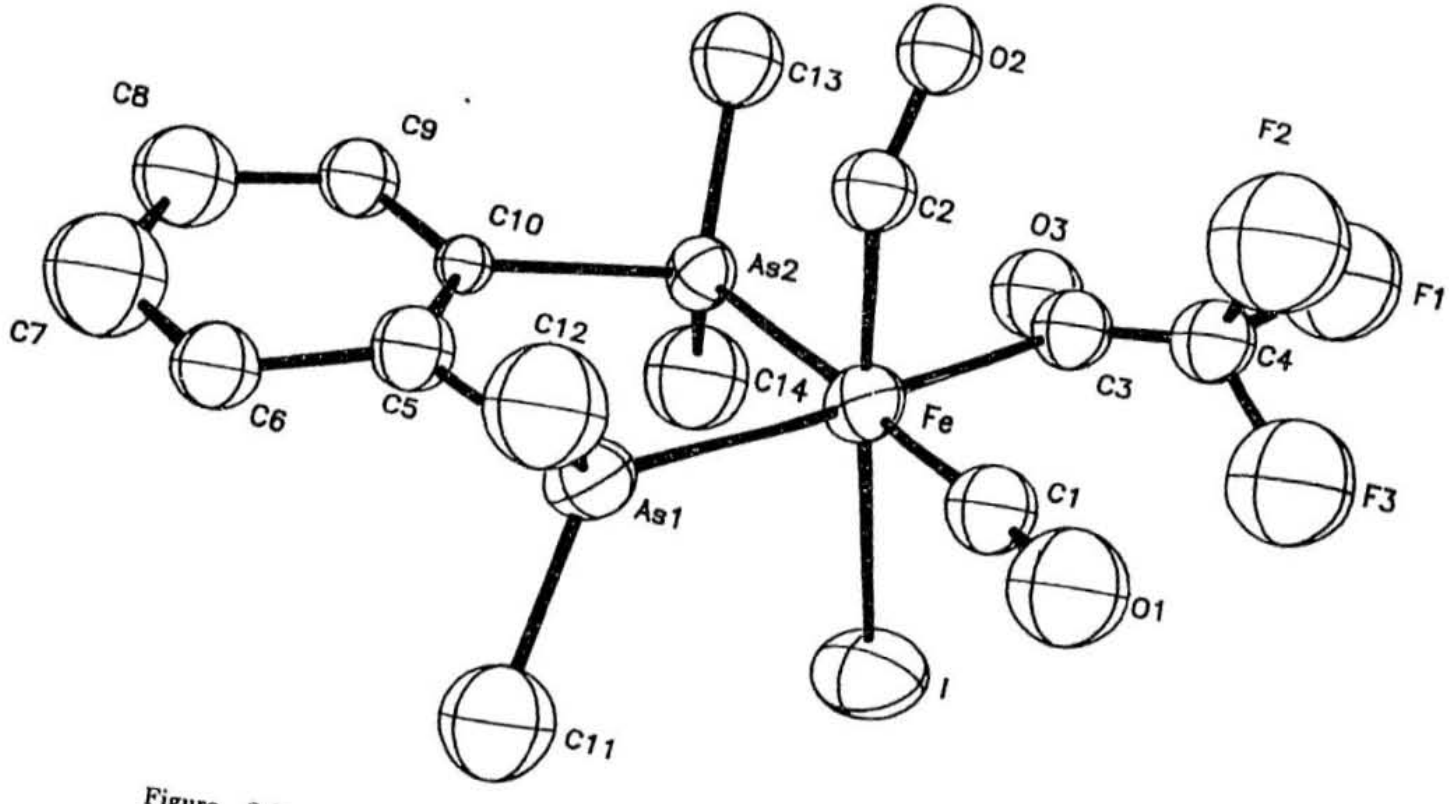

Figure 2.6: ORTEP Drawing of the Crystal Structure of cis,cis-$Fe(CO)_2(diars)(C(O)CF_3)I$ **(17)**

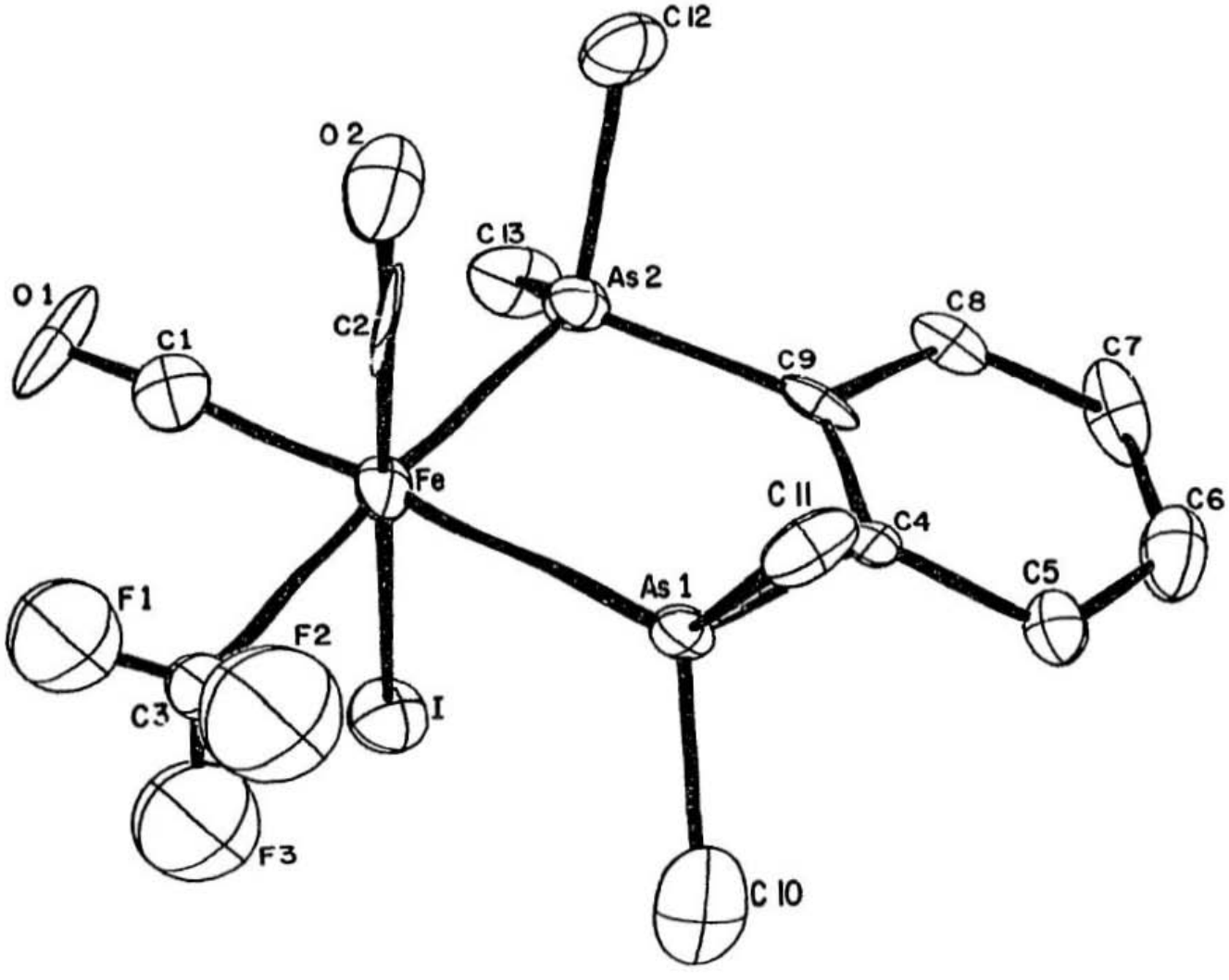

Figure 2.7: ORTEP Drawing of the Crystal Structure of cis,cis-$Fe(CO)_2(diars)(CF_3)I$ (21)

Crystal data	$Fe(CO)_2(diars)(CF_3)I$ **21**	$Fe(CO)_2(diars)(C(O)CF_3)I$ **17**
Empirical formula	$C_{13}H_{16}As_2F_3FeIO_2$	$C_{14}H_{16}As_2F_3FeIO_3$
Molecular weight	577.73	621.86
Crystal dimension(mm)	0.10 x 0.10 x 0.30	0.20 x 0.40 x 0.40
Crystal system	Orthorhombic	Monoclinic
Space group	Pcab	$P2_1$
a(Å)	13.9062(8)	9.183(4)
b(Å)	16.0694(6)	8.987(4)
c(Å)	17.1146(8)	12.175(4)
V(Å^3)	3824.50	986.55
β	-	100.930(20)
Z(molecules/cell)	8	2
F (000) electrons	2255.53	579.88
D_{calcd}(Mg/r.i^3)	2.007	2.093
μ (mm^{-1})	5.84	5.67
λ (A°)	0.70930	0.70930
2θ(max)(deg)	44.8	44.8
No. reflections measured	4066	1379
No. unique reflections	2458	1378
No. unique refl. $I_{net} > n\sigma(I_{net})$	1725(n=2.5)	1185(n=2.5)
Last least sq.cycle calcd. with	38 atoms	40 atoms
	195 parameters	141 parameters
	1725 refls.	1185 refls.
R_f (sig. refl.)	0.072	0.071
R_w (sig. refl.)	0.049	0.081
Goodness of fit	5.115	2.031
R_f (all refl.)	0.106	0.084
R_w (all refl.)	0.049	0.091
Max. shift/σ	0.171	0.191
Last D-map:		
deepest hole, e/Å^3	-1.670	-1.210
highest peak, e/Å^3	2.920	1.770
Transmission factors	0.408956	0.318862
	to	to
	0.554139	0.492092

Table 2.3: Crystallographic Data for Compounds **17** and **21**

Bond	$Fe(CO)_2(diars)(CF_3)I$ (21)	$Fe(CO)_2(diars)(C(O)CF_3)I$ (17)
	bond lengths in Å	
Fe-I	2.654(3)	2.637(5)
Fe-As(1)	2.357(3)	2.354(5)
Fe-As(2)	2.350(3)	2.367(7)
Fe-C(1)	1.842(24)	1.730(4)
Fe-C(2)	1.670(3)	2.080(5)
Fe-C(3)	2.210	2.050(3)
C(1)-O(1)	1.070(3)	1.120(5)
C(2)-O(2)	1.180(4)	0.620(5)
C(3)-O(3)	-	1.210(4)
C(3/4)-F(1)	0.940(3)	1.400(5)
C(3/4)-F(2)	0.990(3)	1.350(4)
C(3/4)-F(3)	1.080(3)	1.400(4)
	Bond angles in degrees	
As(1)-Fe-As(2)	84.78(11)	85.96(20)
As(1)-Fe-I	87.71(12)	92.94(19)
I-Fe-C(3)	-	87.00(9)
C(3)-Fe-C(1)	-	94.00(14)
C(2)-Fe-As(2)	91.00(9)	88.60(12)
I-Fe-C(2)	178.1(9)	178.50(12)
As(1)-Fe-C(1)	173.4(7)	176.80(10)
C(3)-Fe-As(2)	-	174.8(9)

Table 2.4: Selected Bond Lengths and Bond Angles of **17** and **21**

Table 2.5: M-C and C-F Bond Distances from the Literature

Compound	Bond	d_{C-F} in Å	Bond	d_{M-C_t} in Å
π-$C_5H_5Rh(CO)(C_2F_5)I$	C-F	1.310	$Rh-CF_2$	2.080
$(CF_3)Mn(CO)_5$	C-F	1.370	$Mn-CF_3$	2.056
cis-$(HF_2C\ CF_2)_2Fe(CO)_4$	C-F	1.379	$Fe-CF_2$	2.068

M = transition metal

The trans influence of substituted acetyl groups has been studied and is shown to decrease in the series [28]:

$$C(O)CH_3 > C(O)CH_2F > C(O)CHF_2 > C(O)CF_3$$

Accordingly, the Fe-As(1) and Fe-As(2) do not show any difference in their bond lengths. The axial Fe-C(2) bond in **21** is shorter than the equatorial Fe-C(1) bond. A similar observation has been recently reported for four fluoro-organometallic compounds [104]. The Fe-C(3) bond length could not be correctly assigned owing to large thermal factors around it. The Fe-C (perfluoroalkyl) bond lengths reported in literature are given in Table 2.5. From the ^{13}C NMR analysis, it appears that Fe-C (perfluoroalkyl) bond is longer than the Fe-C(O) (perfluoroacyl) bond. The ^{13}C-^{19}F coupling constant in **17** is 302 Hz, while that in **21** is 360 Hz. Hence, the C-F bond is stronger in **21** thereby indicating that the Fe-C (perfluoroalkyl) bond is weaker than the Fe-C(O) (perfluroacyl). The trans influence of the CF_3 group is shown to decrease in the series [28]:

$$CH_3 > CHF_2 \simeq CH_2F > CF_3$$

The Fe-As(1) and Fe-As(2) bond lengths are of similar magnitude to those of **17**.

2.5 Conclusion

Depending on the reaction conditions, $Fe(CO)_3$(diars) reacts with CF_3I to form the perfluoroacyl and/or the perfluoroalkyl compounds. Four isomers of the former and two isomers of the latter were obtained and characterized using spectroscopic and single crystal X-ray data. The parameters controlling the product distribution were investigated and the results are presented in Chapter 4.

Compound	M.P.	Elemental Analysis				IR[a] in cm^{-1}		
		% Carbon		% Hydrogen				
		Calculated	Found	Calculated	Found	ν_{CO}	ν_{COCF_3}	ν_{CF_3}
cis,trans-$Fe(CO)_2$(diars)$(C(O)CF_3)I$ **(16)**	182.0	27.04	27.13	2.59	2.24	1975 2010	1620	1230,1180,1125
cis,cis-$Fe(CO)_2$(diars)$(C(O)CF_3)I$ **(17)**	157.5	27.04	27.45	2.59	2.55	1960 2010	1630	1230, 1180, 1125
cis,cis-$Fe(CO)_2$(diars)$(C(O)CF_3)I$ **(18)**	-	-	-	-	-	1970 2010	1605	1220,1180,1115
trans,cis-$Fe(CO)_2$(diars)$(C(O)CF_3)I$**(19)**	-	-	-	-	-	1975 2010	1600	1220,1180, 1120
cis,trans-$Fe(CO)_2$(diars)$(CF_3)I$ **(20)**	171.5	26.29	26.45	2.72	2.79	1980 2010	-	1080, 990
cis,cis-$Fe(CO)_2$(diars)$(CF_3)I$ **(21)**	170	26.29	25.91	2.72	2.73	1970 2010	-	1050,990
cis,cis-$Fe(CO)_2$(diars)I_2 **(22)**						1960 2010	- -	- -

a = in CH_2Cl_2; Elemental analysis and M.P. of 18 and 19 were not obtained since these were only minor products.

Table 2.6: IR and Element Analysis

Compound	As-CH_3	o-C_6H_4
cis,trans-$Fe(CO)_2$(diars)$(C(O)CF_3)I$ **(16)**	1.62, 2.07	7.70 (m)
cis,cis-$Fe(CO)_2$(diars)$(C(O)CF_3)I$ **(17)**	2.23, 2.02, 1.77,1.65	7.68 (m)
cis,cis-$Fe(CO)_2$(diars)$(C(O)CF_3)I$ **(18)**	1.66, 1.74, 1.90, 2.06	7.58 (m)
trans,cis-$Fe(CO)_2$(diars)$(C(O)CF_3)I$ **(19)**	1.89, 1.69	7.67 (m)
cis,cis-$Fe(CO)_2$(diars)$(CF_3)I$ **(21)**	2.21, 2.09, 1.76, 1.62	7.71 (m)
cis,trans-$Fe(CO)_2$(diars)$(CF_3)I$ **(20)**	2.14,1.77	7.70 (m)
cis,cis-$Fe(CO)_2$(diars)I_2 **(22)**	2.47, 2.10, 1.95, 1.62	7.78 (m)

Solvent : $CDCl_3$; Reference Compound: Me_4Si
Shift values in ppm

Table 2.7: ^1H NMR DATA

Compound	Fe-CO*	$\boxed{CO}$-CF_3	CO-$\boxed{CF_3}$	Fe-CF_3	As-Me	As-Ph
cis,trans-$Fe(CO)_2$(diars)(C(O)CF_3)I **(16)**	212.3 211.9	256 (q) ($^2J_{CF}$ = 29.5 Hz)	113.5 (q) ($^1J_{CF}$ = 303.0 Hz)	-	12.7 15.7	139.08 131.63, 130.05
cis,cis-$Fe(CO)_2$(diars)(C(O)CF_3)I **(17)**	212.3 211.6 (q) ^4J=4 Hz	249.3 (q) ($^2J_{CF}$ = 32.2 Hz)	115.7 (q) ($^1J_{CF}$ = 302.2 Hz)	-	14.6 13.8 13.1 12.8	130.2 130.6 131.5 140.8, 141.1
cis,trans-$Fe(CO)_2$(diars)(CF_3)I **(20)**	212.2	-	-	150.7 (q) ($^1J_{CF}$ = 352.2 Hz)	15.9 14.3	139.6 131.4,129.9
cis,cis-$Fe(CO)_2$(diars)(CF_3)I **(21)**	212.25 209.6	-	-	156.0 (q) ($^1J_{CF}$ = 360.0 Hz)	12.7 13.4 13.7 13.9	129.0 129.5 130.5 139.43, 139.36
cis,cis-$Fe(CO)_2$(diars)I_2 **(22)**	217.4 211.4	-	-		16.4 15.9 15.5 13.8	140.9, 140.4 131.8, 131.5 131.2 129.5

Solvent: $CDCl_3$; Reference compound: Me_4Si
Shift values in ppm

Table 2.8: ^{13}C NMR DATA

Compound	M^+	M^+-CF_3	M^+-CF_3 -CO	M^+-CF_3 -2CO	M^+- -3CO	M^+-CF_3 3CO-CF_2	M^+-2CO	M^+-2CO -CF_2, -F
cis,trans-$Fe(CO)_2$-(diars)(C(O)CF_3)I (16)	622 (2.52)	553 (39.05)	525 (9.23)	497 (8.60)	469 (100.00)	488 (39.05)	-	-
cis,cis-$Fe(CO)_2$-(diars)(C(O)CF_3)I (17)	622 (0.39)	553 (9.30)	525 (2.2)	497 (3.17)	469 (100)	488 (12.60)	-	-
cis,trans-$Fe(CO)_2$-(diars)(CF_3)I (20)	-	-	-	-	-	-	538[a] (0.67)	488 (1.67) 469 (0.25)
cis,cis-$Fe(CO)_2$-(diars)(CF_3)I (21)	594 (0.88)	-	-	-	-	-	538[a] (2.10)	488(5.76) 469 (2.30)
cis,cis-$Fe(CO)_2$-(diars)I_2 (22)	-	-	-	-	-	-	596[a] (0.44)	469 (0.98) (M^+-2CO-I)

a = base peak is 271

Table 2.9: Mass Spectral Data

Compound	ν_{R_f}
cis,trans-$Fe(CO)_2$(diars)($C(O)CF_3$)I **(16)**	-79.4
cis,cis-$Fe(CO)_2$(diars)($C(O)CF_3$)I **(17)**	-78.5
cis,trans-$Fe(CO)_2$(diars)(CF_3)I **(20)**	+12.9
cis,cis-$Fe(CO)_2$(diars)(CF_3)I **(21)**	+10.8

Solvent: $CDCl_3$; Reference compound: $CFCl_3$
Shift values in ppm

Table 2.10: ^{19}F NMR Data

Chapter 3

Reaction of Higher Analogues of CF_3I with $Fe(CO)_3$(diars)

3.1 Introduction

As discussed in Chapter 2, transition metal complexes are known to undergo oxidative addition reactions with perfluoroalkyl iodides. Limited examples are known for the higher analogues of CF_3I, as shown in Table 3.1. $Fe(CO)_3$(diars) reacts with the higher analogues of CF_3I, namely, C_2F_5I,n-C_3F_7I,n-$C_6F_{13}I$,n-$C_7F_{15}I$ as well as CF_3CH_2I to yield the corresponding oxidative addition product, $Fe(CO)_2$(diars)R_fI, in good yield. These results are interesting since in the $Fe(CO)_3L_2$ series, oxidative addition has not been observed for alkyl iodides other than CH_3I. Steric hinderance has been suggested to account for these results [144]. However, oxidative addition of groups larger than CH_3I is facile when a carbonyl ligand in the $Fe(CO)_3L_2$ series is substituted by labile ligands such as N_2 [24, 25] or CH_3CN [43]. Also, in contrast to CF_3I, the higher analogues do not form the perfluoroacyl compound in any significant yield.

Reagent	R_fI	Product	Reference
$Fe(CO)_5$	C_2F_5I C_3F_7I $C_7F_{15}I$	$Fe(CO)_4(C_2F_5)I$ $Fe(CO)_4(C_3F_7)I$ $Fe(CO)_4(C_7F_{15})I$	[124] [124] [109]
trans-$Fe(CO)_3((C_6H_5)_2PC_2H_5)_2$	C_3F_7I	No reaction	[123]
cis-$Fe(CO)_3$(diphos)	C_3F_7I	$Fe(CO)_2$(diphos)$(C_3F_7)I$	[123]
$\pi C_5H_5Co(CO)_2$	C_2F_5I C_3F_7I	$\pi C_5H_5Co(CO)(C_2F_5)I$ $\pi C_5H_5Co(CO)(C_3F_7)I$	[110] [110]

diphos = $P(C_6H_5)_2CH_2CH_2(C_6H_5)_2P$

Table 3.1: Oxidative Addition of Higher Analogues of CF_3I

3.2 Experimental

The perfluoroalkyl iodides C_2F_5I, n-C_3F_7I, n-$C_6F_{13}I$ and CF_3CH_2I were used as purchased from Aldrich. n-$C_7F_{15}I$ showed traces of iodine and hence was stirred with mercury overnight and distilled.

The methodology followed is same as that described in Chapter 2. 424 mg (0.99×10^{-3} moles) of $Fe(CO)_3$(diars) was dissolved in 5 mL of dichloromethane and 50 mL (2.2×10^{-3} moles) of C_2F_5I was syringed into the solution at -78 °C. The yellow solution turned brown immediately and it was stirred for 2 hours at -78 °C. Removal of solvent and other volatiles under vacuum gave a reddish brown product which was isolated as a brown band on preparative thin layer chromatography with toluene as the elutant. This was identified spectroscopically as cis,cis-$Fe(CO)_2$(diars)$(C_2F_5)I$. A thin pink band which also accompanied the above product was isolated and identified by spectroscopy as the di-iodo compound **22**, which was also obtained in the reactions of CF_3I. The reactions of $Fe(CO)_3$(diars) with other R_fI compounds were similar to that of C_2F_5I and the details are shown in Table 3.2. Since it was observed in the case of CF_3I that a concentrated reaction mixture favoured perfluoroacyl formation, the reactions of the higher analogues were carried out with just sufficient solvent to dissolve the $Fe(CO)_3$(diars) (0.5 mL). Only very small perfluoroacyl peaks were observed in the IR spectra and no perfluoroacyl derivatives could be isolated.

Mass of $Fe(CO)_3$(diars) in 5 mL of CH_2Cl_2	R_fI	Qty of R_fI	Mol. Ratio	Product	% Yield
424 mg (0.990 mM)	C_2F_5I	50 mL	1:2.2	cis,cis-$Fe(CO)_2$(diars)$(C_2F_5)I$ (23)	74.49
316 mg (0.742 mM)	C_3F_7I	0.11 mL	1:1	cis,cis-$Fe(CO)_2$(diars)$(C_3F_7)I$ (24)	58.74
406 mg (0.953 mM)	$C_6F_{13}I$	0.20 mL	1:1	cis,cis-$Fe(CO)_2$(diars)$(C_6F_{13})I$ (25)	81.45
452 mg (1.062 mM)	$C_7F_{15}I$	527 mg	1:1	cis,trans-$Fe(CO)_2$(diars)$(C_7F_{15})I$ (26)	49.01
224 mg (0.250 mM)	CH_2CF_3I	111 mg	1:1	cis,cis-$Fe(CO)_2$(diars)$(CH_2CF_3)I$ (27)	48.00

Reaction time = 2 h; Temp = -78 °C

Table 3.2: Reaction Details of Higher Analogues

3.3 Results and Discussion

A single isomer was isolated for all the above oxidative addition reactions. R_fI (R_f = n-C_2F_5I, n-C_3F_7I, n-C_6F_{13}I as well as CH_2CF_3I) formed cis,cis-$Fe(CO)_2$(diars)R_fI, while C_7F_{15}I formed a cis,trans isomer as shown in Fig. 3.1. All these are new compounds. Their physical properties are recorded in Table 3.3, and their ^{1}H, ^{13}C, ^{19}F, IR and mass spectral data are recorded in Tables 3.4 to 3.8 respectively. Compounds **23**,**24**,**25**,and **27** are identified by spectroscopy as cis,cis isomers.

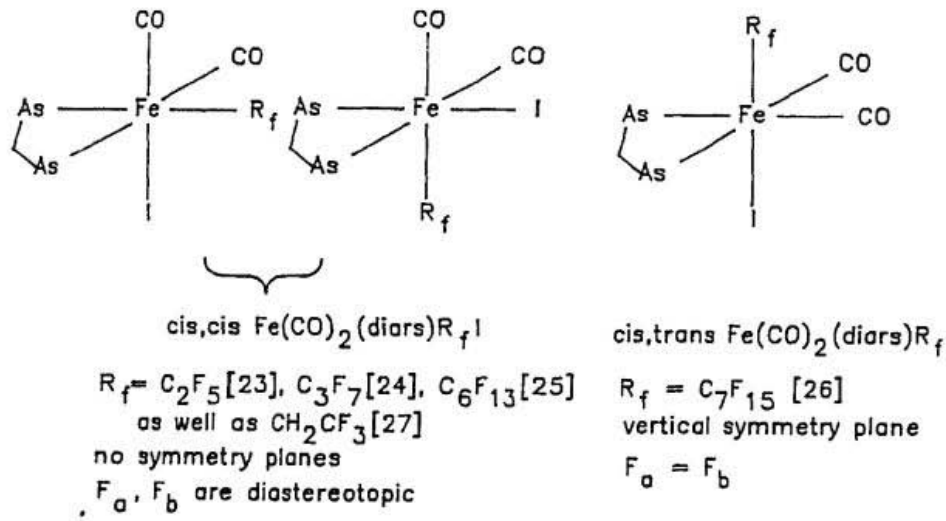

Figure 3.1: Structures of the Perfluoroalkyl Compounds

They have spectral patterns similar to isomers **17** and **18** (cf.Tables 2.6 to 2.10) as discussed below. Since the cis,cis geometry lacks a symmetry plane, the iron atom is chiral and the CF_2 groups are diastereotopic. Similarly in **27**, H_a and H_b of the α-CH_2 group are diastereotopic. Compound **26** is identified as the cis,trans isomer and shows a spectral pattern similar to **16**. A vertical symmetry plane makes the two fluorine atoms of the alpha CF_2 group equivalent.

3.3.1 ^{1}H NMR Spectra

The ^{1}H NMR spectra of cis,cis-Fe(CO)$_2$(diars)R$_f$I isomers **23**, **24**, **25** and **27** show four non-equivalent As-CH$_3$ resonances. In compound **27**, the methylene protons are seen as the AM part of a first order AMX$_3$ multiplet (X=F). The resonance due to H$_a$ is coupled to H$_b$ resulting in a doublet ($J_{H_aH_b}$=12.5Hz) which is further coupled to the three magnetically equivalent ^{19}F nuclei (C$_\beta$), resulting in a doublet of quartets ($^3J_{HF_a}$=16Hz). Similarly, another doublet of quartets is seen for H$_b$ (cf. Fig. 3.2). Compound **26** shows only two As-CH$_3$ resonances due to its vertical symmetry plane.

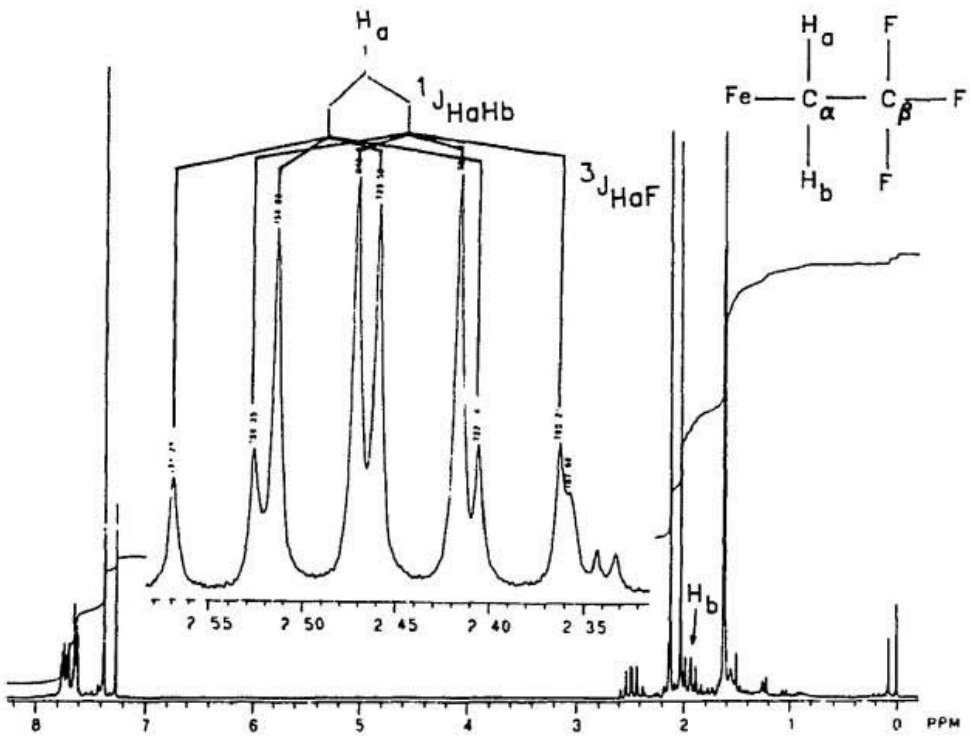

Figure 3.2: 300 MHz ^{1}H NMR Spectrum of Fe(CO)$_2$(diars)(CH$_2$CF$_3$)I (**27**) in CDCl$_3$ Showing the AMX$_3$ Pattern

3.3.2 ^{13}C NMR Spectra

The ^{13}C NMR spectrum of **24** shown in Fig.3.3 is discussed as a typical example. Since the compound has a cis,cis geometry with no symmetry planes, the six carbon atoms of the diars ring are nonequivalent and six o-C_6H_4 resonances are seen. All four methyl groups bonded to the As atoms are nonequivalent. However, only three As-CH_3 resonances are observed due to accidental degeneracy. Two CO resonances are seen with unresolved ^{13}C–^{19}F coupling.

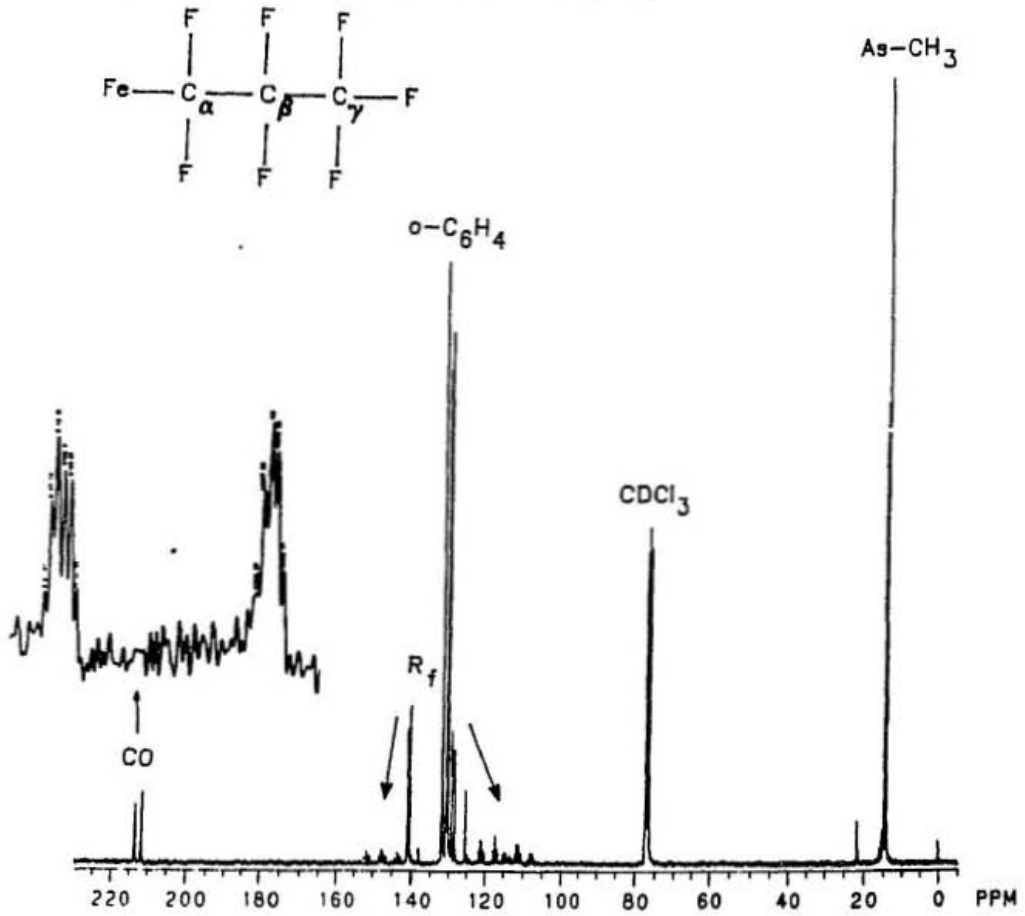

Figure 3.3: 75 MHz ^{13}C NMR Spectrum of $Fe(CO)_2(diars)(C_3F_7)I$ (**24**) in $CDCl_3$

The R_f group shows extensive ^{13}C-^{19}F couplings. The diastereotopic fluorine nuclei, F_a and F_b show slightly different one bond couplings so that C_α appears as a double doublet ($^1J_{CF_a}$ = 300 Hz, $^1J_{CF_b}$ = 291 Hz). Further coupling to the adjacent βCF_2 group results in four triplets as shown in Fig. 3.4 ($^2J_{CF}$ = 52 Hz).

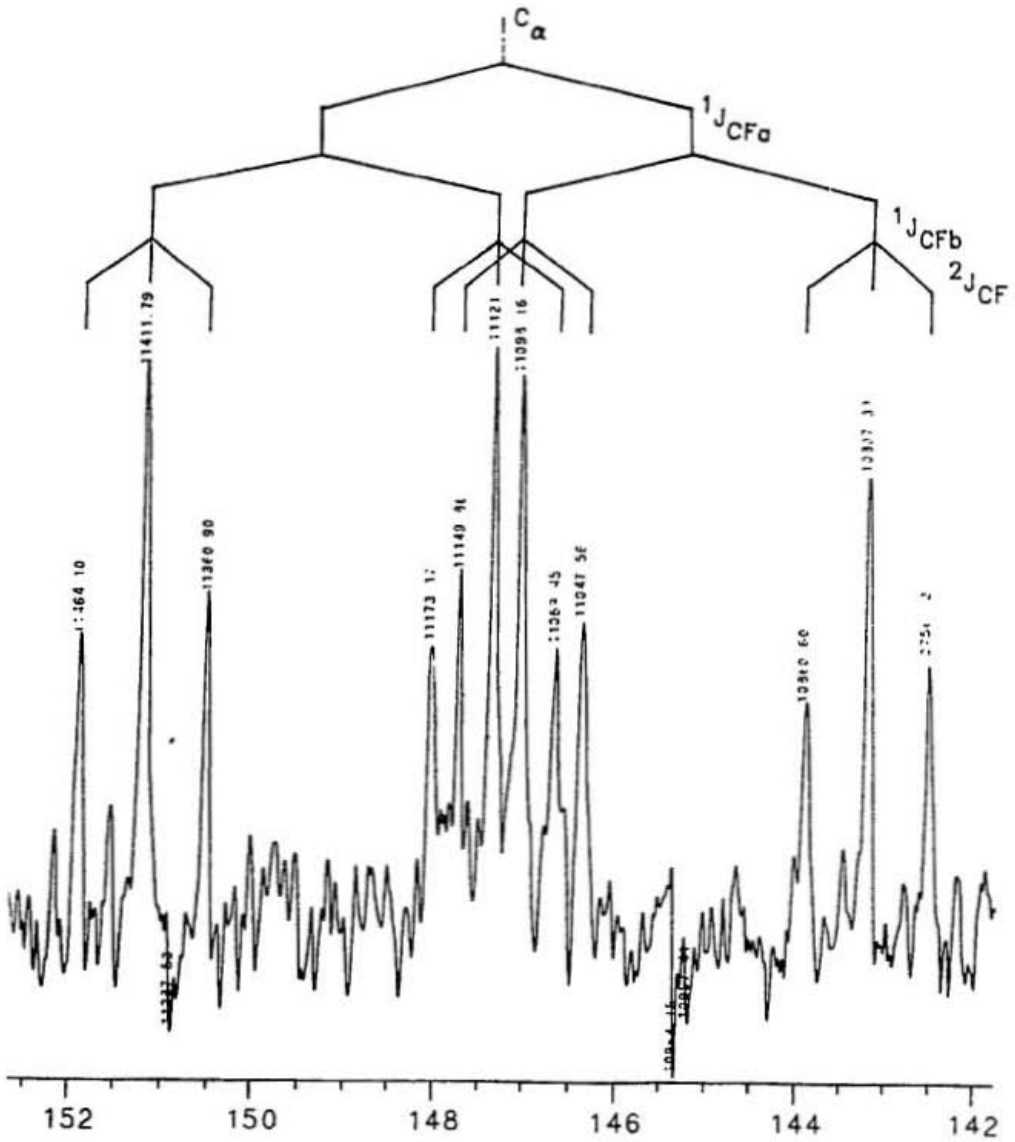

Figure 3.4: 75 MHz Partial ^{13}C NMR Spectrum of $Fe(CO)_2(diars)(C_3F_7)I$ in $CDCl_3$

C_β is coupled to the directly bonded fluorine nuclei resulting in a triplet ($^1J_{CF}$ = 255 Hz) and is further coupled to $C_\gamma F_3$ resulting in a triplet of quartets ($^2J_{CF}$ = 35 Hz). This is further coupled to α-CF_2 which is also a two bond coupling resulting in a triplet of sextets of intensities 1:5:10:10:5:1 ($^2J_{CF}$ = 35Hz). C_γ is coupled to the three magnetically equivalent fluorine atoms and is seen as a quartet ($^1J_{CF}$ = 291 Hz) which is further coupled to $C_\beta F_2$ resulting in a quartet of triplets as shown in Fig. 3.5 ($^2J_{CF}$ = 38 Hz).

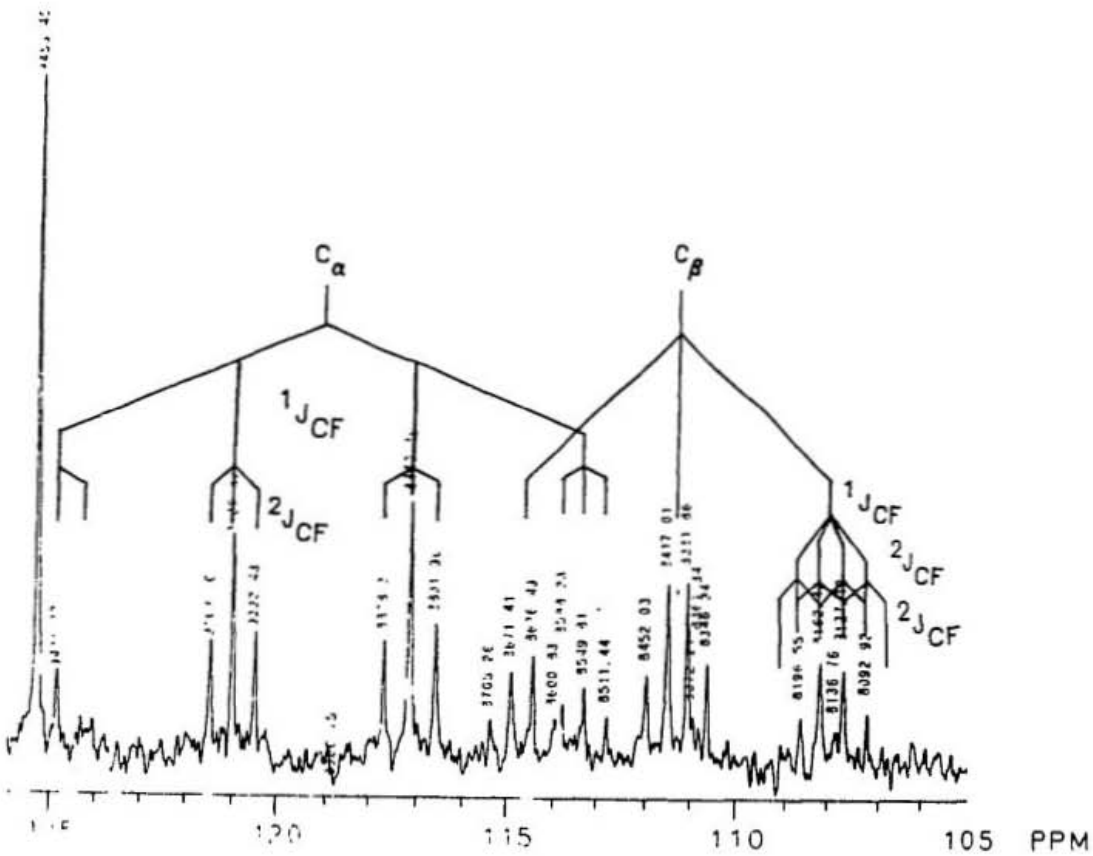

Figure 3.5: 75 MHz Partial ^{13}C NMR Spectrum of $Fe(CO)_2(diars)(C_3F_7)I$ **24** in $CDCl_3$

Compound **23**, $Fe(CO)_2(diars)(C_2F_5)I$, shows a spectral pattern similar to **24** and its partial ^{13}C spectrum is shown in Fig. 3.6. C_α is coupled to the diastereotopic F_a and F_b resulting in a double doublet ($^1J_{CF_a}$ = 300 Hz, $^1J_{CF_b}$ = 293 Hz) which is further coupled to the adjacent CF_3 group resulting in a quartet of quartets ($^2J_{CF}$ = 40.6 Hz). C_β is coupled to the magnetically equivalent fluorine atoms forming a quartet ($^1J_{CF}$ = 286 Hz) which is further oupled to $C_\alpha F_2$ resulting in a quartet of triplets ($^2J_{CF}$ = 33 Hz).

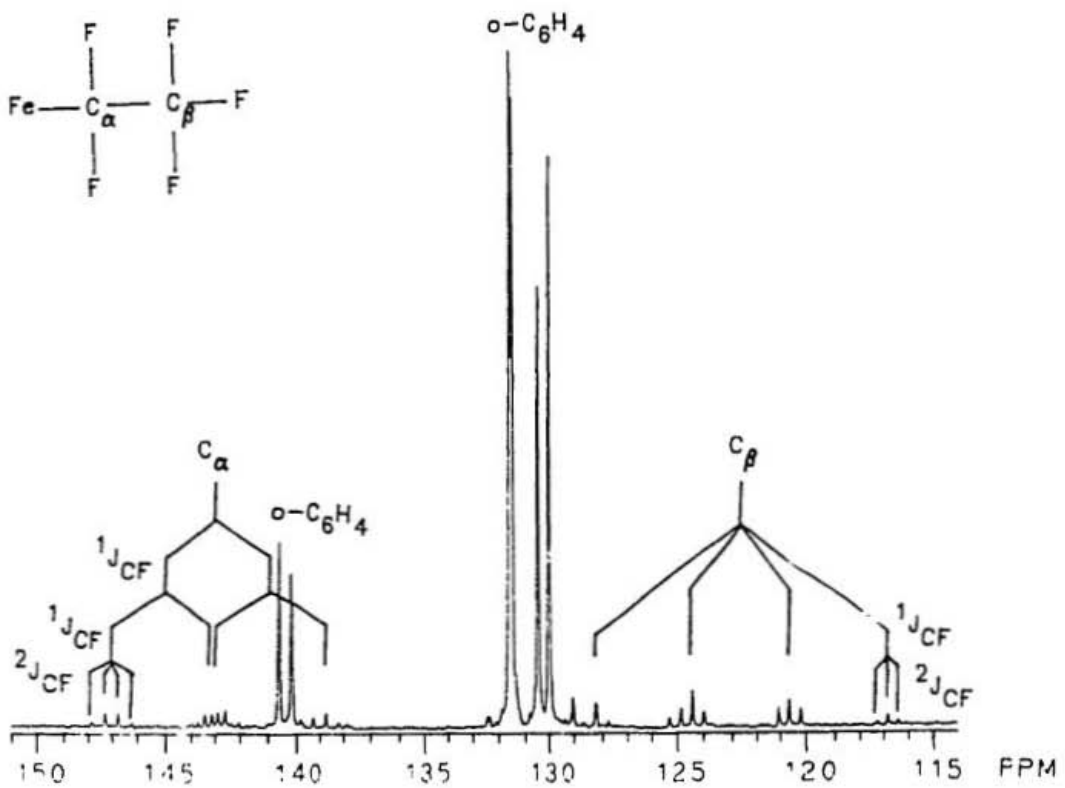

Figure 3.6: 75 MHz Partial ^{13}C NMR Spectrum of $Fe(CO)_2(diars)(C_2F_5)I$ **23** in $CDCl_3$

The spectral pattern of $Fe(CO)_2(diars)(C_6F_{13})I$ (**25**) is similar to those of the above compounds. C_α is found in the same spectral region (148.7 PPM) as compounds **23** and **24** and is seen as a quartet of triplets. C_ζ in the terminal CF_3 group is coupled to the three magnetically equivalent fluorine atoms resulting in a quartet ($^1J_{CF}$ = 288 Hz) in the same spectral region as compounds **23** and **24**. This is further coupled to the adjacent $C_\epsilon F_2$ resulting in a quartet of triplets ($^2J_{CF}$ = 32 Hz). The remaining four carbon atoms C_β, C_γ, C_δ and C_ϵ are split by the directly bonded fluorine atoms into triplets and are seen at 108.8, 110.6, 112.5 and 113.2 ppm ($^1J_{CF}$ = 268 Hz) (cf. Fig. 3.7). Further coupling to the adjacent fluorine nuclei is complex and could not be unambiguously assigned.

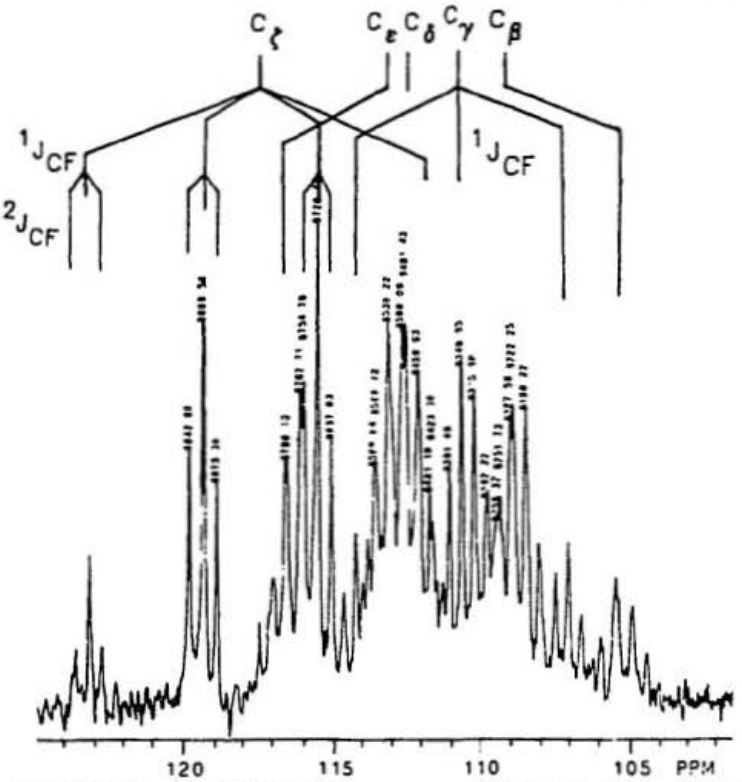

Figure 3.7: 75 MHZ Partial ^{13}C NMR Spectrum of $Fe(CO)_2(diars)(C_6F_{13})I$ **25** in $CDCl_3$

The ^{13}C NMR spectrum of $Fe(CO)_2(diars)CH_2CF_3I$ (**27**) is shown in Fig 3.8. C_α is coupled to the three magnetically equivalent fluorine atoms of C_β resulting in a quartet ($^2J_{CF} = 26$ Hz) at 6.95 ppm. C_β is also a quartet at 134.6 ppm due to coupling with the three directly bonded fluorine atoms ($^1J_{CF} = 275$ Hz).

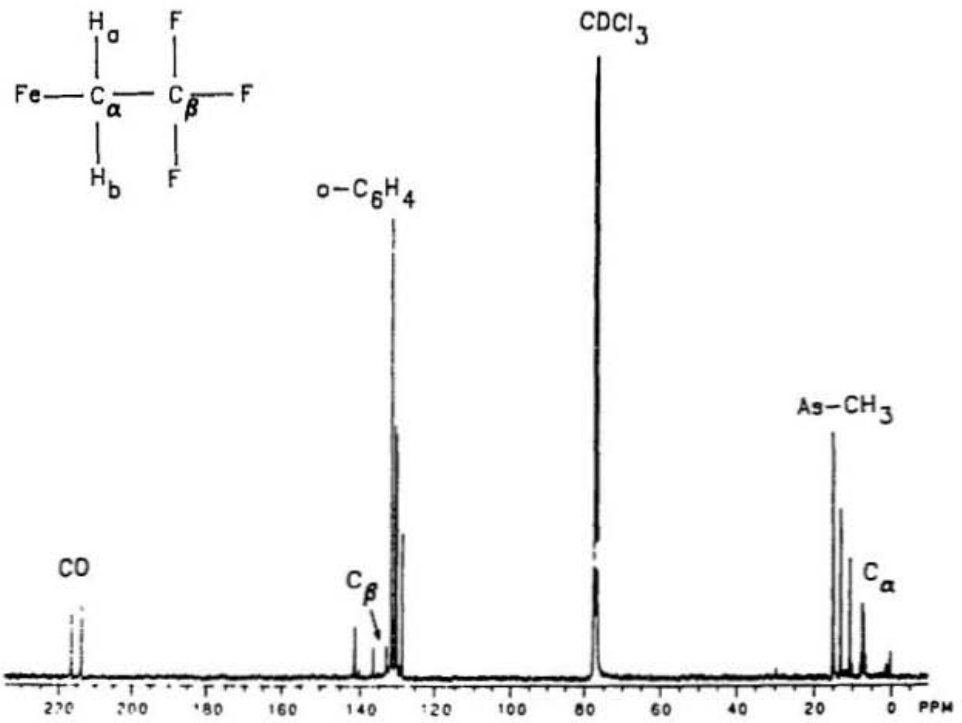

Figure 3.8: 75 MHz ^{13}C NMR Spectrum of $Fe(CO)_2(diars)(CH_2CF_3)I$ **27** in $CDCl_3$

$Fe(CO)_2(diars)(C_7F_{15})I$, **(27)**, has a different symmetry from the other compounds and shows a different spectral pattern. A vertical symmetry plane makes three of the phenyl carbon atoms in diars ligand equivalent and hence only three o-phenylene resonances are seen. Similarly only two As-CH_3 resonances and one CO resonance are seen. The CO resonance is coupled to $C_\alpha F_2$ and $C_\beta F_2$ giving an apparent quintet assuming that $^4J_{CF}$ is almost equal to $^3J_{CF}$. C_α of R_f group is coupled to the two isochronous fluorine nuclei directly bonded to it giving a triplet and further coupling to $C_\beta F_2$ results in a triplet of triplets as shown in Fig. 3.9. C_η is coupled to the three directly bonded magnetically equivalent fluorine atoms and to the adjacent CF_2 group resulting in a triplet of quartets in the same spectral region as compounds **23**, **24** and **25**. Similar to **25**, C_β, C_γ, C_δ and C_ϵ and C_ζ are coupled to the two directly bonded fluorine nuclei and are seen as triplets at 107.3, 108.9, 110.5, 111.7 and 112.6 ppm ($^1J_{CF}$ =279 Hz). Further coupling to the adjacent fluorine nuclei is complex and could not be unambiguously assigned.

3.3.3 ^{19}F NMR Spectra

The ^{19}F NMR spectra of the α-CF_2 group of compounds **23**,**24**,**25** and **27** is an AB spectrum due to the chirality of the iron center. The AB spectrum was analyzed using the equations given below [1]:

$$\begin{aligned} J &= F_1 - F_2 \qquad\qquad F: \text{Frequency} \\ &= F_3 - F_4 \end{aligned}$$

$$\begin{aligned} dv &= v_A - v_B \\ &= \sqrt{(F_1 - F_4)(F_2 - F_3)} = y \\ v_A &= v_B + y \qquad\qquad \ldots 1 \\ \tfrac{1}{2}(v_A + v_B) &= \text{center of the AB spectrum} = x \\ v_B &= 2x - v_A \qquad\qquad \ldots 2 \end{aligned}$$

v_A & v_B were computed from Eqs. 1 and 2. The detailed calculations for compounds **23**, **24**, **25**, and **27** are given in Appendix A.

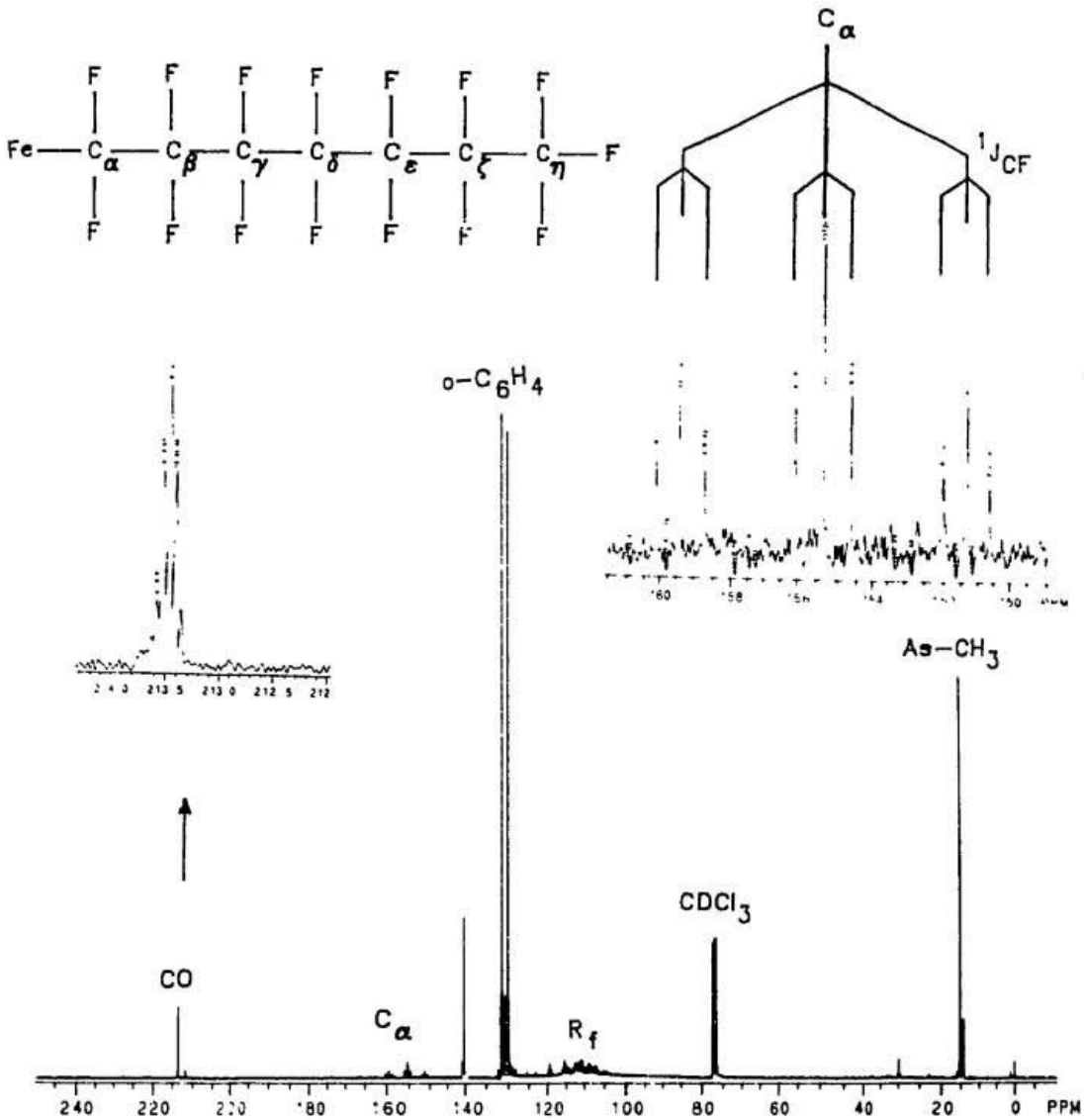

Figure 3.9: 75 MHz Partial ^{13}C NMR Spectrum of $Fe(CO)_2(diars)(C_7F_{15})I$ **26** in $CDCl_3$

The ^{19}F NMR spectrum of compound **23** is shown in Fig. 3.10. The diastereotopic C_α fluorine atoms appear as a typical four line AB pattern ($^2J_{F_aF_b}$ = 263 Hz). Vicinal coupling with the adjacent $C_\beta F_3$ group results in further splitting of each component into a quartet. The CF_3 group is coupled to F_a and F_b resulting in a double doublet. ($^3J_{F_aF}$ = 7.5 Hz, $^3J_{F_bF}$ = 5 Hz) The different coupling constants are not surprising since F_a and F_b are diastereotopic.

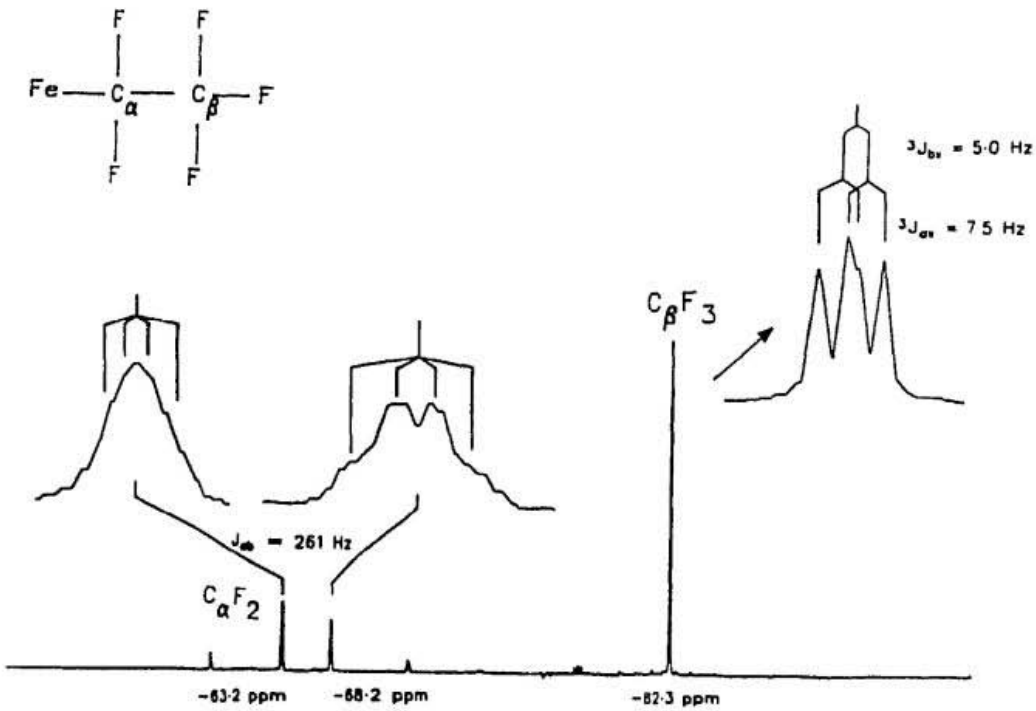

Figure 3.10: 282 MHz ^{19}F NMR Spectrum of $Fe(CO)_2(diars)(C_2F_5)I$ **23** in $CDCl_3$

The ^{19}F NMR spectrum of compound **24** is shown in Fig. 3.11. The four line AB pattern of $C_\alpha F_a F_b$ is further coupled to the C_γ fluorine atoms instead of C_β giving four quartets ($^1J_{F_aF_b}$ = 268 Hz, $^4J_{F_aF}$ = 12.5 Hz, $^4J_{F_bF}$ =10.9 Hz). This four bond coupling is as expected since it is generally observed that $^4J_{FF} > {}^3J_{FF}$ [147]. The CF_3 group is observed in the same spectral region as that of compound **23** and $C_\beta F_2$ and $C_\gamma F_3$ are observed as unresolved multiplets.

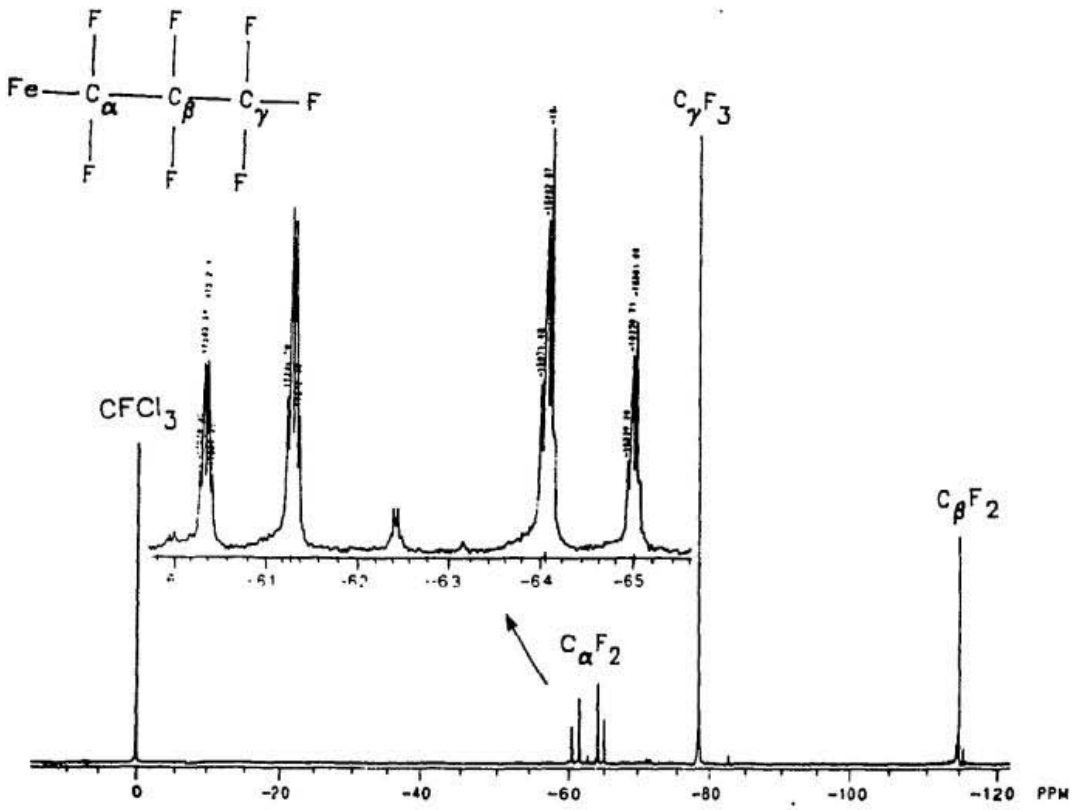

Figure 3.11: 282 MHz ^{19}F NMR Spectrum of $Fe(CO)_2(diars)(C_3F_7)I$ **24** in $CDCl_3$

The ^{19}F NMR spectrum of compound 25 is shown in Fig.3.12. The four line AB pattern of C_α fluorine nuclei is further coupled and results in four triplets ($^1J_{FaFb}$ = 271 Hz). The coupling constant of the triplets is 18 Hz suggesting a four bond coupling with $C_\gamma F_2$ since $^3J_{FaF}$ is only 7.5Hz in **23**. The terminal CF_3 group occurs at the same spectral region as compounds **23** and **24**. The AB resonance at -110 ppm is assigned to $C_\beta F_2$ since in compound **24** $C_\beta F_2$ is seen at -115 ppm. A similar shift has been reported for many other transition metal compounds [146]. $C_\gamma F_2$, $C_\delta F_2$ and $C_\varepsilon F_2$ are assigned to the three unresolved multiplets upfield from $C_\beta F_2$ at -121 ppm, -123 ppm and -127 ppm respectively.

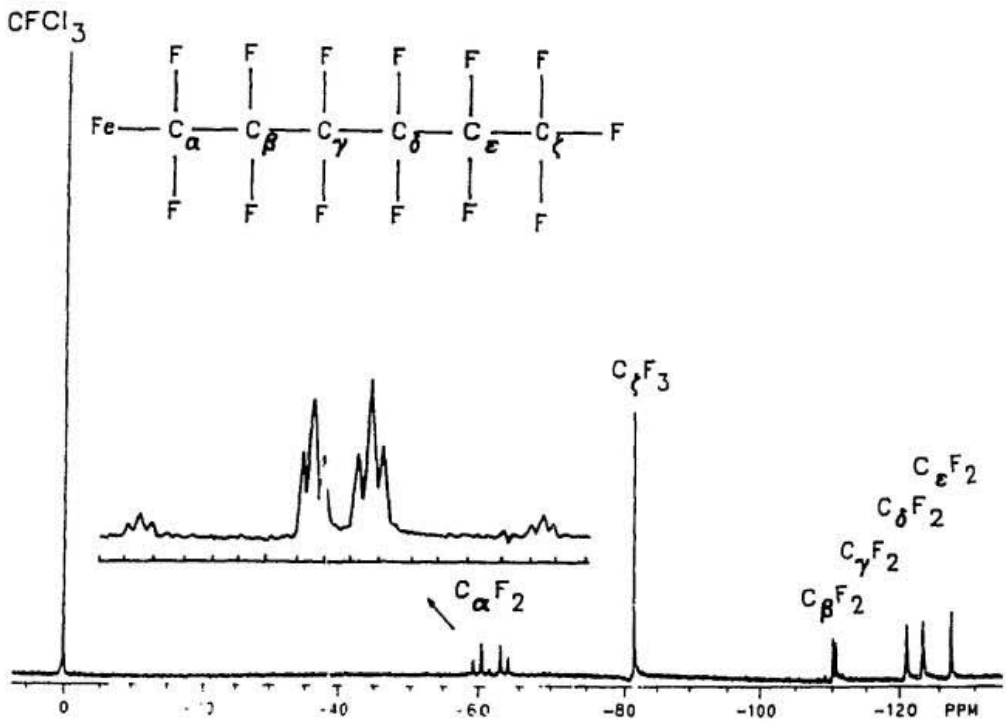

Figure 3.12: 75 MHz ^{19}F NMR Spectrum of $Fe(CO)_2(diars)(C_6F_{13})I$ **25** in $CDCl_3$

The ^{19}F NMR spectrum of compound **27** is shown in Fig. 3.13. $C_\beta F_3$ shows identical coupling to H_a and H_b and is seen as a double doublet ($^3J_{FH_a} = {}^3J_{FH_b}$ = 16 Hz).

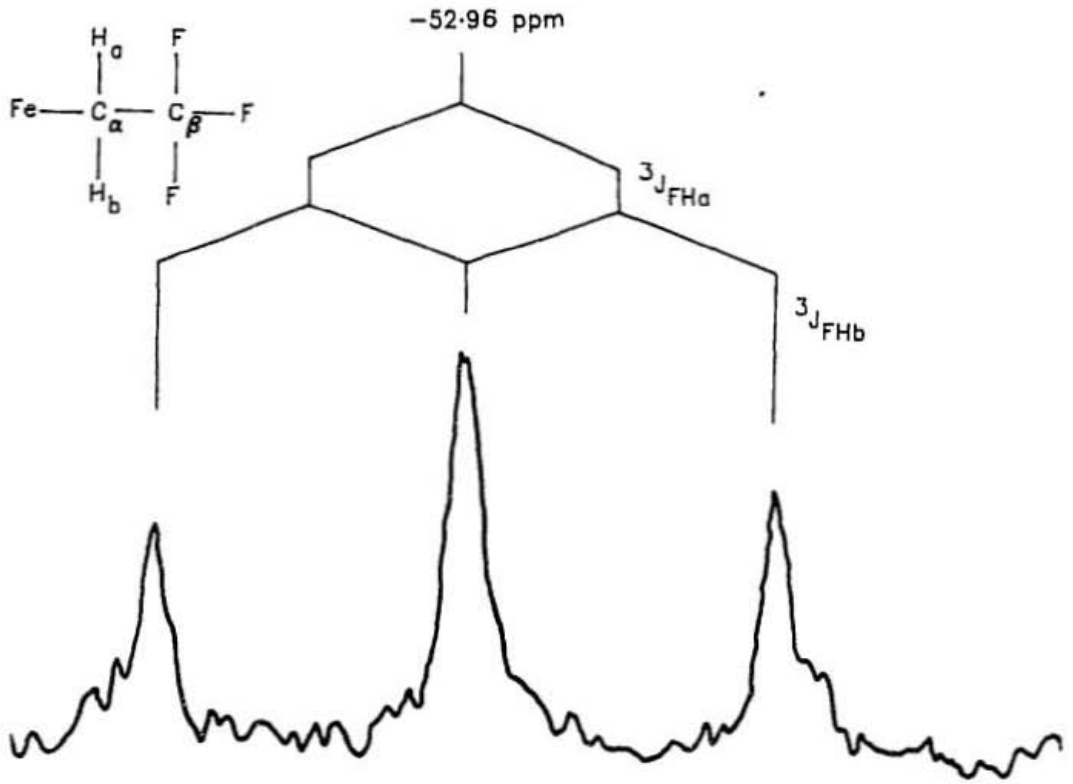

Figure 3.13: 75 MHz ^{19}F NMR Spectrum of $Fe(CO)_2(diars)(CH_2CF_3)I$ **27** in $CDCl_3$

The ^{19}F NMR spectrum of compound **26** is shown in Fig.3.14. Due to the vertical symmetry plane, the C_α fluorine atoms are isochronous. Four bond coupling with $C_\gamma F_2$ results in a triplet ($^4J_{FF} = 18$ Hz). $C_\eta F_3$ is observed in the same spectral region as compounds **23**, **24** and **25**. Similar to **25**, $C_\beta F_2$, $C_\gamma F_2$, $C_\delta F_2$, $C_\varepsilon F_2$ and $C_\zeta F_2$ are assigned in increasing upfield shifts as -111 ppm, -121 ppm, -122 ppm, -123 ppm and -127 pprn respectively. These are observed as unresolved multiplets. A similar assignment has been made for $Fe(CO)_4(C_7F_{15})I$ [109].

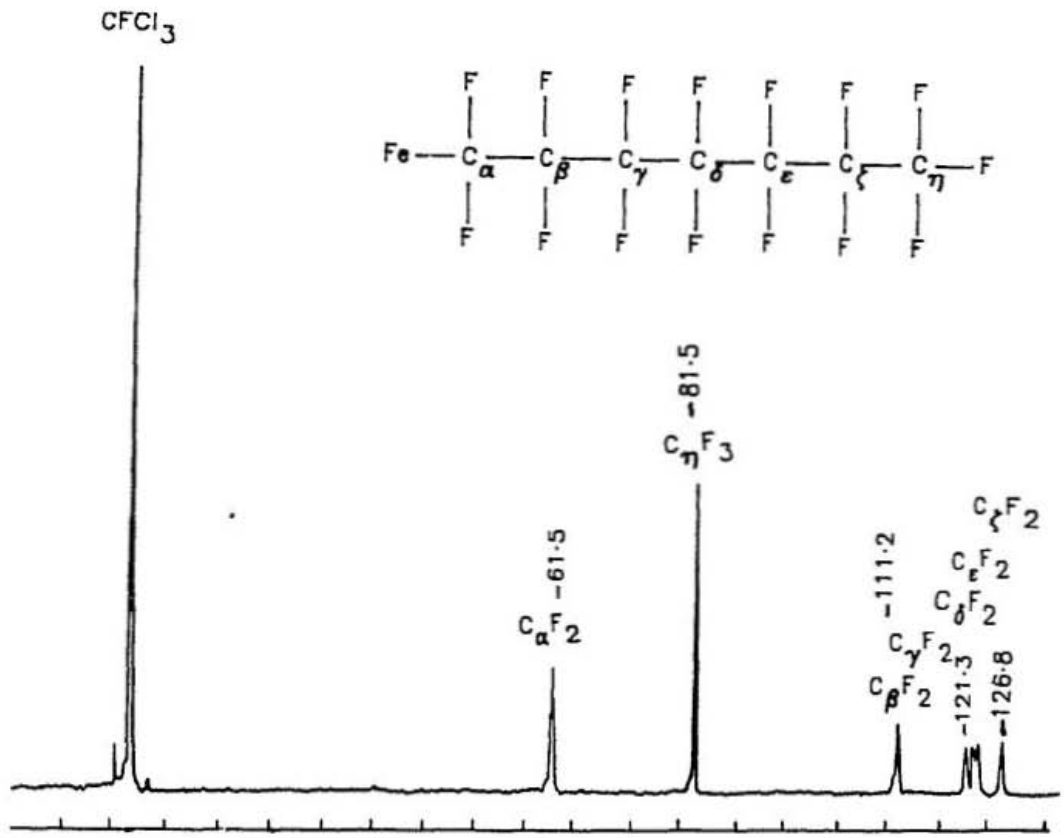

Figure 3.14: 75 MHz ^{19}F NMR Spectrum of $Fe(CO)_2(diars)(C_7F_{15})I$ **26** in $CDCl_3$

3.3.4 IR and Mass Spectra

In general, perfluoroalkyl transition metal carbonyls show strong CO stretches at appreciably higher frequencies than alkyl transition metal carbonyls [148]. The CO stretches for cis,cis-Fe(diars)$(CO)_2(C_2F_5)I$ are 2010 and 1960 cm^{-1} and similar stretches are seen for the other compounds (cf. Table 3.7). The CO stretching frequencies of the fluorocarbon metal carbonyls are found to be similar to those of the corresponding metal carbonyl halides [148]. Accordingly, the CO stretching frequencies of the di-iodo compound **22** are similar to those of the perfluoroalkyl compounds. The C-F stretches for compounds **23**, **24**,**25** and **26** vary from 1310 to 960 cm^{-1} [148] (cf. Table 3.7).

The mass spectra of metal carbonyls are characterized by sequential loss of CO from the parent molecular ion and only processes with very low energy requirements compete with this decarbonylation. The mass spectra of all the new compounds discussed in this chapter show simultaneous loss of two carbonyls. Similar observations have been made for $[Fe(CO)_2(diars)CH_3\ L]^+$ (L = phosphorus donor ligands) [85] and other metal carbonyl complexes with phosphorus donor ligands [121].

3.3.5 Isomerization Study

Cis,cis-$Fe(CO)_2$(diars)$(C_3F_7)I$, **24**, was dissolved in d_8-toluene and the AB spectrum of the $C_\alpha F_2$ followed by ^{19}F NMR at different temperatures. The AB spectrum remained undisturbed even at 100 °C (cf.Fig. 3.15) indicating that the chiral iron center is configurationally stable on the NMR time scale. Pankowski et al. report that the solution stabilities of iron chiral complexes are strongly dependent on steric strain. $Fe(CO)_2(P(CH_3)_3)RL$ is stable in solution at 30 °C when L is small such as $PhP(CH_3)(OR)$, but when L is moderately large such as

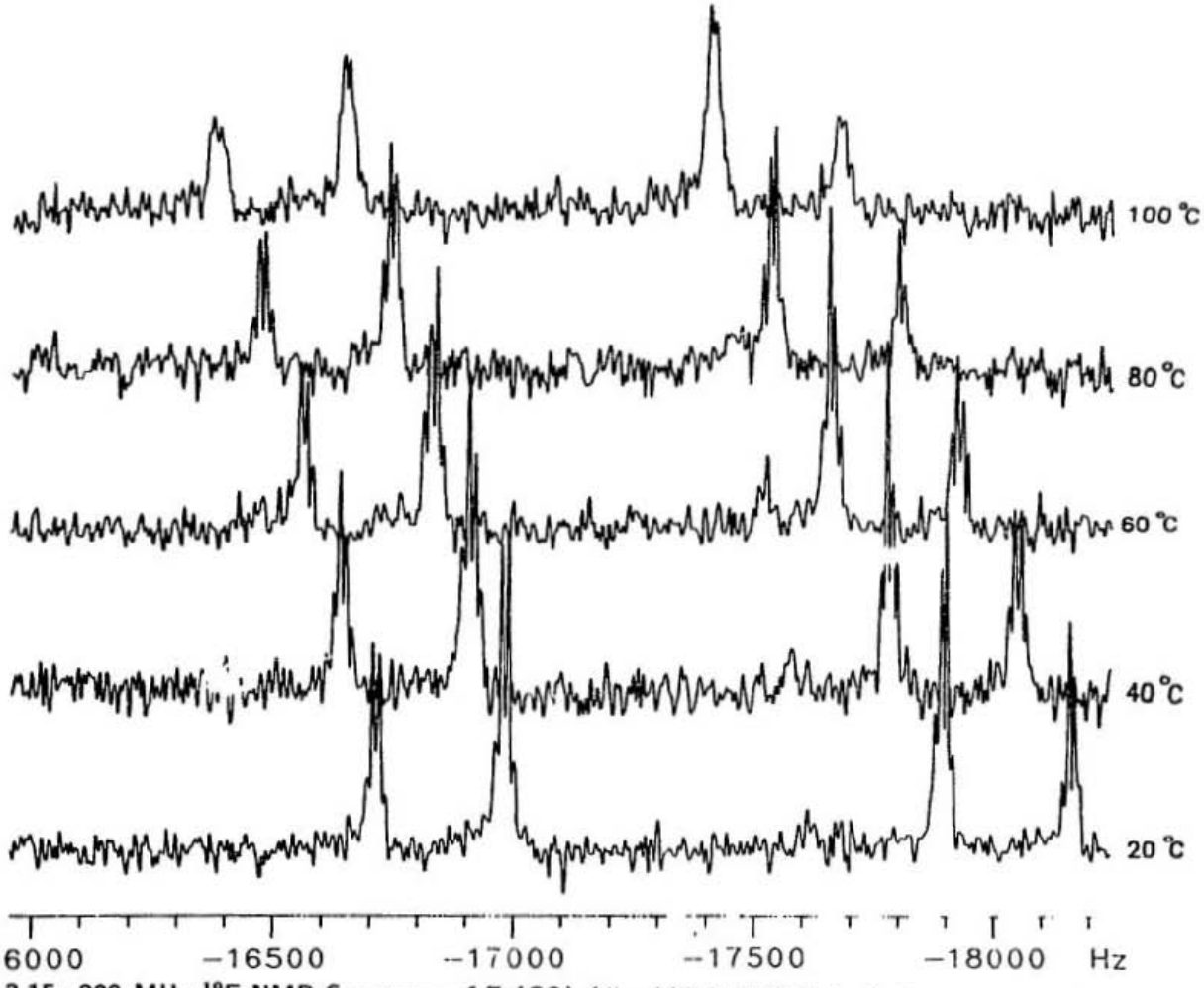

Figure 3.15: 282 MHz ^{19}F NMR Spectrum of $Fe(CO)_2(diars)(C_3F_7)I$ (**24**) in d_8-Toluene Showing the AB Spectrum at Various Temperatures

$PhP(CH_3)(CH_2Ph)$, it is stable only at –30 °C [142].

3.4 Conclusion

$Fe(CO)_3$(diars) reacts with various perfluoroalkyl iodides forming single isomers of the oxidative addition product in good yield (cis,cis-$Fe(CO)_2$(diars)R_fI for R_f = C_2F_5, n-C_3F_7, n-C_6F_{13} as well as CH_2CF_3 and the cis,trans isomer for R_f = C_7F_{15}). No perfluoroacyl compounds were isolated. Evidence supporting a free radical mechanism is given in Chapter 4. The isolation of single isomers is most probably due to thermodynamic factors. The formation of a different isomer for R_f = n-C_7F_{15} may be due to steric factors, since C_7F_{15} and iodine atoms are bulky and hence prefer to be mutually trans.

Compound	% Yield	M.P. (°C)	Elemental Analysis			
			% Carbon		% Hydrogen	
			Calculated	Found	Calculated	Found
cis,cis $Fe(CO)_2(diars)(C_2F_5)I$ (23)	74.49	116 - 117	26.12	25.64	2.50	2.10
cis,cis $Fe(CO)_2(diars)(C_3F_7)I$ (24)	58.74	115 - 116	25.97	26.16	2.32	1.92
cis,cis $Fe(CO)_2(diars)(C_6F_{13})I$ (25)	81.45	141 - 142	25.62	25.68	1.91	1.68
cis,trans $Fe(CO)_2(diars)(C_7F_{15})I$ (26)	49.01	142 - 143	25.53	25.46	1.80	1.82

Table 3.3: Physical Data

Compound	As-Me	O-C_6H_4
cis,cis $Fe(CO)_2(diars)(C_2F_5)I$ **(23)**	2.205, 2.133, 1.726, 1.616	7.67 (m)
cis,cis $Fe(CO)_2(diars)(C_3F_7)I$ **(24)**	2.167, 2.106, 1.69, 1.582	7.70 (m)
cis,cis $Fe(CO)_2(diars)(C_6F_{13})I$ **(25)**	2.197, 2.133, 1.722, 1.609	7.71 (m)
cis,trans $Fe(CO)_2(diars)(C_7F_{15})I$ **(26)**	2.182, 1.693	7.68 (m)
cis,cis $Fe(CO)_2(diars)(CH_2CF_3)I$ **(27)**	2.118, 2.023, 1.628, 1.612 $H_a = 2.48$ $H_b = 1.25$ $J_{H_aH_b} = 12.9$ Hz $^3J_{HF} = 16.4$ Hz	7.67 (m)

Table 3.4: ^{1}H NMR Spectral Data

Cpd.	Fe-CO	As-Me	As-Ph	α-CF_2	β-CF_2	γ-CF_2	δ-CF_2	ϵ-CF_2	ζ-CF_2	CF_3
23	213.3 (d, J=9) 211.5	14.1 14.3 14.4 14.7	130.0,140.0 130.1,140.2 131.5,131.7	142.9(m, $^1J_{CF_a}$=300, $^1J_{CF_b}$=293)						122.7(qt, $^1J_{CF}$=286, $^3J_{CF}$=40.6)
24	213.0 (m, J=4) 211.0	15.1 14.7 14.6	129.9,140.6 130.4,140.1 131.5,131.3	147.3(m, $^1J_{CF_a}$=320, $^1J_{CF_b}$=291, $^2J_{CF}$=52)	111.3(ts, $^1J_{CF}$=255, $^2J_{CF}$=35)					119.0(qt, $^1J_{CF}$=291, $^2J_{CF}$=38)
25	213.6 211.8	14.7 14.2 15.2 15.1	130.5,140.7 130.0,140.2 131.9,131.6	148.7(m, $^1J_{CF_a}$=315, $^1J_{CF_b}$=293, $^2J_{CF}$=53)	108.8(t, $^1J_{CF}$=268)	110.6	112.5	113.2		117.6(qt, $^1J_{CF}$=288, $^2J_{CF}$=32)
26	213.5 (p, J=4)	15.2 15.3	130.0 131.4 140.9	155.4(tt, $^1J_{CF}$=304, $^2J_{CF}$=53)	107.3(t, $^1J_{CF}$=279	108.9	110.5	11.7	112.6	117.2(qt, $^1J_{CF}$=289, $^2J_{CF}$=33)
27	216.0 213.3	14.9 14.8 12.8 ı0.3	128.3,141.2 129.8,141.1 130.4,131.2	6.95(q, $^2J_{CF}$=26.4)						134.6(q, $^1J_{CF}$=275)

Table 3.5: ^{13}C NMR Spectral Data

Solvent: $CDCl_3$; reference Me_4Si; shift values are in ppm and coupling constants are in Hz
m=multiplet; qt=quartet of triplets; tt=triplet of triplets; ts=triplet of sextets; q=quartet; d=doublet; t=triplet

Compound	αCF_2	β CF_2	γ CF_2	δ CF_2	ϵ CF_2	ε CF_2	CF_3
cis,cis-$Fe(CO)_2$ (diars)(C_2F_5)I [a] (23)	F_a =-67.9 (m, $^1J_{F_aF_b}$=262.6 $^3J_{F_aF}$=7.5) F_b =-63.5 (m, $^1J_{F_aF_b}$=262.6 $^3J_{F_bF}$=5)	-	-	-	-	-	83.4 (m, $^3J_{FF_b}$=5.0, $^3J_{FF_a}$=7.5)
cis,cis-$Fe(CO)_2$ (diars)(C_3F_7)I [a] (24)	F_a =-63.2 (m, $^1J_{F_aF}$=267.9 $^4J_{F_aF}$=12.5) F_b =-60.0 (m, $^1J_{F_bF}$=268.0 $^4J_{F_bF}$=10.8)	-114.9	-	-	-	-	-79.5
cis,cis-$Fe(CO)_2$ (diars)(C_6F_{13})I [b] (25)	F_a =-64.5 (m, $^1J_{F_aF}$=270.9 $^4J_{F_aF}$=18.0) F_b =-60.9 (m, $^1J_{F_bF}$=270.0 $^4J_{F_bF}$=18)	-110.5	-121.2	-123.2	-126.8	-	-81.5
cis,trans-$Fe(CO)_2$ (diars)(C_7F_{15})I [b] (26)	-61.5 (t, $^4J_{F_bF}$=18.3)	-111.2	-121.3	-122.6	-123.4	-126.8	-83.37
cis,cis-$Fe(CO)_2$ (diars)(CH_2CF_3)I (27)	-	-53.0 ($C_\beta F_3$)					-53.0 ($^3J_{FH}$=16)

Table 3.6: ^{19}F NMR Spectral Data

a : Compared with Pitcher et. al; b : Compared with King et. al
Solvent: $CDCl_3$; Reference compound:$CFCl_3$(0.0 ppm)
Shift values in ppm and coupling constant in Hz

Compound	Solvent	ν_{CO} (cm^{-1})	ν_{R_f} (cm^{-1})
cis,cis-$Fe(CO)_2$(diars)$(C_2F_5)I$ (23)	CH_2Cl_2	1960, 2010	1285,1175,1165,1030,960
cis,cis-$Fe(CO)_2$(diars)$(C_3F_7)I$ (24)	CH_2Cl_2	1962,2010	131υ,1210,1180,1150,1075
cis,cis-$Fe(CO)_2$(diars)$(C_6F_{13})I$ (25)	Toluene	1965, 2010	1350,1230,1200,1140
cis,trans-$Fe(CO)_2$(diars)$(C_7F_{15})I$ (26)	CH_2Cl_2	1980, 2010	1355,1230,1200,1140,1010,970

Table 3.7: IR Spectral Data

Compound	M^+	M^+-2CO	M^+-2CO-R_f
cis,cis-$Fe(CO)_2$(diars)(C_2F_5)I **(23)**	644	588	469
cis,cis-$Fe(CO)_2$(diars)(C_3F_7)I **(24)**	694	638	469
cis,cis-$Fe(CO)_2$(diars)(C_6F_{13})I **(25)**	844	-	469
cis,trans-$Fe(CO)_2$(diars)(C_7F_{15})I **(26)**	894	838	469

Table 3.8: Mass Spectral Data

Chapter 4

Mechanism of Carbonyl Insertion and Oxidative Addition in the Reaction of $Fe(CO)_3(diars)$ with CF_3I

4.1 Introduction

Both the perfluoroalkyl Fe-CF_3 and the perfluoroacyl Fe-C(O)CF_3 compounds are formed on treating $Fe(CO)_3$(diars) with CF_3I gas as shown in Eq. 4.1. The formation of the perfluoroacyl compound is contradictory to experimental observations [40, 104, 106] and theoretical predictions [8, 20, 153]. As discussed in Chapter 2, Fe-C(O)CF_3 is the major product at high concentrations while Fe-CF_3 is the major product at low concentrations when the amount of $Fe(CO)_3$(diars) and CF_3I is kept constant and the volume of CH_2Cl_2(solvent) varied.

$$Fe(CO)_3(diars) + CF_3\,I \longrightarrow \begin{array}{l} Fe(CO)_2(diars)(C(O)CF_3)I \\ +Fe(CO)_2(diars)(CF_3)I + CO \end{array} \qquad (4.1)$$

The perfluoroalkyl is the product of simple oxidative addition while the perfluoroacyl is the result of apparent insertion. The reaction mechanism was investigated by following the concentration vs. time profile of the reaction sequence by ^{19}F NMR under various reaction conditions. Mechanisms are proposed for the apparent carbonyl insertion and the oxidative addition reaction.

4.2 Experimental

4.2.1 General

All experiments were done under a nitrogen atmosphere in an NMR tube and the reaction sequence was followed by ^{19}F NMR using a Bruker-WP80 NMR spectrometer. Fifteen experiments were done to study the course of the carbonyl insertion and oxidative addition reactions. All the experiments were repeated and reproducible trends were seen, although the final product ratio varied slightly.

4.2.2 Concentration vs. Time Experiments

Three sets of concentration vs. time experiments (1 to 12) were done following the procedure as outlined in this section. $Fe(CO)_3$(diars) was weighed into an NMR tube and degassed by three freeze-pump-thaw cycles. 0.5 mL of CD_2Cl_2 (degassed by bubbling nitrogen gas into the solvent) and 1 μL of C_6F_6 (as reference) were added, and the solution cooled to -90 ° to -100 °C. The required amount of CF_3I gas was taken in a syringe at room temperature and one atmospheric pressure and syringed into the NMR tube. The reaction mixture was stirred with a platinum stirrer to make the solution homogeneous. Tipping the NMR tube to make the solution homogeneous was avoided since this warmed up the solution, and irreproducible results were obtained. The solution was then quickly transferred to the NMR probe maintained at -90 °C and the spectrum was recorded as a function of time. For the first set of experiments, [$Fe(CO)_3$(diars)][1] was varied keeping all the other parameters constant. For the second set of experiments, [CF_3I] was varied. The third set held [$Fe(CO)_3$(diars)] and [CF_3I] constant and a free radical inhibitor, (galvinoxyl,Experiments 9 to 11) or CO gas (Experiment 12) was added. The details are presented in Tables 4.1 to 4.3.

[1]Square brackets indicate concencentration.

Experiment No.	$Fe(CO)_3$(diars) (mg)	CF_3I[d] (mL)	Mole ratio of $Fe(CO)_3$(diars):CF_3I	Product Rati. Data[e]		
				$Fe\text{-}CF_3$	CF_3H	$Fe\text{-}C(O)CF_3$ (Interm.)[f]
1	7.5[a]	10	1:25	1.00	0.33	0
2	16.3	10	1:12	1.00	0.56	0.34
3	31.2[b]	10	1:6	1.00	0.16	0.76(0.25)
4	60.0[c]	10	1:3	1.00	1.00	3.17

Table 4.1: Experimental Data at -90°C - Set I

CD_2Cl_2 = 0.5 mL; Reference = C_6F_6 = 1 μL;
a = 0.35 ml of CD_2Cl_2; b = reaction studied for 6500 seconds;
c = concentration determined from peak height data;
d = at 20°C/1 atm.; e = normalized to $Fe\text{-}CF_3$ = 1.00;
f = figures in brackets refer to intermediate shown to be the precursor to $Fe\text{-}C(O)CF_3$

Experiment No.	$Fe(CO)_3$(diars) (mg)	CF_3I[a] (mL)	Mole ratio of $Fe(CO)_3$(diars):CF_3I	Product Ratio Data[b]		
				Fe-CF_3	CF_3H	Fe-C(O)CF_3 (Interm.)[c]
5	17.5	20	1:22	1.00	0.25	0
2	16.3	10	1:12	1.00	0.56	0.34
6	17.4	5	1:6	1.00	1.67	4.00 (1.5)
7	21.1	3	1:3	1.00	0.66	1.93(0.84)
8	20.8	2	1:2	1.00	0.63	2.39(1.38)

Table 4.2: Experimental Data at -90°C - Set II

CD_2Cl_2 = 0.5 mL; Reference = C_6F_6 = 1 μL;
a: at 20 °C/1 atm.; b: normalized to Fe-CF_3 = 1.00;
c: values in brackets refer to intermediate shown to be the precursor to Fe-C(O)CF_3

Experiment No.	$Fe(CO)_3$(diars) (mg)	CF_3I [a] (mL)	Additional Reagents (mole %)	Mole ratio of $Fe(CO)_3$(diars):CF_3I	Product Ratio Data[b]		
					$Fe\text{-}CF_3$	CF_3H	$Fe\text{-}COCF_3$ (Interm.)[c]
9	20.4	3	Galvanoxyl 0.09	1:2.8	1.00	0.50	1.25 (0.75)
10	24.1	3	Galvanoxyl ~ 2	1:2.4	1.00	2.73	9.09 (4.55)
11	20.0	3	Galvanoxyl 14.0	1:2.9	1.00	12.86	6.14 (4.00)
12	17.6	3	CO 1 atm	1:3.2	1.00	0.83	3.23 (1.01)

Table 4.3: Experimental Data - Set III

CD_2Cl_2 = 0.5 mL;Reference = C_6F_6 = 1.0 μL ;
a : at 20°C/1 atm.; b : normalized to $Fe\text{-}CF_3$ = 1.00;
c : values in bracket refer to intermediate shown to be the precursor to $Fe\text{-}C(O)CF_3$

Since the reaction profile indicated the formation of an unstable intermediate, an attempt was made to determine its identity. 20 mg of $Fe(CO)_3$(diars) was dissolved in 0.5 mL of CD_2Cl_2 and treated with 3 mL of CF_3I gas at -90°C (Experiment 13). The reaction was allowed to proceed until the build-up of the intermediate was maximum (5500 seconds as determined in Experiment 7) and then quenched by cooling in liquid nitrogen. 7.0 mg of HBF_4 (less than one equivalent) in diethyl ether was added to the solution via syringe. The tube was then allowed to warm up to -100°C and the reaction mixture stirred with a platinum stirrer to make a homogeneous solution. Subsequently the reaction was monitored by ^{19}F NMR at -90°C for three hours.

Reaction of Perfluoroacyl 16, 17 with $AgBF_4$ and Bu_4NI

According to the principle of microscopic reversibility, creating a vacant site in perfluoroacyl, **17**, should lead to the reverse of the migratory insertion and afford the perfluoromethyl compound. Experiment 14 tested the feasibility of such a reaction, to confirm Fe-CF_3 as the intermediate giving Fe-$C(O)CF_3$. A solution of 20 mg of $Fe(CO)_2$(diars)($C(O)CF_3$)I in 0.5 mL of d_6-acetone was prepared in an NMR tube. A solution of $AgBF_4$ in d_6-acetone was slowly syringed into the tube at room temperature, causing an immediate yellow precipitation of AgI. The addition of $AgBF_4$ was continued until no more precipitation occurred. The ^{19}F NMR spectra were measured before and after one equivalent of Bu_4NI in d_6-acetone was added.

Reaction of Perfluoromethyl (21) with CO

Further information regarding the intermediacy of Fe-CF_3 in the formation of Fe-$C(O)CF_3$ was obtained by treating $Fe(CO)_2$(diars)(CF_3)I with carbon monoxide

(Experiment 15). 20 mg of $Fe(CO)_2(diars)(CF_3)I$ (**21**) was dissolved in 0.5 mL of CD_2Cl_2 and CO gas was syringed into the tube at atmospheric pressure and 25 °C. The reaction was monitored by ^{19}F NMR at 20 °C.

4.3 Results

Concentration vs. time profiles were determined for 3 to 4 hours and 30 ^{19}F NMR spectra taken at time-intervals as shown in Tables 4.4 to 4.16. The integral of each peak (shown in Tables 4.4 to 4.16) was plotted against time. The plots of concentration vs. time are shown in Figs. 4.11 to 4.23.

A typical ^{19}F spectrum observed in the kinetic experiments for the reaction shown in Eq. 4.1 at -90 °C is shown in Fig. 4.1. The resonance at 13.1 ppm (at -90 °C) is assigned to $Fe(CO)_2(diars)(CF_3)I$ and that at -76.1 ppm is assigned to $Fe(CO)_2(diars)(C(O)CF_3)I$. Two perfluoroacyl isomers are formed under conditions favouring kinetic control. Two peaks are resolved at -80 °C (-76.9 and -77.1 ppm) and only a single peak is observed at -90 °C. At room temperature the two peaks appear at -79.5 and -78.7 ppm and their product ratio remains the same. A large temperature gradient is also seen for the other peaks which is shown in Appendix B. By comparing with the shifts of the isolated perfluoroacyl and perfluoroalkyl products, the peak at -78.7 ppm is assigned to cis,cis-$Fe(CO)_2(diars)(C(O)CF_3)I$ **17** and that at -79.5 ppm to the corresponding cis,trans isomer **16**. Two closely spaced peaks were observed with chemical shifts similar to the perfluoroacyl. These were identified as due to CHF_3 as follows. Experiments at varying field strengths (1.9T and 7T) confirmed them to be a doublet with a constant coupling constant of 78 Hz. Broad band proton decoupling collapses the doublet into a singlet (cf. Fig. 4.2), confirming that the doublet is due to coupling between H^1 and ^{19}F nuclei. The proton spectrum of the reaction mixture shows a quartet at 6.6 ppm

($^2J_{HF}$=79Hz) (cf. Fig. 4.3). On adding D_2O to the reaction mixture, a triplet assigned to CF_3D is seen instead of the usual doublet of CF_3H (cf. Fig. 4.4).

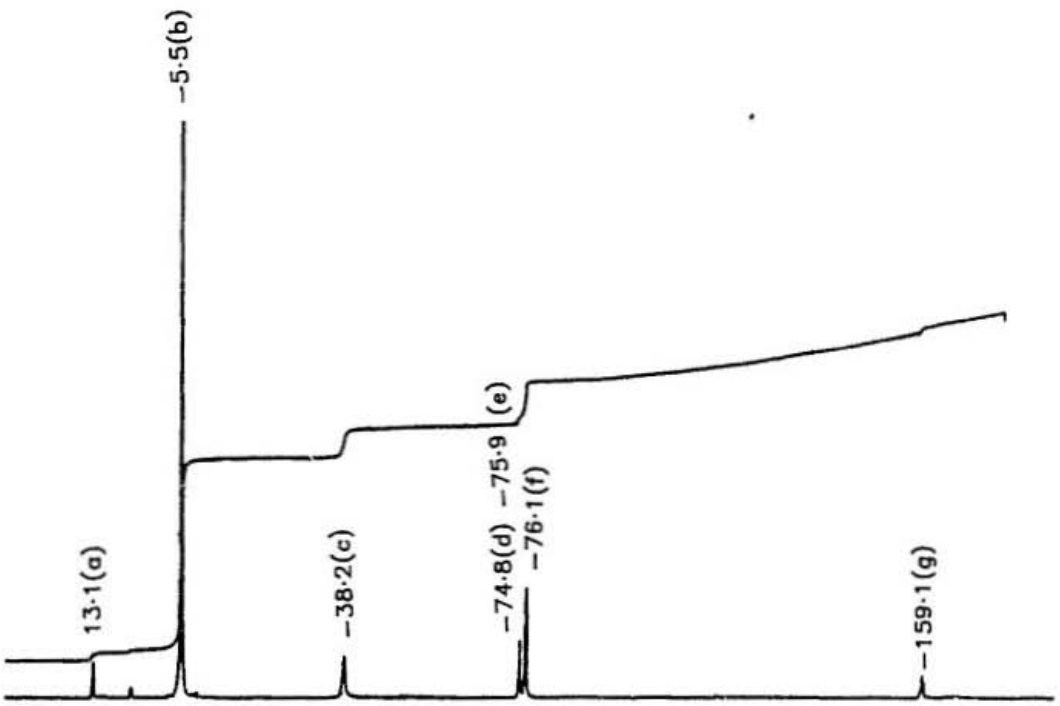

Figure 4.1: Typical 75 MHz ^{19}F NMR Spectrum for the Concentration vs. Time Experiments of Eq. 4.1 in CD_2Cl_2
Temperature = -90 °C; a = Fe-CF_3; b = CF_3I; c = Intermediate; d, e = CF_3H; f = Fe-C(O)CF_3; g = C_6F_6; chemical shifts are in ppm

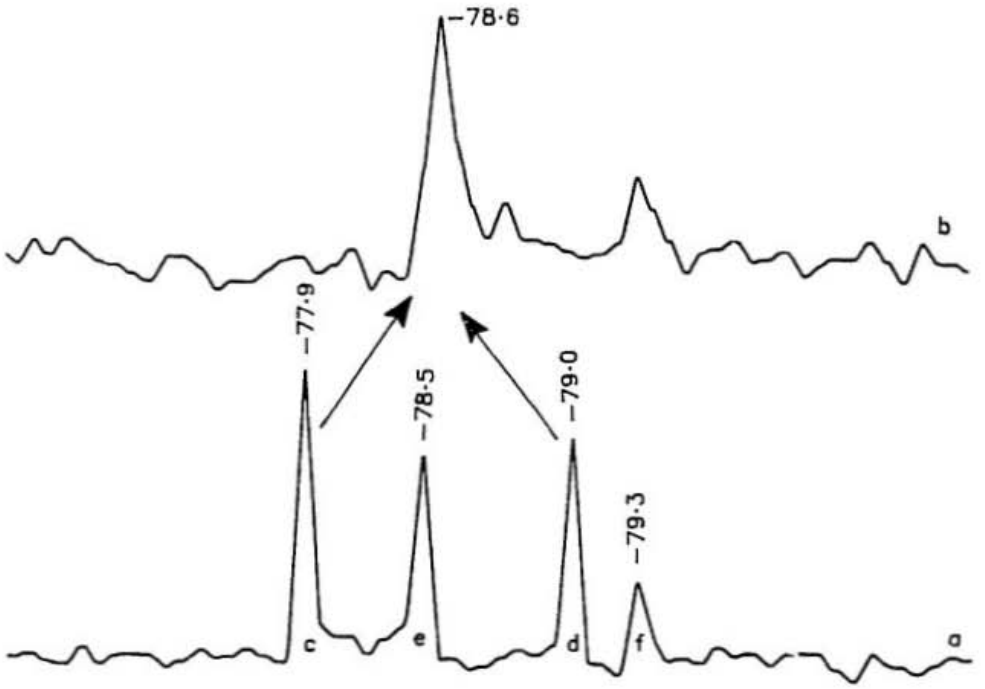

Figure 4.2: Partial 75 MHz ^{19}F NMR Spectrum of CF_3H Resonance in CD_2Cl_2 Temperature = 20 °C; a = decoupler off; b = 0.5 watts decoupler on; c, d = CF_3H; ($^2J_{FH}$ = 78 Hz); e, f = 2 Isomers of Fe-C(O)CF_3; chemical shifts are in ppm

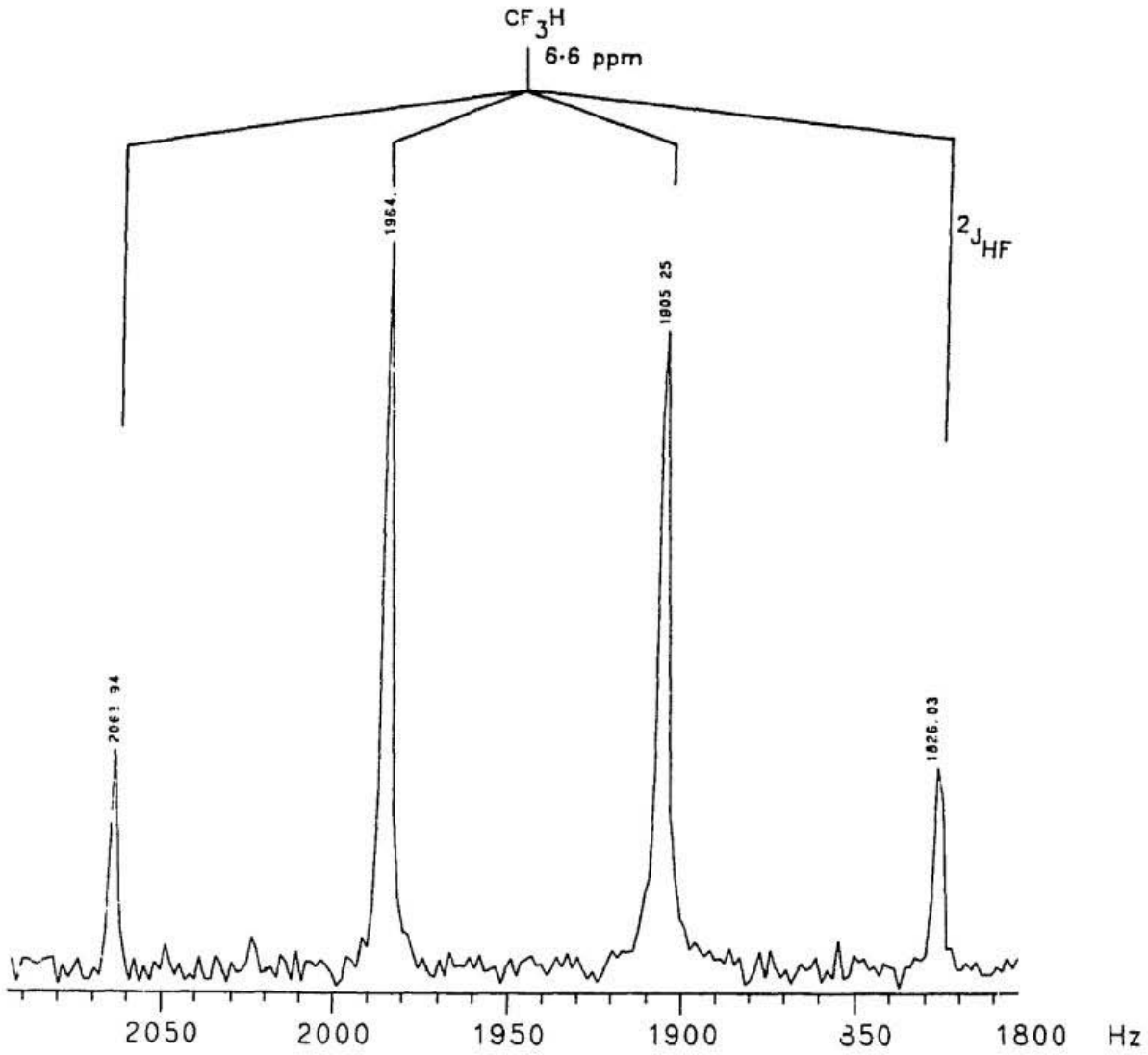

Figure 4.3: 300 MHz ^{1}H NMR Spectrum of $Fe(CO)_3$(diars) and CF_3I Solution Showing CF_3H Quartet in CD_2Cl_2

Temperature = 20°C

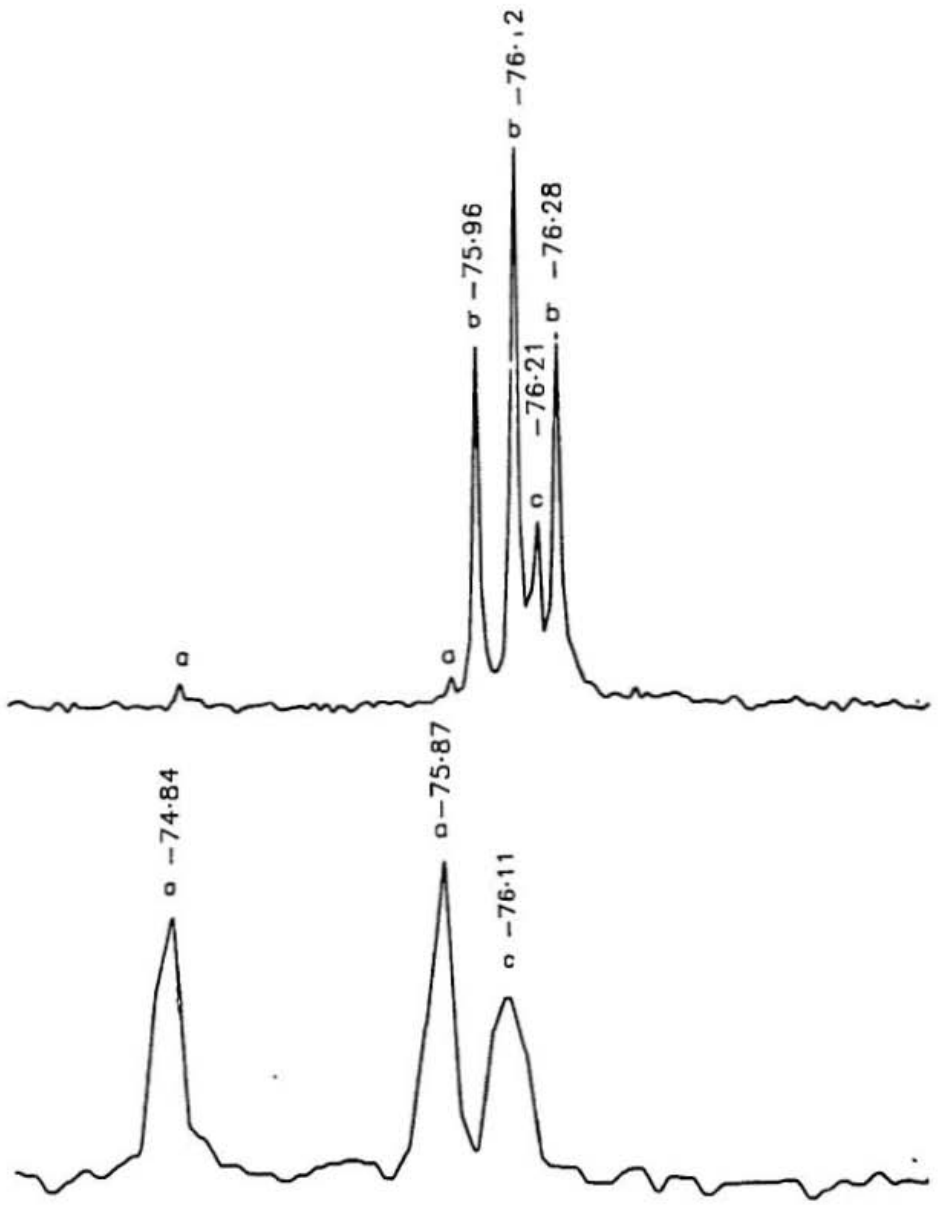

Figure 4.4: 75 MHz ^{19}F NMR Spectrum of CF_3D and CF_3H in CD_2Cl_2
Temperature = -90 °C; a = CF_3H ($^2J_{FH}$ = 78 Hz); b = CF_3D ($^2J_{DF}$ = 12 Hz);
c = Isomeric mixture of Fe-[illegible](O)CF_3 (see text); chemical shifts are in ppm

The ^{19}F NMR spectrum of CF_3D shows an upfield shift of 0.8 ppm which may be due to an isotope effect. $^2J_{DF}$=12.4 Hz, which is in agreement with the calculated value of 12.7Hz.

$$J_{HF}.\frac{\gamma_D}{\gamma_F} = \frac{78 \times 0.857}{5.255} = 12.7$$

Thus the doublet beside the perfluoroacyl peaks is confirmed to be that of fluoroform. The literature value of $^1J_{HF}$ is 79.7 Hz and the ^{19}F chemical shift is 78.6 $\pm$0.7 ppm [77]. The peak at 38.2 ppm is assigned to an intermediate species, which decays to Fe-C(O)CF_3.

Concentration vs. time curves of the first set of experiments, where the amount of $Fe(CO)_3$(diars) was varied (Experiments 1 to 4 in Figs. 4.11 to 4.14, product ratios in Table 4.1), show that perfluoroacyl formation is favoured by increasing concentration of $Fe(CO)_3$(diars). Thus in experiment 4, Fe-C(O)CF_3 is formed as the major product. Fe-CF_3 is favoured with decreasing concentration of $Fe(CO)_3$(diars), and thus in experiment 1 Fe-CF_3 is formed as the major product. This trend is similar to the preparative results in Chapter 2, where the molar reactant ratio of $Fe(CO)_3$(diars) and CF_3I was kept constant and the concentration of the solution was varied by changing the volume of the solvent.

Concentration vs. time profiles of the second set of experiments, where the volume of CF_3I was varied (Experiments 5 to 8 in Figs. 4.15 to 4.18, product ratios in Table 4.2), show a different trend. Perfluoroacyl is favoured as the concentration of CF_3I decreases. Thus, in experiment 8, Fe-C(O)CF_3 is formed as the major product while, in experiment 5, Fe-CF_3 is formed as the major product.

Concentration vs. time profiles for the third set of experiments where the effect of external reagents was examined are shown in Figs. 4.19 to 4.22. Three different concentrations of galvinoxyl, a free radical inhibitor, were tested on the solution. Experiment 9 used 0.01 mole per cent of galvinoxyl but had no effect on the rates

rates of Fe-CF_3 and Fe-$C(O)CF_3$ reactions. Experiment 10 tested 5 mole per cent galvinoxyl and resulted in a marked decrease in the rate of formation of Fe-CF_3 with no effect on the rate of formation of the intermediate, CF_3H or Fe-$C(O)CF_3$ (cf. Figs. 4.5 and 4.6). This experiment also indicates that CF_3H is related to the intermediate and Fe-$C(O)CF_3$, since the intermediate and the Fe-$C(O)CF_3$ peaks rise only after the CF_3H peaks cease to grow.

25 mole per cent galvinoxyl (Experiment 11) showed the same retarding effect on the rate of Fe-CF_3 formation. However, the CF_3H peaks dominate and the Fe-$C(O)CF_3$ is suppressed presumably because galvinoxyl (**28**) serves as a proton donor, trapping CF_3^- as CF_3H.

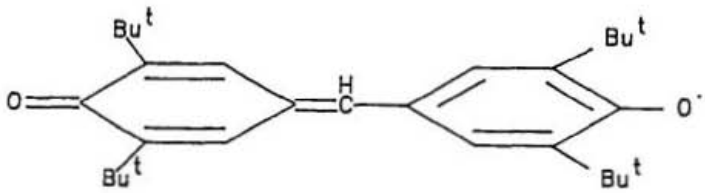

28

The intermediate is formed late in the reaction leading to Fe-$C(O)CF_3$. Consistent with the proposal that CF_3^- is present, introduction of HBF_4 to the solution at the peak concentration of the intermediate, diverts the reaction to the formation of CF_3H instead of the usual Fe-$C(O)CF_3$ (cf. Fig. 4.7). A concentration vs. time profile is shown in Fig. 4.23. Time zero is taken as the spectrum indicating the maximum peak concentration of the intermediate when the Fe-$C(O)CF_3$ peak just begins to rise. Subsequent spectra taken after one hour correspond to the

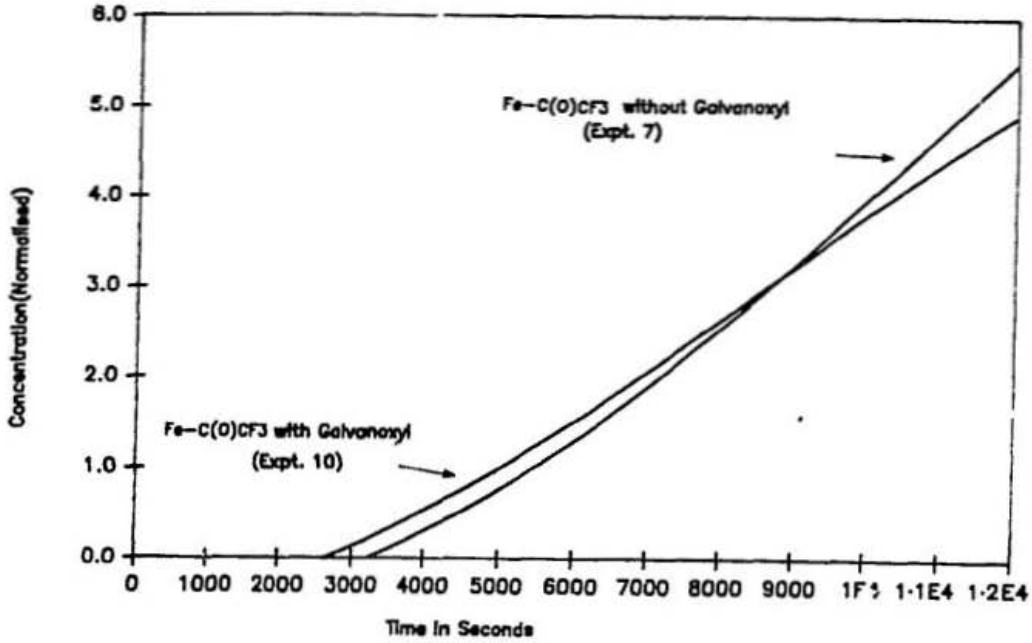

Figure 4.5: Effect of Galvanoxyl on Perfluoroacyl

Temp: −90°C
Solvent :CD2Cl2

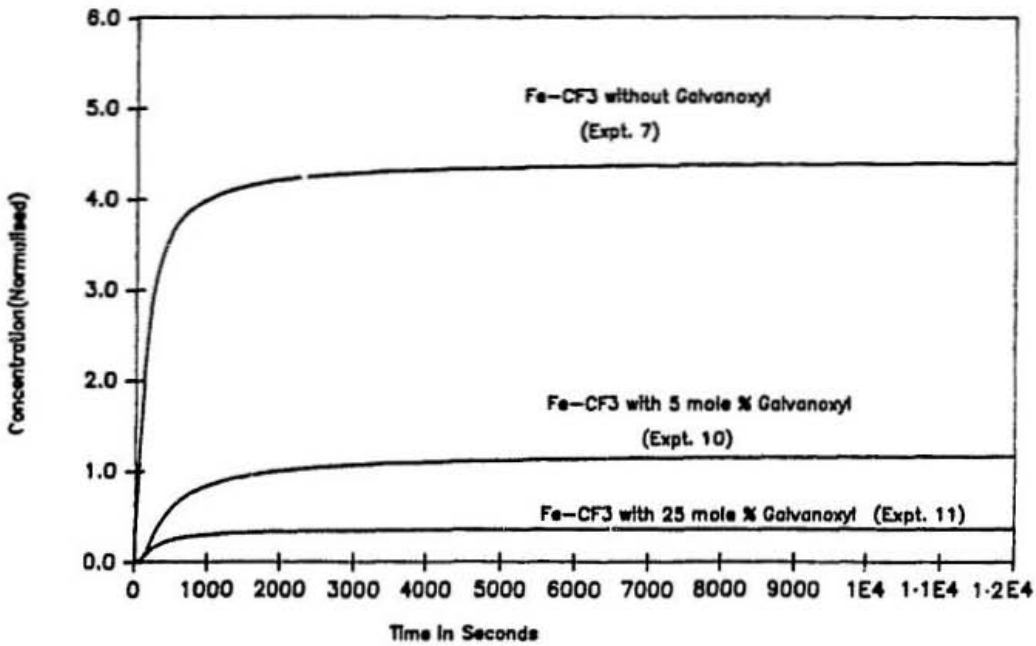

Figure 4.6: Effect of Galvanoxyl on Perfluoroalkyl

Temp: −90°C
Solvent :CD2Cl2

reaction after addition of HBF_4. The reaction was followed for a further two hours and the Fe-$C(O)CF_3$ signal showed no significant growth, while the CF_3H peak continued to grow and the Fe-CF_3 peak remained constant. Thus HBF_4 effectively traps the intermediate and prevents perfluoroacyl formation. The intermediate therefore appears to serve as the source of CF_3^- ions suggesting that the structure of the intermediate could be $[Fe(CO)_3(diars)I]^+CF_3^-$. Experiment 12 tested the effect of CO on Eq. 4.1. The addition of 1 atmosphere of CO gas had no observable effect on the rates of formation of Fe-$C(O)CF_3$ or Fe-CF_3.

Halide abstraction of the perfluoroacyl compound with $AgBF_4$ followed by treatment with iodide did not lead to the formation of the perfluoroalkyl compound (Experiment 14). The ^{19}F NMR peaks at -79.5 and -78.7 ppm due to Fe-$C(O)CF_3$, disappear on adding $AgBF_4$, but a new signal tentatively assigned to a perfluoroacyl compound, appears at -78.6 ppm. The IR spectrum of this new compound shows strong C-F

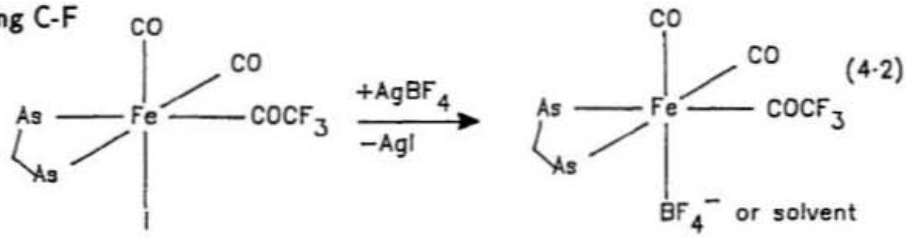

[17] [28]

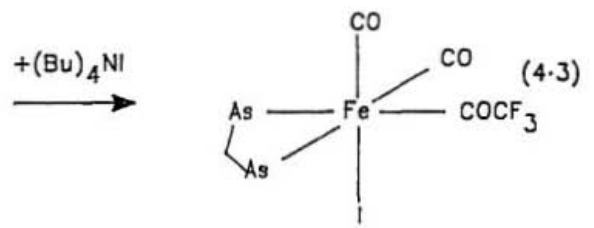

[17]

stretches at 1230, 1180 and 1120 cm^{-1}, and an acyl stretch at 1620 cm^{-1} confirming that the $C(O)CF_3$ group is still intact. Adding I^- restores the original Fe-$C(O)CF_3$ peaks (cf. Eq. 4.2 and 4.3). **28** may have the vacant site filled

either by BF_4^- [17, 30, 80, 92, 158, 159, 160, 164] or the solvent CH_2Cl_2 [70]. The ^{19}F NMR spectra are shown in Fig. 4.7. Therefore the extrusion reaction Fe-C(O)CF_3 to Fe-CF_3 does not take place suggesting, by the principle of microscopic reversibility, that the insertion reaction, Fe-CF_3 to Fe-(CO)CF_3 does not occur and that Fe-CF_3 is not an intermediate leading to Fe-C(O)CF_3.

The perfluoroalkyl compound **21** does not react with CO under the conditions of Eq. 4.1 (Experiment 15). These results are in agreement with Experiment 14 and confirm that Fe-CF_3 does not carbonylate to Fe-C(O)CF_3 and cannot be an intermediate.

4.4 Discussion

The concentration vs. time curves obtained by F^{19} NMR for Eq. 4.1 show several characteristic features as shown in the stacked plot in Fig. 4.8.

1. The Fe-CF_3 and CF_3H peaks rapidly attain a constant limiting concentration.

2. The CF_3H peaks are related to both Fe-CF_3 and the observed intermediate. Build up of the intermediate occurs only after [Fe-CF_3] and [CF_3H] attain their limiting values.

3. The intermediate and Fe-C(O)CF_3 peaks are related. Perfluoroacyl formation was always preceded by the rise and fall of an intermediate peak.

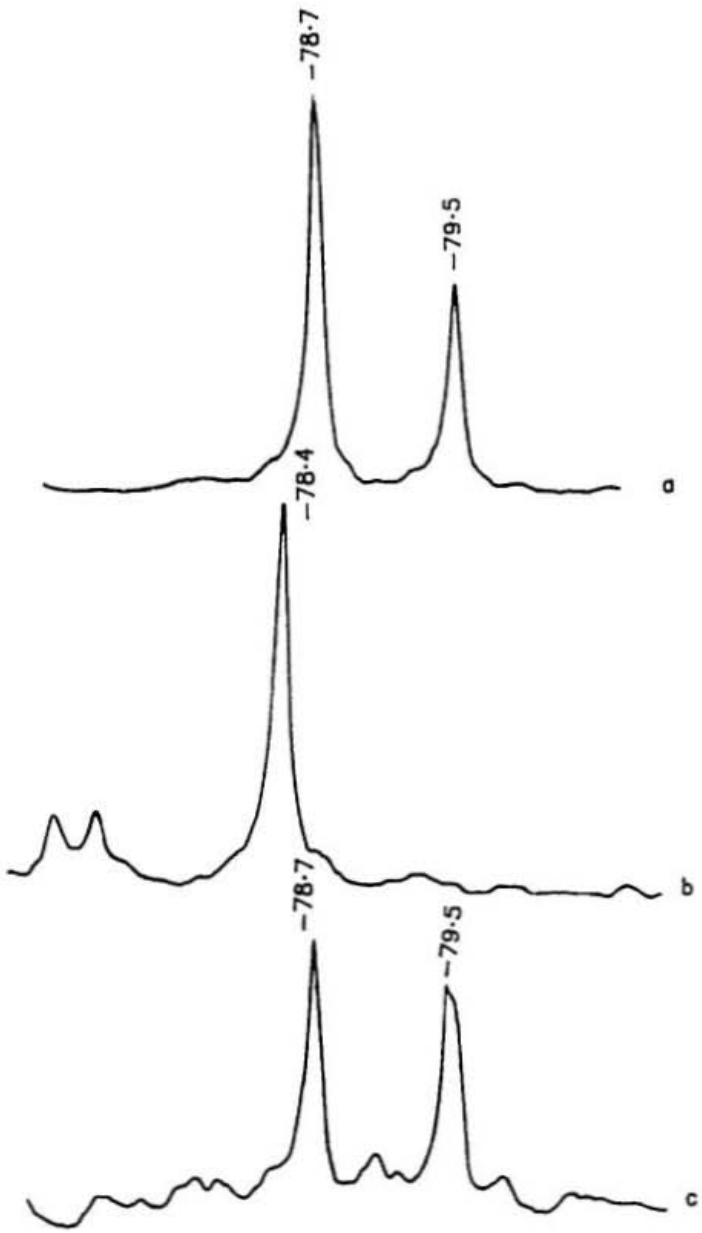

Figure 4.7: 75 MHz ^{19}F NMR Spectra of the Reaction of $Fe(CO)_2(diars)(C(O)CF_3)I$ with $AgBF_4$ and Bu_4NI in CD_2Cl_2
Temperature = 20 °C; a = 2 Isomers of Fe $C(O)CF_3$;
b = after adding $AgBF_4$; c = after adding Bu_4NI; chemical shifts are in ppm

The formation of both Fe-C(O)CF_3 and Fe-CF_3 compounds raises the question of whether Fe-CF_3 is an intermediate leading to Fe-C(O)CF_3. In all the concentration vs. time plots, [Fe-CF_3] reaches a plateau, indicating that it is either not consumed in a subsequent step or that it is in a fast equilibrium as shown in Eq. 4.4. Experiment 14 which tested the feasibility of the reverse of migratory insertion and experiment 15 which attempted to induce insertion in Fe-CF_3 bond indicate that Fe-CF_3 is not an intermediate leading to Fe-C(O)CF_3. The equilibrium in Eq. 4.4 is unlikely since the perfluoroalkyl concentration is unaffected by the addition of CO (experiment 12).

$$Fe(CO)_3(diars) + CF_3I \rightleftharpoons Fe(CO)_2(diars)(CF_3)I + CO \qquad (4.4)$$

These results are consistent with the formation of Fe-C(O)CF_3 and Fe-CF_3 in two parallel reactions where the perfluoroalkyl is formed very rapidly compared to the perfluoroacyl (cf. Eq. 4.5).

$$Fe(CO)_3(diars) + CF_3I \rightarrow Fe(CO)_2(diars)(C(O)CF_3)I \qquad (4.5a)$$

$$Fe(CO)_3(diars) + CF_3I \rightarrow Fe(CO)_2(diars)(CF_3)I \qquad (4.5b)$$

4.5b >> 4.5a

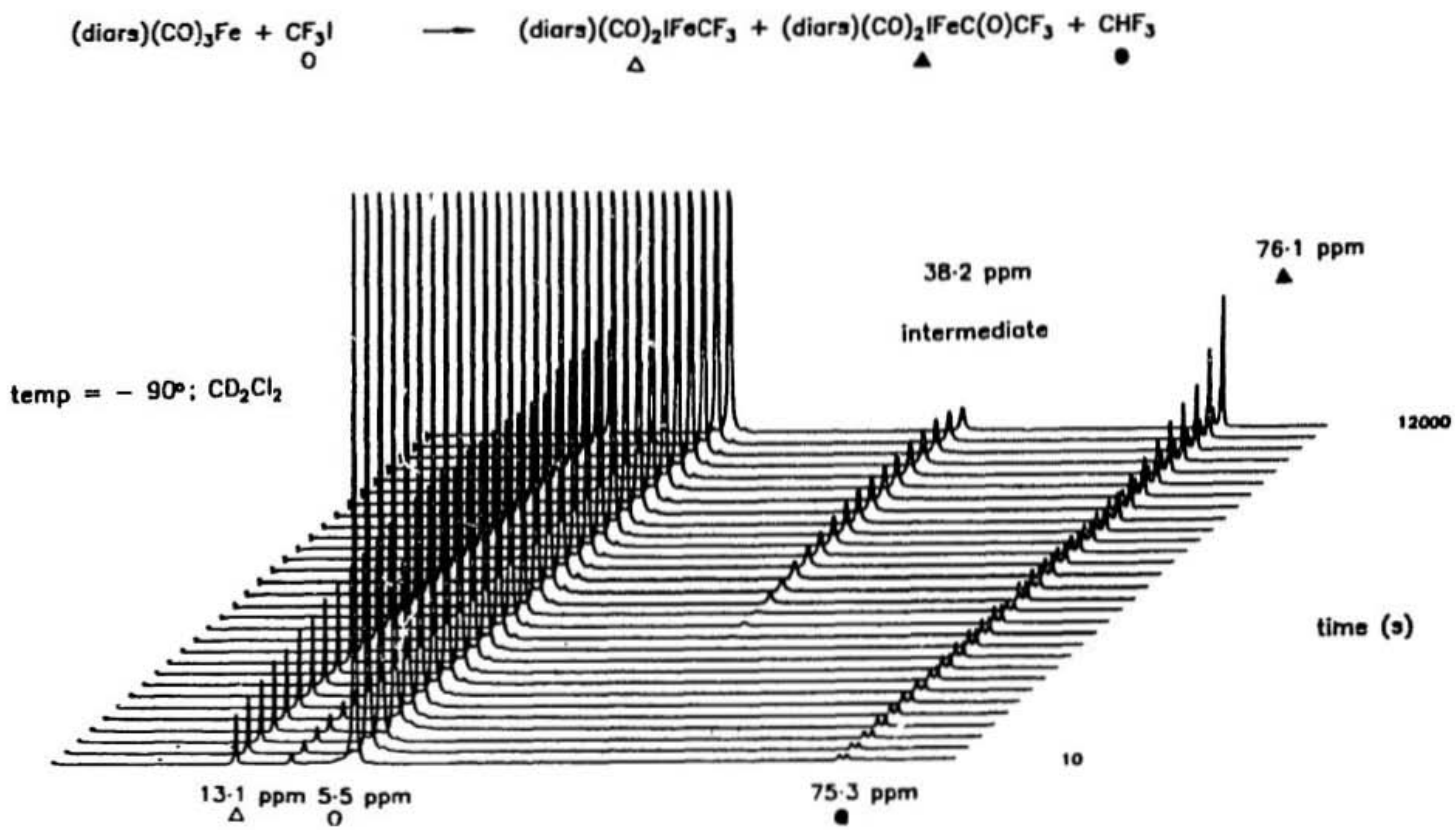

Figure 4.8: Stacked Plot of ^{19}F NMR Spectra of Concentration vs. Time Curves (Experiment 7)

Several trends became apparent on considering the molar ratio of CF_3I to $Fe(CO)_3$(diars) for each of the above kinetic runs. When the ratio is 25:1 or more, the rate of Eq. 4.5b dominates and Fe-CF_3 is the major product. When the ratio is 5:1 or less, the rate of Eq. 4.5a dominates and Fe-$C(O)CF_3$ is the major product. Intermediate ratios form both Fe-$C(O)CF_3$ and Fe-CF_3. Reliable quantitative data could not be obtained and only qualitative estimates could be made. Thus a high concentration of CF_3I with respect to $Fe(CO)_3$(diars) favours Fe-CF_3 while a lower concentration favours Fe-$C(O)CF_3$.

The reaction mechanism leading to Fe-$C(O)CF_3$ appears to be non-radical. Experiments 9 to 11 show that galvinoxyl does not retard the formation of Fe-$C(O)CF_3$, the intermediate or the CF_3H. The galvinoxyl experiments also show that CF_3^- does not originate from free radical reactions, which is in agreement with the conclusions of Experiment 13 where the intermediate has been shown to be the source of the CF_3^- ions. Thus the picture which emerges is as shown in Eq. 4.6.

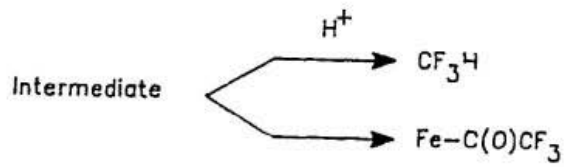

(4.6)

The reaction mechanism leading to Fe-CF_3 is free radical in nature. This conclusion is arrived at from the following four experimental observations. Firstly, tipping of the NMR tube for homogenizing the solution did not yield consistent results while stirring with a platinum stirrer did. A 1:3 molar ratio of reactants generally formed Fe-$C(O)CF_3$ as a major product; tipping of the tube formed Fe-CF_3 as the major product consistently. Tipping of the NMR tube causes warming of the solution and it is possible that this initiates free radical reactions. Secondly, Fe-CF_3 is

favoured by increased concentration of CF_3I (cf. Table 4.2) which is known to participate in many free radical reactions [102, 156]. Thirdly, in all the kinetic experiments, formation of Fe-C(O)CF_3 continues even after Fe-CF_3 peak rises rapidly to a plateau. Thus one or more of the reactants leading to Fe-CF_3 are depleted, but the continued formation of Fe-C(O)CF_3 demands the presence of $Fe(CO)_3$(diars) and CF_3I. Hence we can only conclude that the formation of Fe-CF_3 ceases when adventitious radicals are depleted from the solution. This is confirmed by the observation in experiments 10 and 11 where galvinoxyl inhibits the rate of formation of Fe-CF_3.

We conclude that $Fe(CO)_3$(diars) reacts with CF_3I at -90°C through two parallel routes: a radical reaction forming Fe-CF_3 and a non-radical reaction forming Fe-C(O)CF_3. This is in agreement with the recent observation that mono and di substituted derivatives of iron pentacarbonyl react with alkyl halides and poly halides through both radical and molecular paths [18]. Also, studies on the oxidative addition of alkyl halides to Ir(I) complex indicate the existence of two different mechanistic patterns, a radical path and a non-radical path. Reactions of saturated alkyl halides (except methyl), and vinyl and aryl halides, alpha halo esters show characteristics consistent with radical chain pathway while those of methyl, benzyl and allyl halides, and alpha halo ethers follow a non-radical path [115]. A similar mechanistic duality has been observed for Pt(0) complexes [111]. The reaction of $Fe(CO)_3$(diars) with CF_3I is interesting since both the mechanisms are seen to operate in the same system, with the same perfluoroalkyl halide.

4.4.1 Mechanism of CO "Insertion" in Fe-CF_3 bond

$Fe(CO)_3(L_2)$ reacts with CH_3I to give the carbonyl inserted product $Fe(CO)_2$(diars)$(C(O)CH_3)I$ via an ionic intermediate [18, 95] (cf. Eqs. 4.7 and 4.8).

$$Fe(CO)_3(L_2) + CH_3I \longrightarrow [Fe(CO)_3(L_2)CH_3]^+I^- \qquad (4.7)$$

$$[Fe(CO)_3(L_2)CH_3]^+I^- \longrightarrow [Fe(CO)_3(L_2)(C(O)CH_3)I] \qquad (4.8)$$

L_2 = diars, 2 PMe_3

However, the polarity of CF_3I is reversed compared with CH_3I due to the three strong electronegative fluorine atoms [13]. Assuming the reaction is charge controlled the analogous reaction of CF_3I with $Fe(CO)_3$(diars) would be as suggested in Eq. 4.11.

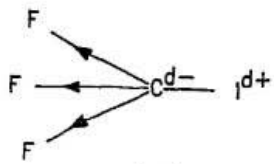

[29]

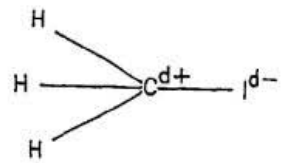

[30]

Ionic intermediates as shown in Eqs. 4.7 and 4.8 are also formed when $Fe(CO)_3L_2$ compounds are treated with halogens [35, 140] (cf. Eq. 4.9).

$$Fe(CO)_3L_2 + X_2 \longrightarrow [Fe(CO)_3L_2X]^+X^- \qquad (4.9)$$

CF_3I is reported to behave like a pseudo-halogen[2] [67, 87, 110, 116, 122] and hence a similar ionic intermediate is not unlikely in the reaction of $Fe(CO)_3$(diars) with CF_3I.

[2] CF_3I mimicks I_2 in its reaction with the neutral metal carbonyl $Fe(CO)_5$. I_2 reacts with $Fe(CO)_5$ forming $Fe(CO)_3I_2$. Similarly, CF_3I reacts with $Fe(CO)_5$ forming $Fe(CO)_3(CF_3)I$. However, CF_3I does not show all the characteristics of a pseudohalogen. Though it forms the acid CF_3H, CF_3^- ion is highly reactive and cannot remain as a free ion in solution. The dimer, C_2F_6, is a gas at room temperature and unreactive under ordinary conditions.

The mechanism of oxidative addition of alkyl halides to metal carbonyls is usually associated with a nucleophilic attack of an electron-rich transition metal on the alkyl group. However, in the reaction of $Mn(CO)_5^-$ with 2-bromo-substituted acyl halides, a direct attack of the metal center on Br is reported [127]. The feasibility of such a halogen abstraction reaction has been explored theoretically by Hartree-Fock-Slater calculations and is found to be energetically favourable with a reaction enthalpy of -118 $kJMol^{-1}$ with no activation barrier (cf. Eq. 4.10).

(4.10)

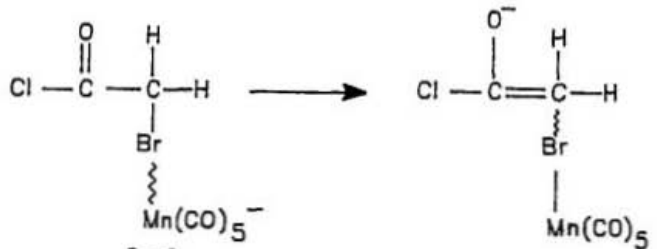

[33] [34]

Therefore, the first step in the reaction of $Fe(CO)_3$(diars) with CF_3I may occur via nucleophilic attack of Fe on the iodine atom as in Eq. 4.11. The resulting product, presumably formed as a tight ion pair, is consistent with the results of Experiment 13 which suggests that the intermediate is a source of CF_3^- ions.

(4.11)

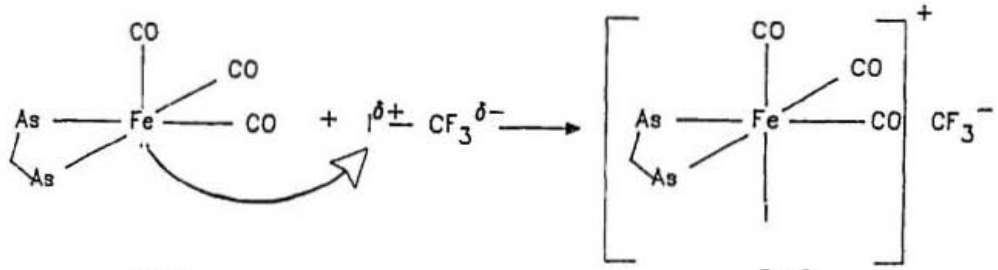

[31] [32]

CF_3^- is reported to have a high affinity for protons [14, 19, 88, 132]. The intermediate is therefore rapidly quenched by available proton sources forming CF_3H. As the concentration of proton donors is depleted, the CF_3H concentration reaches a plateau and the concentration of the intermediate rises.

The intermediate affords the cis,cis **17** and the cis,trans **16** isomers of Fe-$C(O)CF_3$ in the kinetically determined ratio of 2:1 respectively (cf. Fig. 4.9). Assumption of intermolecular nucleophilic addition accounts for the observed ratio of the two perfluoroacyl isomers (cf. Fig. 4.10).

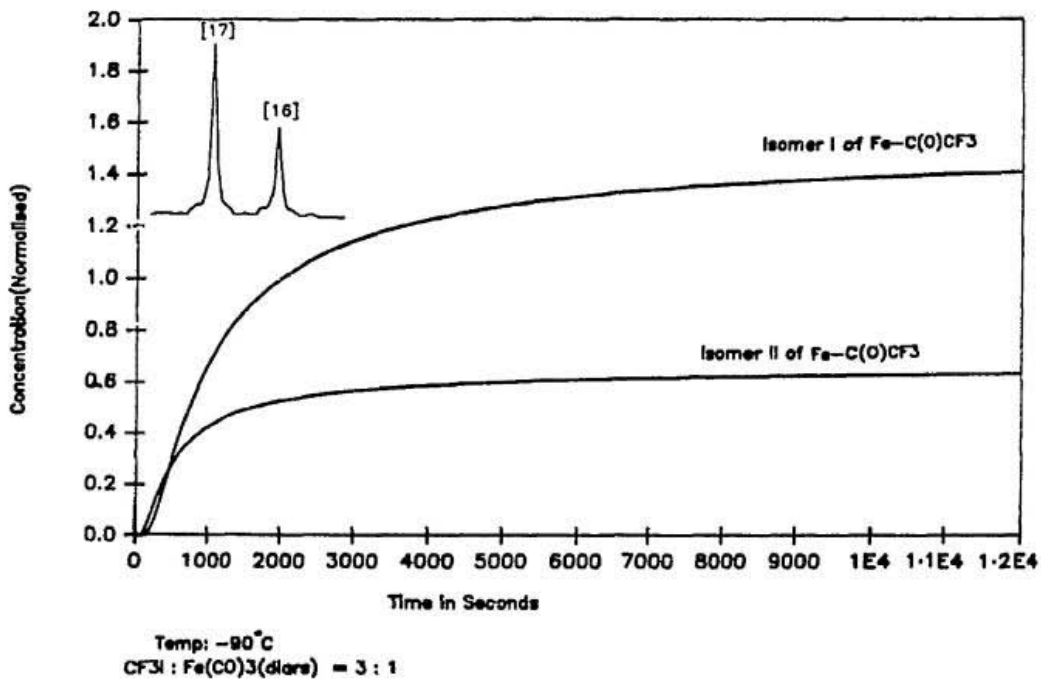

Figure 4.9: The Two Isomers of Fe-$C(O)CF_3$

The CF_3^- ion could attack any one of the three coordinated electron-poor carbonyl groups instead of the iron centre of **32**, thus forming the perfluoroacyl group. The statistical distribution of the cis,cis and cis,trans isomers would then be in the ratio of 2:1 respectively. Only one of the two possible cis,cis isomers can form via this mechanism, **17** and not **18**. Accordingly, in the preparative results (Chapter 2), it was seen that **17** is formed as the major product with **18** only as a minor product. The geometry of **17** was confirmed by crystallography thus providing strong support for the mechanism of Fig. 4.10. There is extensive precedence for nucleophilic attack on coordinated carbonyl groups [32, 65, 101, 103]. I^- in nitromethane or acetone solvents, attacks the coordinated carbonyl of $[Fe(CO)_3(dienyl)]^+$, (dienyl = C_6H_7, C_7H_9) forming the acyl iodide complex (cf. Eq. 4.12) [101].

$$[Fe(CO)_3(dienyl)]^+ + I^- \longrightarrow [Fe(CO)_2(dienyl)(C(O)I)] \qquad (4.12)$$

Semi-empirical molecular orbital calculations on Group VI octahedral, hexacarbonyl complexes favour nucleophilic attack of halide ion (X^-) on a coordinated CO ligand forming the acyl halide complex [60] (cf. Eq. 4.13).

$$Cr(CO)_6 + X^- \longrightarrow Cr(CO)_5C(O)X^- \qquad (4.13)$$

Alkoxy carbonyl complexes are prepared by nucleophilic addition of alkoxide to a co-ordinated CO ligand (cf. Eq. 4.14). Several cationic complexes of Fe, Ru, Os, Mn, Re, Co, Ir and Rh are known to react in this manner. Other complexes which are formed in a similar manner include the carbamoyl and carbazoyl complexes [2].

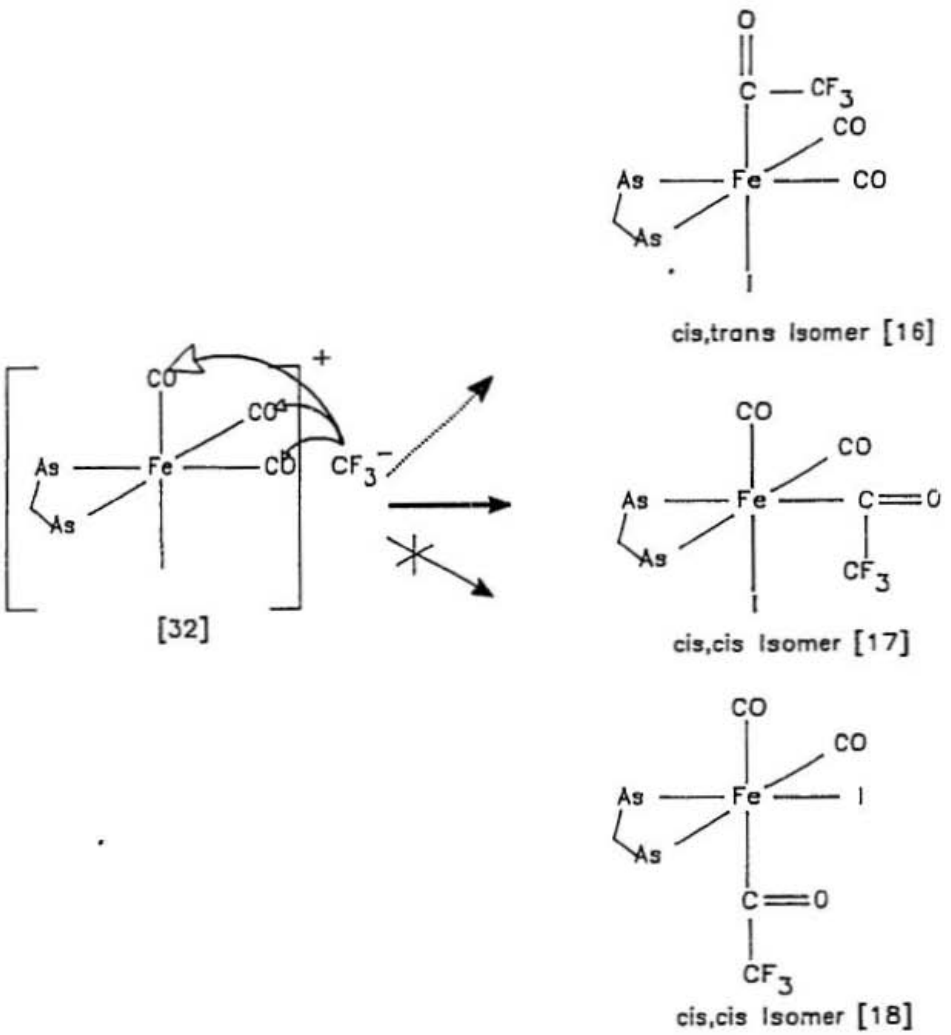

cis, trans Isomer [16] : cis, cis Isomer [17] = 1 : 2

Figure 4.10: The Intermolecular Nucleophilic Addition in $[Fe\text{-}(CO)_3(diars)I]^+[CF_3]^-$

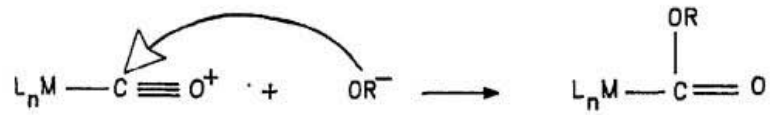

(4.14)

A positive charge on the metal complex, a co-ordinative unsaturation and a reactive nucleophile appear to be key factors in these reactions [52, 61]. All these factors appear to be satisfied in the proposed intermediate, **32**, which leads to the Fe-C(O)CF_3 compound. Thus, the mechanism of carbonyl insertion in M-CF_3 can be summarized as follows:

(4.15)

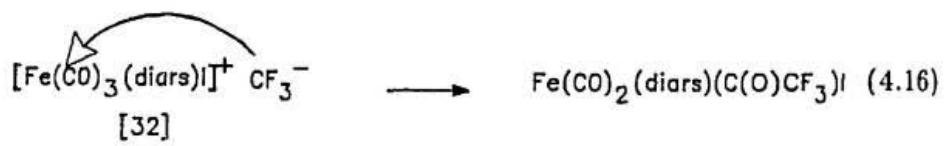

(4.16)

4.4.2 Mechanism of Oxidative Addition of CF_3I to $Fe(CO)_3$(diars)

Evidence from the concentration vs. time experiments suggests that Fe-CF_3 is formed by a nonchain, free radical reaction. Fe-CF_3 formation ceases even though both CF_3I and $Fe(CO)_3$(diars) are present. This observation is in accord with a non-chain, radical mechanism. Nonchain free radical oxidative addition is reported for the reaction of certain alkyl halides RX to $Pt(PPh_3)_3$ (R = methyl, ethyl, X=I; R = $PhCH_2$, X=Br) [112, 118, 119, 120] The reaction of $Fe(CO)_3(AsPh_3)_2$ with

CCl_4 was found to give $Fe(CO)_2(AsPh_3)_2Cl_2$ via a free radical mechanism [18]. Similar mechanisms have been proposed for the reaction of $Fe(CO)_3L_2$ (L= PPh_3, $AsPh_3$, $P(CH_3)Ph_2$, $P(N(CH_3)_2)_3$, $P(OPh)_3$, or $L_2 = Ph_2PCH_2CH_2PPh_2$ (dppe) or $Ph_2PCH_2PPh_2$ (dppm)) with I_2. Baker et al. suggest that 17 electron and 19 electron species are involved which are known to function as reactive intermediates in many reactions [4, 10, 11, 163] including catalytic cycles [9, 69, 150, 161]. CF_3I behaves like a pseudohalogen and the system studied above is similar to the system of this study. Hence a similar mechanism is possible. A more detailed mechanism could not be arrived at for this particular system, however, a suggestion consistent with the qualitative results obtained is presented in Eqs. 4.17 to 4.24.

The industrial preparation of perfluoroalkyl iodides is reported to involve free radicals [13]. Pyrolysis of an anhydrous mixture of silver trifluroacetate and excess iodine produces CF_3I via formation of acyl hypohalides (cf. Eqs. 4.25 and 4.26). Hence, adventitious free radicals in CF_3I are likely to be present and would serve to initiate the free radical reaction. Another potential source of free radicals is adventitious oxygen which could initiate the free radical reaction to form $CF_3^{\cdot}$ and $I^{\cdot}$. The solvent, however, cannot be the source of free radicals since the radical reaction occurs even in the absence of the solvent (cf. Table 2.2). The proposed mechanism explains the abrupt levelling of Fe-CF_3 concentration. As the $I^{\cdot}$ and $CF_3^{\cdot}$ concentrations are depleted from the solution, the path to Fe-CF_3 ...ids. Formation of the di-iodo side product is consistent with a radical mechanism and is explained by Eqs. 4.20 to 4.22.

FORMATION OF THE PERFLUOROALKYL PRODUCT

$$Fe(CO)_3L_2 + CF_3^{\cdot} \longrightarrow [Fe(CO)_3L_2(CF_3)]^{\cdot} \quad (4.17)$$

$$[Fe(CO)_3L_2(CF_3)]^{\cdot} + I^{\cdot} \longrightarrow [Fe(CO)_3L_2(CF_3)]^{+} + I^{-} \quad (4.18)$$

$$[Fe(CO)_3L_2(CF_3)]^{+} + I^{-} \longrightarrow Fe(CO)_2L_2(CF_3)I + CO \quad (4.19)$$

FORMATION OF THE DI-IODIDE PRODUCT

$$Fe(CO)_3L_2 + I^{\cdot} \longrightarrow [Fe(CO)_3L_2I]^{\cdot} \quad (4.20)$$

$$[Fe(CO)_3L_2I]^{\cdot} + I^{\cdot} \longrightarrow [Fe(CO)_3L_2I]^{+} + I^{-} \quad (4.21)$$

$$[Fe(CO)_3L_2I]^{+} + I^{-} \longrightarrow Fe(CO)_2L_2I_2 + CO \quad (4.22)$$

An alternative route from Eq. 4.17 would be

$$[Fe(CO)_3L_2(CF_3)]^{\cdot} + I^{\cdot} \longrightarrow [Fe(CO)_2L_2(CF_3)]^{\cdot} + CO \quad (4.23)$$

$$[Fe(CO)_2L_2(CF_3)]^{\cdot} + I^{-} \longrightarrow Fe(CO)_2L_2(CF_3)I \quad (4.24)$$

L_2 = (diars)

$$CF_3CO_2Ag + I_2 \longrightarrow CF_3CO_2I + AgI \tag{4.25}$$

$$CF_3CO_2I \longrightarrow I^{\cdot} + CF_3CO_2^{\cdot} \longrightarrow CO_2 + CF_3^{\cdot}$$
$$\xrightarrow{CF_3CO_2I} CF_3I + CF_3CO_2^{\cdot} \longrightarrow \ etc. \tag{4.26}$$

A kinetic observation which remains unaccounted for is the CF_3H concentration vs. time profile, which appears to parallel that of Fe-CF_3. This could mean that the free radical reaction is the source of either CF_3^- or H^+ ions. Experiments 10, 11 and 13 suggest that the formation of CF_3^- leading to CF_3H is non-radical in nature. Hence the other option, that the free radical reaction is the source of H^+ ions seems more reasonable. In the reaction under study, the only source of protons is the methyl or phenyl groups of the diars ligand. Since there is no precedent for acidic protons in the diars ligand, the source of protons in the reaction and the above kinetic observation remains unresolved. It may be from adventitious moisture present in the system.

The rate of free radical oxidative addition reactions is proportional to the stability of the R radical in alkyl iodides and it decreases according to the series: tertiary > secondary > primary > methyl [61]. A similar trend has been observed for the perfluoroalkyl iodides. The ultraviolet spectra of perfluoroalkyl iodides in light petroleum were shown to lie at longer wavelengths with increasing size of the R_f group. This was interpreted as indicating a decrease in carbon-iodine bond dissociation energy caused by an increase in the stability of the free radical $R_f^{\cdot}$. Therefore the stability of the R_f radical decreases according to the series tertiary > secondary > primary > perfluoromethyl [89]. Also, Brace [31] carried out competitive experiments to demonstrate the above trend and interpreted the results in terms of the dissociation energy of R_fI, the stability of $R_f^{\cdot}$, and the

stability of the radical adducts in the addition reaction of R_fI to olefins. Similarly, in the addition reactions of R_fI to ethylene or propargyl alcohol, an increase in the resonance energy of $R_f^{\cdot}$ with increasing size of the R_f group has been suggested as the reason for the greater reactivity of C_3F_7I over CF_3I [145]. Thus, with the higher analogues of CF_3I (C_2F_5I, n-C_3F_7I, n-$C_6F_{13}I$, and n-$C_7F_{15}I$ as well as CF_3CH_2I) the extent of the free radical reaction should be much larger owing to their greater stability. A similar observation has been made in a d^8 Ir(I) complex. The higher analogues of methyl iodide undergo free radical oxidative addition while methyl iodide follows a non-radical S_N2 path [115]. This suggests that the free radical reaction of the higher analogues of CF_3I in d^8 Fe(0) and CH_3I in d^8 Ir(I) is due to the greater stability of the alkyl/perfluoroalkyl radicals. Therefore, in the reaction of $Fe(CO)_3$(diars) with R_fI (R_f = higher analogues of CF_3I), the mechanism leading to Fe-C(O)CF_3 is dominated by the radical path and hence only the perfluoroalkyl compounds are formed.

4.5 Conclusion

$Fe(CO)_3$(diars) appears to react with CF_3I at -90 °C via two parallel pathways: radical and molecular. The radical path leads to the oxidative addition product of $Fe(CO)_2$(diars)(CF_3)I while the molecular path leads to $Fe(CO)_2$(diars)(C(O)CF_3)I through an ionic intermediate $[Fe(CO)_3(diars)I]^+$ CF_3^-, which subsequently undergoes intermolecular insertion, also known as nucleophilic addition. The results are consistent with the prevalent theoretical and preparative results which suggest that the observed perfluoroacyl compounds are not the result of intramolecular insertion. For the higher analogues of CF_3I namely C_2F_5I, n-C_3F_7I, n-$C_6F_{13}I$ and n-$C_7F_{15}I$ as well as CF_3CH_2I, the free radical path dominates, resulting in simple oxidative addition.

Table 4.4: Concentration vs. Time Data for Experiment I

$[CF_3I] = a = 1.28$ mol/L
$[Fe(CO)_3(diars)] = b = 5.03 \times 10^{-2}$ mol/L
Ratio **a:b** = 25:1

Temperature : -90 °C

Time	Raw Data		Normalised Data	
(s)	$Fe\text{-}CF_3$	CF_3H	$Fe\text{-}CF_3$	CF_3H
10.	0.200	0.020	2.857	0.286
100.	0.300	0.030	4.286	0.429
200.	0.300	0.050	4.286	0.714
300.	0.300	0.070	4.286	1.000
400.	0.300	0.090	4.286	1.286
500.	0.300	0.090	4.286	1.286
600.	0.300	0.100	4.286	1.429
700.	0.300	0.100	4.286	1.429
800.	0.300	0.100	4.286	1.429
900.	0.300	0.100	4.286	1.429
1000.	0.300	0.100	4.286	1.429
1200.	0.300	0.100	4.286	1.429
1400.	0.300	0.100	4.286	1.429
1600.	0.300	0.100	4.286	1.429
1800.	0.300	0.100	4.286	1.429
2000.	0.300	0.100	4.286	1.429
2500.	0.300	0.100	4.286	1.429
3000.	0.300	0.100	4.286	1.429
3500.	0.300	0.100	4.286	1.429
4000.	0.300	0.100	4.286	1.429
4500.	0.300	0.100	4.286	1.429
5000.	0.300	0.100	4.286	1.429
5500.	0.300	0.100	4.286	1.429
6000.	0.300	0.100	4.286	1.429
6500.	0.300	0.100	4.286	1.429
7000.	0.300	0.100	4.286	1.429
7500.	0.300	0.100	4.286	1.429
8000.	0.300	0.100	4.286	1.429
10000.	0.300	0.100	4.286	1.429
12000.	0.300	0.100	4.286	1.429

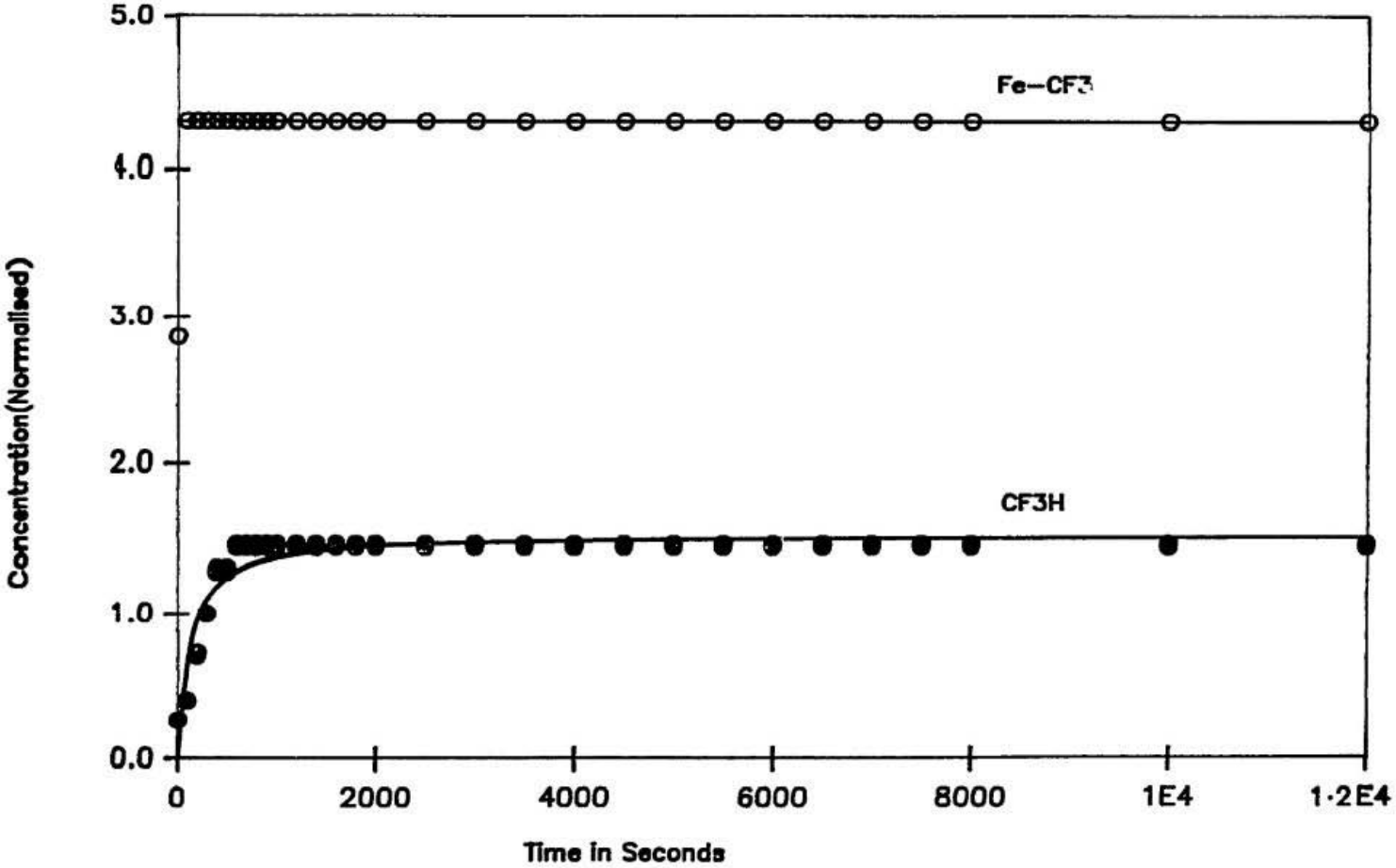

Figure 4.11: Concentration vs. Time Graph for Experiment I

Table 4.5: Concentration vs. Time Data for Experiment II

$[CF_3I] = a = 0.893$ mol/L
$.[Fe(CO)_3(diars)] = b = 7.65 \times 10^{-2}$ mol/L
Ratio a:b = 12:1

Temperature : -90 °C

Time	Raw Data				Normalised Data			
(s)	$Fe\text{-}CF_3$	CF_3H	$Fe\text{-}C(O)CF_3$	Interm.	$Fe\text{-}CF_3$	CF_3H	$Fe\text{-}C(O)CF_3$	Interm.
100.	0.800	0.300	0.000	0.000	0.727	0.273	0.000	0.000
200.	0.850	0.350	0.000	0.000	0.773	0.318	0.000	0.000
300.	0.900	0.400	0.000	0.000	0.818	0.364	0.000	0.000
400.	0.900	0.450	0.000	0.000	0.818	0.409	0.000	0.000
500.	0.950	0.500	0.000	0.000	0.864	0.455	0.000	0.000
600.	0.950	0.500	0.000	0.080	0.864	0.455	0.000	0.073
700.	0.950	0.500	0.000	0.100	0.864	0.455	0.000	0.091
800.	0.950	0.500	0.000	0.170	0.864	0.455	0.000	0.155
900.	0.950	0.500	0.000	0.190	0.864	0.455	0.000	0.173
1000.	0.950	0.500	0.030	0.200	0.864	0.455	0.027	0.182
1200.	0.950	0.500	0.050	0.250	0.864	0.455	0.045	0.227
1400.	0.950	0.500	0.100	0.250	0.864	0.455	0.091	0.227
1600.	0.950	0.500	0.150	0.280	0.864	0.455	0.136	0.255
1800.	0.950	0.500	0.170	0.250	0.864	0.455	0.155	0.227
2000.	0.950	0.500	0.200	0.230	0.864	0.455	0.182	0.209
2500.	0.950	0.500	0.230	0.190	0.864	0.455	0.209	0.173
3000.	0.950	0.500	0.300	0.130	0.864	0.455	0.273	0.118
3500.	0.900	0.500	0.300	0.100	0.818	0.455	0.273	0.091
4000.	0.900	0.500	0.300	0.070	0.818	0.455	0.273	0.064
4500.	0.900	0.500	0.300	0.050	0.818	0.455	0.273	0.045
5000.	0.900	0.500	0.300	0.050	0.818	0.455	0.273	0.045
5500.	0.900	0.500	0.300	0.000	0.818	0.455	0.273	0.000
6000.	0.900	0.500	0.300	0.000	0.818	0.455	0.273	0.000
6500.	0.900	0.500	0.300	0.000	0.818	0.455	0.273	0.000
7000.	0.900	0.500	0.300	0.000	0.818	0.455	0.273	0.000
7500.	0.900	0.500	0.300	0.000	0.818	0.455	0.273	0.000
8000.	0.900	0.500	0.300	0.000	0.818	0.455	0.273	0.000
9000.	0.850	0.500	0.300	0.000	0.773	0.455	0.273	0.000
10000.	0.900	0.500	0.300	0.000	0.818	0.455	0.273	0.000

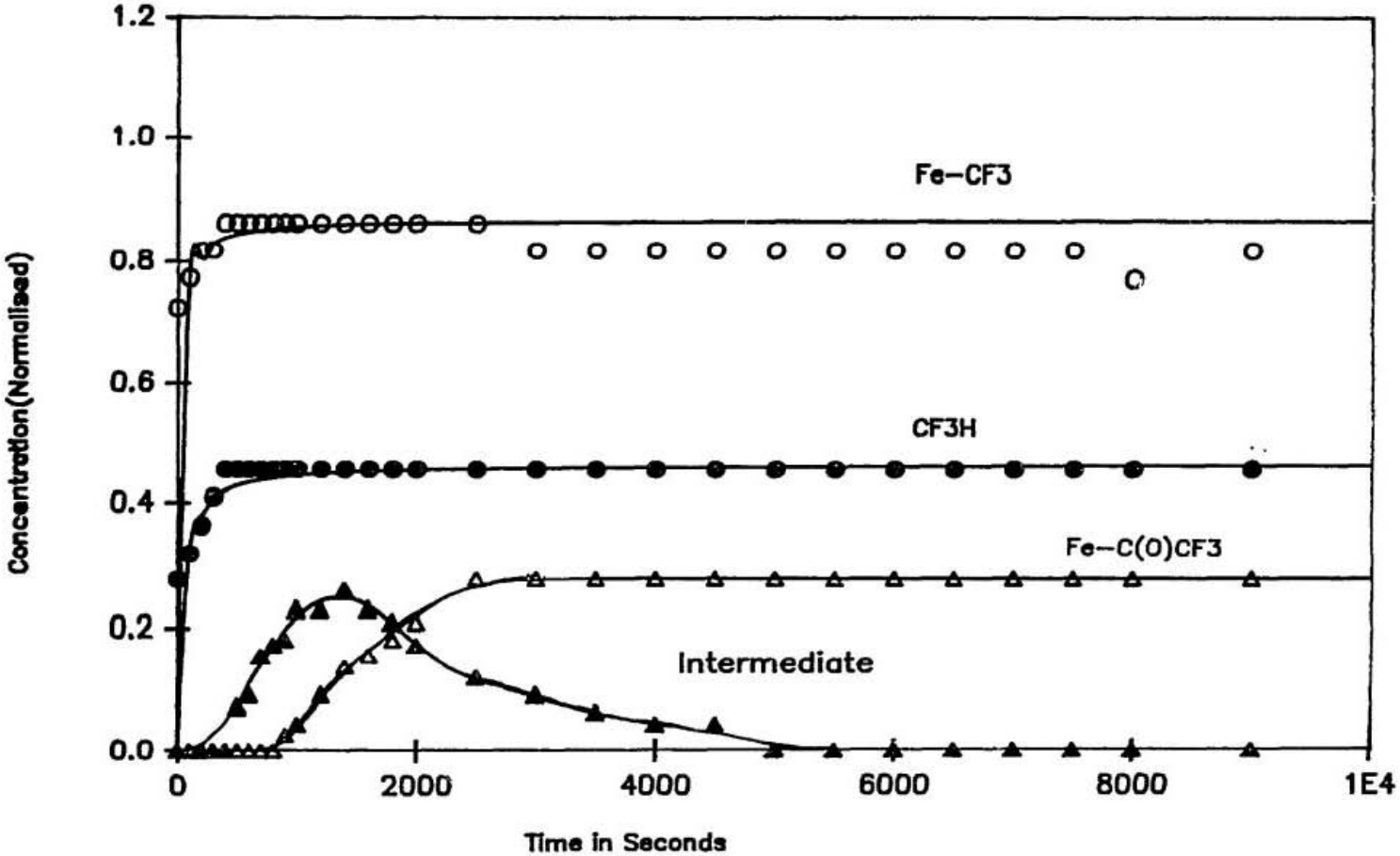

Figure 4.12: Concentration vs. Time Graph for Experiment II

Temp: −90 °C

CF3I : Fe(CO)3(diars) = 12 : 1

Table 4.6: Conc ntration vs Time Data for Experiment III

$[CF_3I] = a = 0.893$ mol/L
.$[Fe(CO)_3(diars)] = b = 14.65 \times 10^{-2}$ mol/L
Ratio a:b = 6:1

Temperature : -90 °C

Time	Raw Data				Normalised Data			
(s)	$Fe\text{-}CF_3$	CF_3H	$Fe\text{-}C(O)CF_3$	Interm.	$Fe\text{-}CF_3$	CF_3H	$Fe\text{-}C(O)CF_3$	Interm.
10.	1.200	0.200	0.000	0.000	1.714	0.286	0.000	0.000
100.	1.200	0.200	0.000	0.100	1.714	0.286	0.000	0.143
200.	1.200	0.200	0.000	0.200	1.714	0.286	0.000	0.286
300.	1.200	0.200	0.000	0.300	1.714	0.286	0.000	0.429
400.	1.200	0.200	0.010	0.350	1.714	0.286	0.014	0.500
500.	1.200	0.200	0.030	0.400	1.714	0.286	0.043	0.571
600.	1.200	0.200	0.050	0.490	1.714	0.286	0.071	0.700
700.	1.200	0.200	0.070	0.540	1.714	0.286	0.100	0.771
800.	1.200	0.200	0.090	0.560	1.714	0.286	0.129	0.800
900.	1.200	0.200	0.100	0.580	1.714	0.286	0.143	0.829
1000.	1.200	0.200	0.100	0.680	1.714	0.286	0.143	0.971
1200.	1.200	0.200	0.100	0.700	1.714	0.286	0.143	1.000
1400.	1.200	0.200	0.130	0.750	1.714	0.286	0.186	1.071
1600.	1.200	0.200	0.180	0.750	1.714	0.286	0.257	1.071
1800.	1.200	0.200	0.200	0.810	1.714	0.286	0.286	1.157
2000.	1.200	0.200	0.230	0.730	1.714	0.286	0.329	1.043
2500.	1.200	0.200	0.300	0.680	1.714	0.286	0.429	0.971
3000.	1.200	0.200	0.300	0.650	1.714	0.286	0.429	0.929
3500.	1.200	0.200	0.350	0.600	1.714	0.286	0.500	0.857
4000.	1.200	0.200	0.400	0.500	1.714	0.286	0.571	0.714
4500.	1.200	0.200	0.450	0.450	1.714	0.286	0.643	0.643
5000.	1.200	0.200	0.500	0.400	1.714	0.286	0.714	0.571
5500.	1.200	0.200	0.550	0.350	1.714	0.286	0.786	0.500
6000.	1.200	0.200	0.600	0.300	1.714	0.286	0.857	0.429
6500.	1.200	0.200	0.600	0.300	1.714	0.286	0.857	0.429

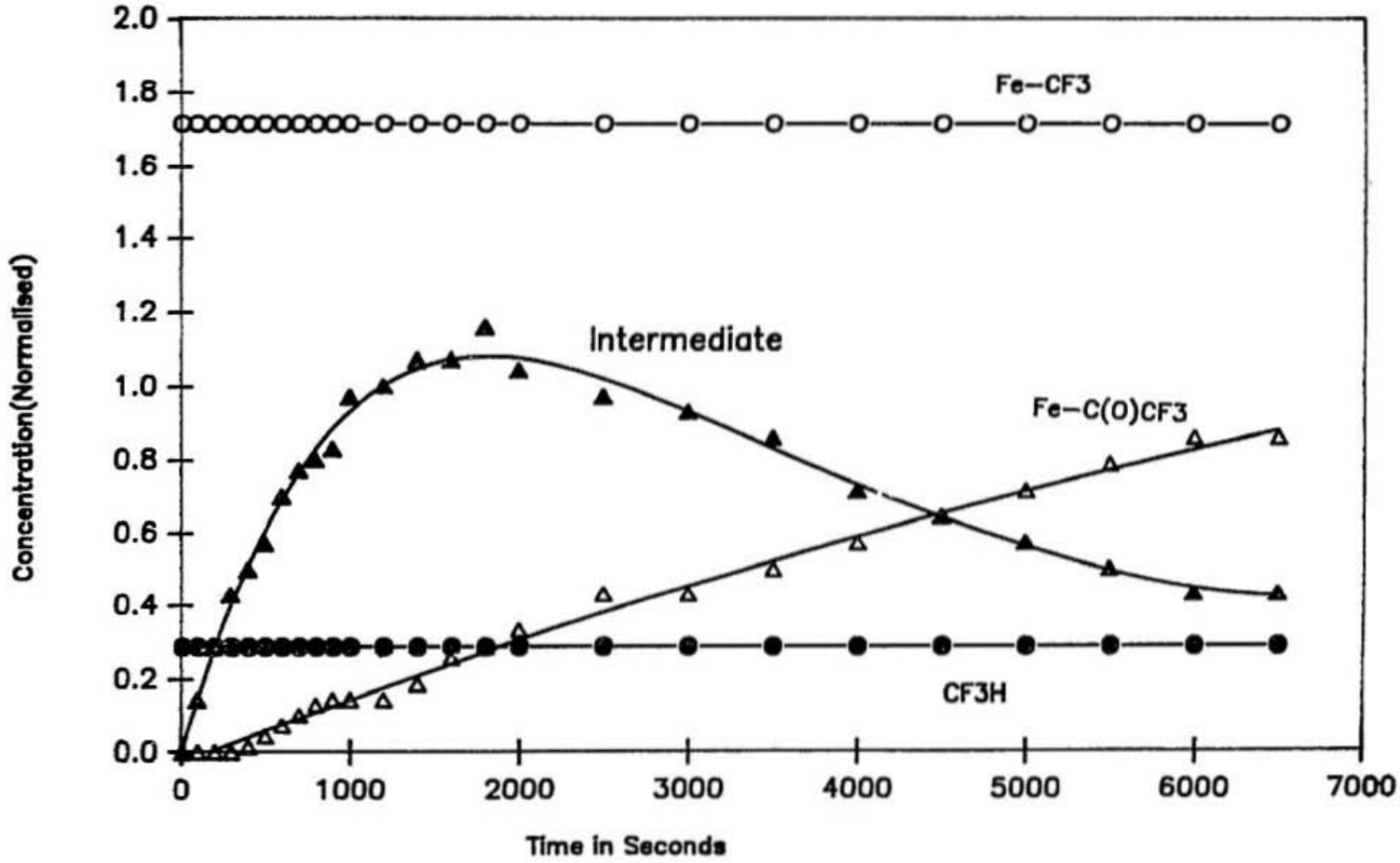

Figure 4.13: Concentration vs. Time Graph for Experiment III

Table 4.7: Concentration vs. Time Data for Experiment IV

$[CF_3I] = a = 0.893$ mol/L
.$[Fe(CO)_3(diars)] = b = 28.17 \times 10^{-2}$ mol/L
Ratio **a:b** = 3:1

Temperature : -80 °C

Time	Raw Data			Ref	Normalised Data		
(s)	Acyl I	Acyl II	Interm.		Acyl I	Acyl II	Interm.
10.	0.300	0.200	0.400	9.400	0.032	0.021	0.043
100.	0.900	0.600	0.500	12.700	0.071	0.047	0.039
200.	2.200	1.300	0.600	11.400	0.193	0.114	0.053
300.	2.450	1.600	0.600	12.700	0.193	0.126	0.047
400.	3.800	2.320	0.600	13.700	0.277	0.169	0.044
500.	5.400	3.300	0.600	14.400	0.375	0.229	0.042
600.	5.400	3.600	0.600	14.300	0.378	0.252	0.042
700.	6.200	4.000	0.550	15.000	0.413	0.267	0.037
800.	8.900	5.800	0.500	15.300	0.582	0.379	0.033
900.	10.400	6.800	0.250	15.700	0.662	0.433	0.016
1000.	10.400	7.200	0.200	15.500	0.671	0.465	0.013
1200.	11.200	8.100	0.180	15.900	0.704	0.509	0.011
1400.	12.000	8.600	0.150	16.400	0.732	0.524	0.009
1600.	13.000	9.200	0.120	16.300	0.798	0.564	0.007
1800.	14.400	9.400	0.100	16.600	0.867	0.566	0.006
2000.	15.600	9.800	0.080	16.500	0.945	0.594	0.005
2500.	18.400	9.700	0.080	17.300	1.064	0.561	0.005
3000.	18.400	9.600	0.080	17.200	1.070	0.558	0.005
3500.	20.000	9.680	0.080	17.300	1.156	0.560	0.005
4000.	20.400	10.400	0.080	17.300	1.179	0.601	0.005
4500.	22.000	10.000	0.080	17.400	1.264	0.575	0.005
5000.	23.200	10.400	0.080	17.400	1.333	0.598	0.005
5500.	22.400	10.400	0.080	17.300	1.295	0.601	0.005
6000.	23.600	11.200	0.080	17.900	1.318	0.626	0.004
6500.	24.400	10.800	0.080	18.000	1.356	0.600	0.004
7000.	25.200	10.800	0.080	17.800	1.416	0.607	0.004
7500.	25.600	10.800	0.080	17.800	1.438	0.607	0.004
8000.	25.600	10.800	0.080	18.100	1.414	0.597	0.004
10000.	25.600	11.200	0.080	18.200	1.407	0.615	0.004
12000.	27.200	10.400	0.080	19.400	1.402	0.536	0.004

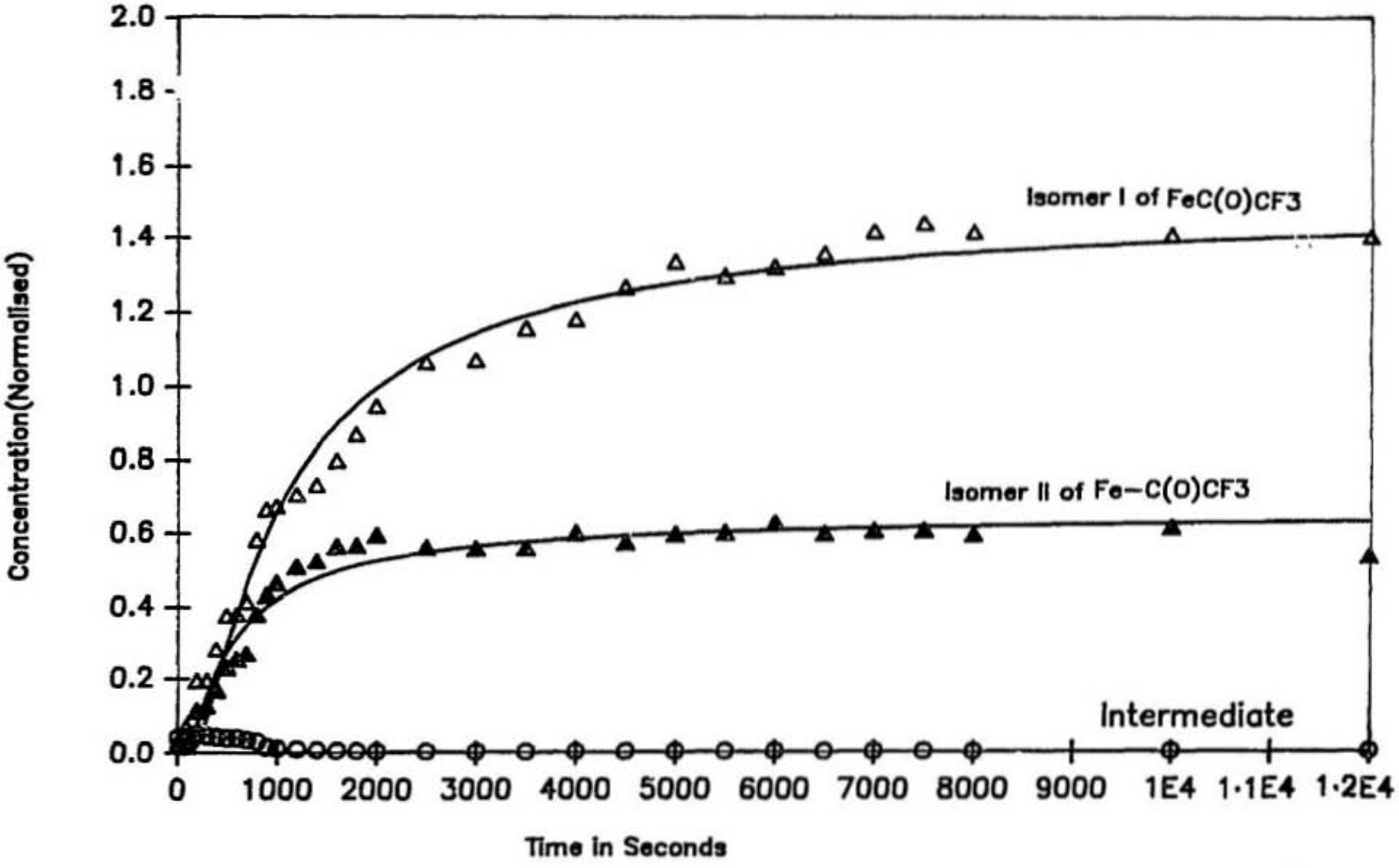

Figure 4.14: Concentration vs. Time Graph for Experiment IV

Table 4.8: Concentration vs. Time Data for Experiment V

$[CF_3I]$ = a = 1.79 mol/L
$[Fe(CO)_3(diars)]$ = b = 8.22 x 10^{-2} mol/L
Ratio a:b = 22:1

Temperature : -90 °C

Time	Raw Data		Normalised Data	
(s)	Fe-CF_3	CF_3H	Fe-CF_3	CF_3H
10.	0.400	0.050	1.333	0.167
100.	0.400	0.060	1.333	0.200
200.	0.400	0.060	1.333	0.200
300.	0.400	0.060	1.333	0.200
400.	0.400	0.080	1.333	0.267
500.	0.400	0.080	1.333	0.267
600.	0.400	0.080	1.333	0.267
700.	0.400	0.090	1.333	0.300
800.	0.400	0.100	1.333	0.333
900.	0.400	0.100	1.333	0.333
1000.	0.400	0.100	1.333	0.333
1200.	0.400	0.100	1.333	0.333
1400.	0.400	0.100	1.333	0.333
1600.	0.400	0.100	1.333	0.333
1800.	0.400	0.100	1.333	0.333
2000.	0.400	0.100	1.333	0.333
2500.	0.400	0.100	1.333	0.333
3000.	0.400	0.100	1.333	0.333
3500.	0.400	0.100	1.333	0.333
4000.	0.400	0.100	1.333	0.333
4500.	0.400	0.100	1.333	0.333
5000.	0.400	0.100	1.333	0.333
5500.	0.400	0.100	1.333	0.333
6000.	0.400	0.100	1.333	0.333
6500.	0.400	0.100	1.333	0.333
7000.	0.400	0.100	1.333	0.333
7500.	0.400	0.100	1.333	0.333
8000.	0.400	0.100	1.333	0.333
9000.	0.400	0.100	1.333	0.333
10000.	0.400	0.100	1.333	0.333

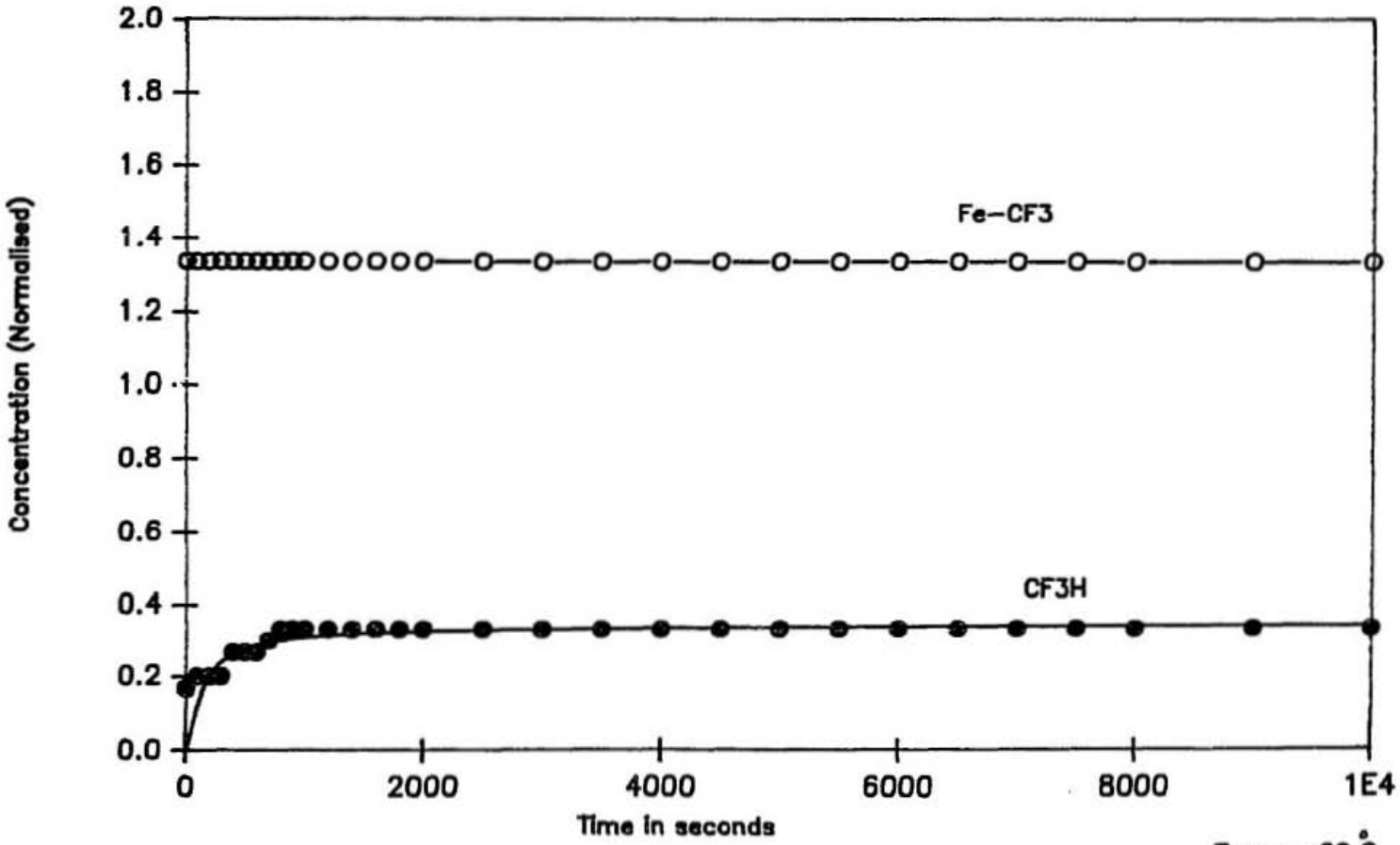

Figure 4.15: Concentration vs. Time Graph for Experiment V

Table 4.9: Concentration vs. Time Data for Experiment VI

$[CF_3I] = a = 0.446$ mol/L
.$[Fe(CO)_3(diars)] = b = 8.17 \times 10^{-2}$ mol/L
Ratio a:b = 6:1

Temperature : -90 °C

Time	Raw Data				Normalised Data			
(s)	$Fe\text{-}CF_3$	CF_3H	$Fe\text{-}C(O)CF_3$	Interm.	$Fe\text{-}CF_3$	CF_3H	$Fe\text{-}C(O)CF_3$	Interm.
10.	0.030	0.110	0.000	0.000	0.075	0.275	0.000	0.000
100.	0.060	0.130	0.000	0.000	0.150	0.325	0.000	0.000
200.	0.080	0.150	0.000	0.000	0.200	0.375	0.000	0.000
300.	0.090	0.170	0.000	0.000	0.225	0.425	0.000	0.000
400.	0.100	0.190	0.000	0.000	0.250	0.475	0.000	0.000
500.	0.110	0.200	0.000	0.000	0.275	0.500	0.000	0.000
600.	0.120	0.200	0.000	0.000	0.300	0.500	0.000	0.000
700.	0.120	0.200	0.000	0.000	0.300	0.500	0.000	0.000
800.	0.120	0.200	0.000	0.000	0.300	0.500	0.000	0.000
900.	0.120	0.200	0.000	0.000	0.300	0.500	0.000	0.000
1000.	0.120	0.200	0.000	0.000	0.300	0.500	0.000	0.000
1200.	0.120	0.200	0.000	0.000	0.300	0.500	0.000	0.000
1400.	0.120	0.200	0.000	0.050	0.300	0.500	0.000	0.125
1600.	0.120	0.200	0.000	0.060	0.300	0.500	0.000	0.150
1800.	0.120	0.200	0.000	0.080	0.300	0.500	0.000	0.200
2000.	0.120	0.200	0.000	0.100	0.300	0.500	0.000	0.250
2500.	0.120	0.200	0.000	0.130	0.300	0.500	0.000	0.325
3000.	0.120	0.200	0.020	0.190	0.300	0.500	0.050	0.475
3500.	0.120	0.200	0.020	0.200	0.300	0.500	0.050	0.500
4000.	0.120	0.200	0.040	0.210	0.300	0.500	0.100	0.525
4500.	0.120	0.200	0.060	0.230	0.300	0.500	0.150	0.575
5000.	0.120	0.200	0.080	0.240	0.300	0.500	0.200	0.600
5500.	0.120	0.200	0.100	0.240	0.300	0.500	0.250	0.600
6000.	0.120	0.200	0.110	0.240	0.300	0.500	0.275	0.600
6500.	0.120	0.200	0.140	0.230	0.300	0.500	0.350	0.575
7000.	0.120	0.200	0.160	0.230	0.300	0.500	0.400	0.575
7500.	0.120	0.200	0.200	0.230	0.300	0.500	0.500	0.575
8000.	0.120	0.200	0.230	0.210	0.300	0.500	0.575	0.525
10000.	0.120	0.200	0.250	0.200	0.300	0.500	0.625	0.500
12000.	0.120	0.200	0.300	0.180	0.300	0.500	0.750	0.450

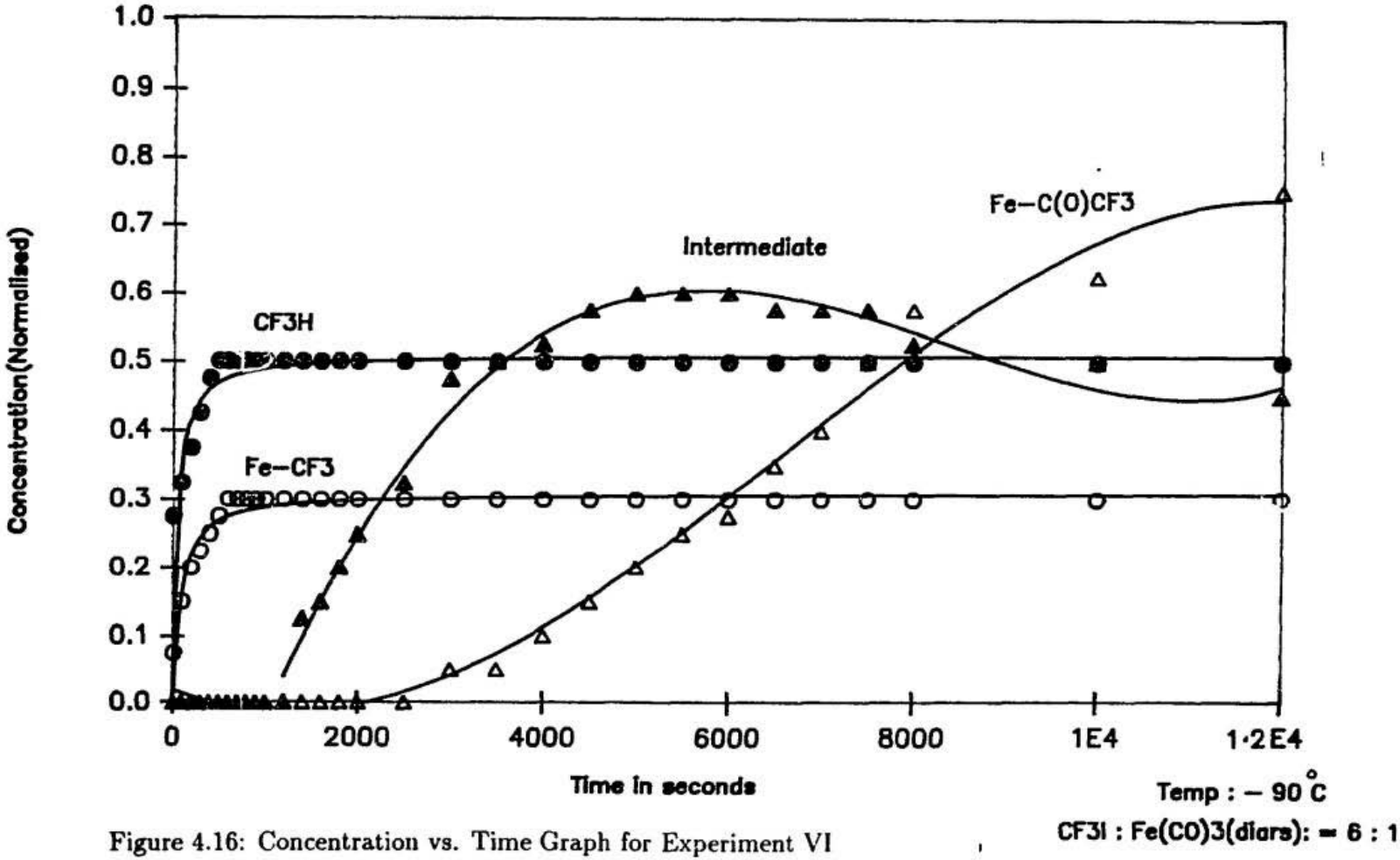

Figure 4.16: Concentration vs. Time Graph for Experiment VI

Table 4.10: Concentration vs. Time Data for Experiment VII

$[CF_3I] = a = 0.268$ mol/L
.$[Fe(CO)_3(diars)] = b = 9.91 \times 10^{-2}$ mol/L
Ratio a:b = 3:1

Temperature : -90 °C

Time	Raw Data				Normalised Data			
(s)	$Fe\text{-}CF_3$	CF_3H	$Fe\text{-}C(O)CF_3$	Interm.	$Fe\text{-}CF_3$	CF_3H	$Fe\text{-}C(O)CF_3$	Interm.
10.	0.180	0.080	0.000	0.000	2.571	1.143	0.000	0.000
100.	0.200	0.080	0.000	0.000	2.857	1.143	0.000	0.000
200.	0.200	0.100	0.000	0.000	2.857	1.429	0.000	0.000
300.	0.200	0.100	0.000	0.000	2.857	1.429	0.000	0.000
400.	0.230	0.100	0.000	0.000	3.286	1.429	0.000	0.000
500.	0.230	0.100	0.000	0.000	3.286	1.429	0.000	0.000
600.	0.250	0.100	0.000	0.000	3.571	1.429	0.000	0.000
700.	0.280	0.130	0.000	0.000	4.000	1.857	0.000	0.000
800.	0.290	0.130	0.000	0.000	4.143	1.857	0.000	0.000
900.	0.290	0.150	0.000	0.000	4.143	2.143	0.000	0.000
1000.	0.300	0.150	0.000	0.000	4.286	2.143	0.000	0.000
1200.	0.300	0.150	0.000	0.010	4.286	2.143	0.000	0.143
1400.	0.300	0.150	0.000	0.050	4.286	2.143	0.000	0.714
1600.	0.300	0.150	0.000	0.100	4.286	2.143	0.000	1.429
1800.	0.300	0.150	0.000	0.120	4.286	2.143	0.000	1.714
2000.	0.300	0.180	0.000	0.140	4.286	2.571	0.000	2.000
2500.	0.300	0.200	0.000	0.200	4.286	2.857	0.000	2.857
3000.	0.300	0.200	0.000	0.240	4.286	2.857	0.000	3.429
3500.	0.300	0.200	0.000	0.250	4.286	2.857	0.000	3.571
4000.	0.300	0.200	0.000	0.300	4.286	2.857	0.000	4.286
4500.	0.300	0.200	0.030	0.300	4.286	2.857	0.429	4.286
5000.	0.300	0.200	0.050	0.320	4.286	2.857	0.714	4.571
5500.	0.300	0.200	0.070	0.330	4.286	2.857	1.000	4.714
6000.	0.300	0.200	0.090	0.380	4.286	2.857	1.286	5.429
6500.	0.300	0.200	0.110	0.330	4.286	2.857	1.571	4.714
7000.	0.300	0.200	0.130	0.330	4.286	2.857	1.857	4.714
7500.	0.300	0.200	0.190	0.310	4.286	2.857	2.714	4.429
8000.	0.300	0.200	0.200	0.300	4.286	2.857	2.857	4.286
10000.	0.300	0.200	0.230	0.290	4.286	2.857	3.286	4.143
12000.	0.300	0.200	0.400	0.250	4.286	2.857	5.714	3.571

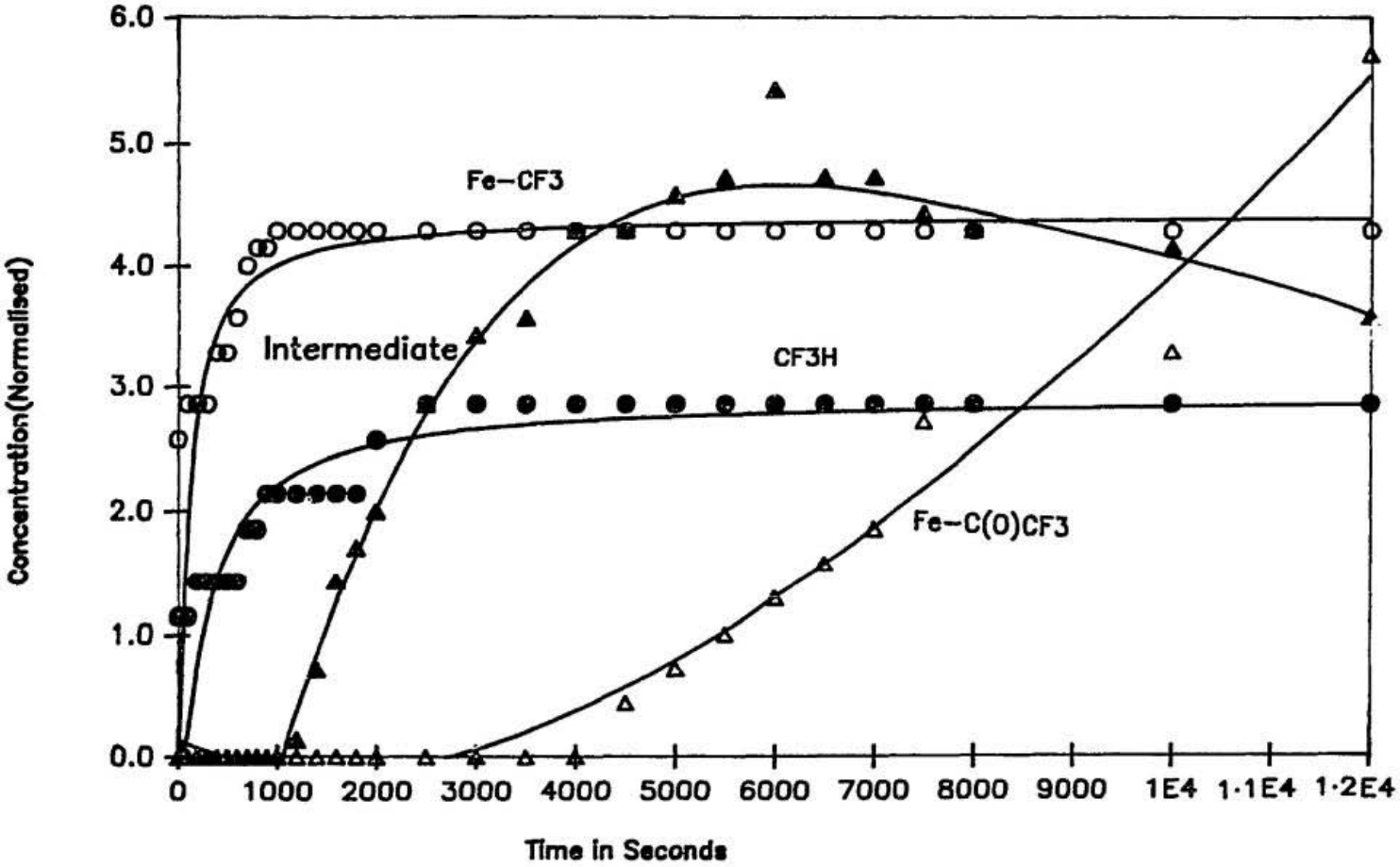

Figure 4.17: Concentration vs. Time Graph for Experiment VII

Table 4.11: Concentration vs.Time Data for Experiment VIII

$[CF_3I] = a = 0.179$ mol/L
$[Fe(CO)_3(diars)] = b = 9.77 \times 10^{-2}$ mol/L
Ratio a:b = 2:1

Temperature : -90 °C

Time	Raw Data				Normalised Data			
(s)	$Fe\text{-}CF_3$	CF_3H	$Fe\text{-}C(O)CF_3$	Interm.	$Fe\text{-}CF_3$	$CF_3'!$	$Fe\text{-}C(O)CF_3$	Interm.
10.	0.100	0.050	0.000	0.000	0.333	0.167	0.000	0.000
100.	0.150	0.050	0.000	0.000	0.500	0.167	0.000	0.000
200.	0.200	0.080	0.000	0.000	0.667	0.267	0.000	0.000
300.	0.250	0.100	0.000	0.000	0.833	0.333	0.000	0.000
400.	0.300	0.130	0.000	0.000	1.000	0.433	0.000	0.000
500.	0.350	0.150	0.000	0.000	1.167	0.500	0.000	0.000
600.	0.400	0.180	0.000	0.000	1.333	0.600	0.000	0.000
700.	0.400	0.200	0.000	0.000	1.333	0.667	0.000	0.000
800.	0.400	0.250	0.000	0.000	1.333	0.833	0.000	0.000
900.	0.470	0.280	0.000	0.000	1.567	0.933	0.000	0.000
1000.	0.500	0.300	0.000	0.000	1.667	1.000	0.000	0.000
1200.	0.550	0.300	0.000	0.000	1.833	1.000	0.000	0.000
1400.	0.600	0.300	0.000	0.000	2.000	1.000	0.000	0.000
1600.	0.600	0.360	0.000	0.000	2.000	1.200	0.000	0.000
1800.	0.650	0.380	0.000	0.000	2.167	1.267	0.000	0.000
2000.	0.680	0.400	0.000	0.000	2.267	1.333	0.000	0.000
2500.	0.700	0.450	0.000	0.000	2.333	1.500	0.000	0.000
3000.	0.750	0.500	0.000	0.100	2.500	1.667	0.000	0.333
3500.	0.800	0.500	0.000	0.300	2.667	1.667	0.000	1.000
4000.	0.800	0.500	0.000	0.400	2.667	1.667	0.000	1.333
4500.	0.800	0.500	0.030	0.600	2.667	1.667	0.100	2.000
5000.	0.800	0.500	0.050	0.700	2.667	1.667	0.167	2.333
5500.	0.800	0.500	0.080	0.800	2.667	1.667	0.267	2.667
6000.	0.800	0.500	0.100	0.900	2.667	1.667	0.333	3.000
6500.	0.800	0.500	0.150	1.000	2.667	1.667	0.500	3.333
7000.	0.800	0.500	0.200	1.000	2.667	1.667	0.667	3.333
7500.	0.800	0.500	0.200	1.100	2.667	1.667	0.667	3.667
8000.	0.800	0.500	0.260	1.150	2.667	1.667	0.867	3.833
10000.	0.800	0.500	0.350	1.200	2.667	1.667	1.167	4.000
12000.	0.800	0.500	0.800	1.100	2.667	1.667	2.667	3.667

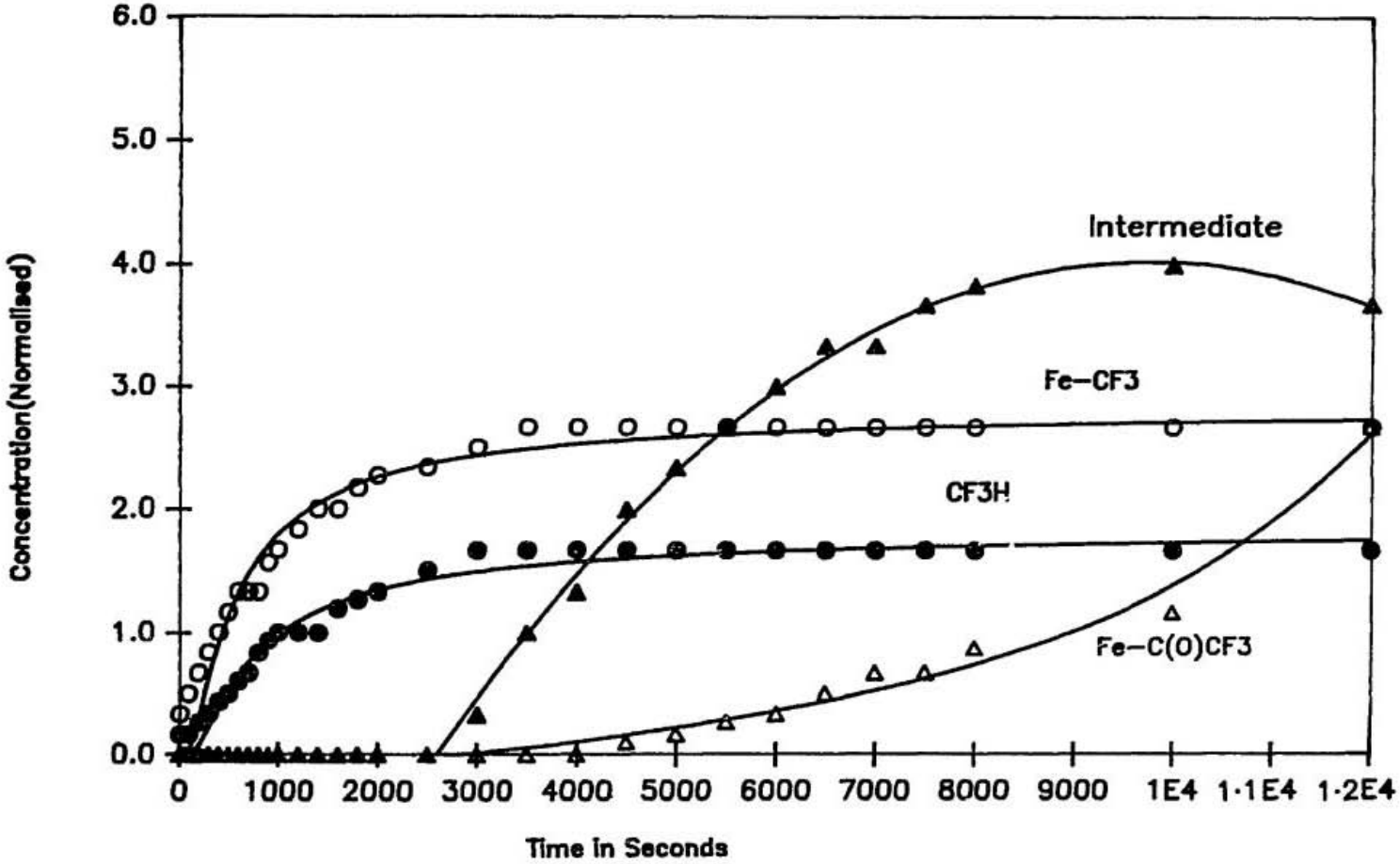

Figure 4.18: Concentration vs. Time Graph for Experiment VIII

Table 4.12: Concentration vs. Time Data for Experiment IX

$[CF_3I]$ = a = 0.268 mol/L
.$[Fe(CO)_3(d\ ars)]$ = b = 9.58 x 10^{-2} mol/L
Ratio **a:b** = 2.8:1

Temperature : -90 °C

Time	Raw Data				Normalised Data			
(s)	$Fe\text{-}CF_3$	CF_3H	$Fe\text{-}C(O)CF_3$	Interm.	$Fe\text{-}CF_3$	CF_3H	$Fe\text{-}C(O)CF_3$	Interm.
10.	0.200	0.010	0.000	0.000	2.000	0.100	0.000	0.000
100.	0.200	0.030	0.000	0.000	2.000	0.300	0.000	0.000
200.	0.200	0.030	0.000	0.000	2.000	0.300	0.000	0.000
300.	0.200	0.100	0.000	0.000	2.000	1.000	0.000	0.000
400.	0.200	0.100	0.000	0.000	2.000	1.000	0.000	0.000
500.	0.230	0.100	0.000	0.000	2.300	1.000	0.000	0.000
600.	0.250	0.100	0.000	0.000	2.500	1.000	0.000	0.000
700.	0.250	0.100	0.000	0.000	2.500	1.000	0.000	0.000
800.	0.250	0.100	0.000	0.000	2.500	1.000	0.000	0.000
900.	0.270	0.150	0.000	0.000	2.700	1.500	0.000	0.000
1000.	0.270	0.150	0.000	0.000	2.700	1.500	0.000	0.000
1200.	0.290	0.150	0.000	0.000	2.900	1.500	0.000	0.000
1400.	0.290	0.180	0.000	0.000	2.900	1.800	0.000	0.000
1600.	0.300	0.180	0.000	0.000	3.000	1.800	0.000	0.000
1800.	0.300	0.200	0.000	0.000	3.000	2.000	0.000	0.000
2000.	0.300	0.200	0.000	0.000	3.000	2.000	0.000	0.000
2500.	0.350	0.200	0.000	0.000	3.500	2.000	0.000	0.000
3000.	0.350	0.200	0.000	0.030	3.500	2.000	0.000	0.300
3500.	0.350	0.200	0.000	0.100	3.500	2.000	0.000	1.000
4000.	0.350	0.200	0.030	0.150	3.500	2.000	0.300	1.500
4500.	0.400	0.200	0.050	0.180	4.000	2.000	0.500	1.800
5000.	0.400	0.200	0.070	0.200	4.000	2.000	0.700	2.000
5500.	0.400	0.200	0.090	0.250	4.000	2.000	0.900	2.500
6000.	0.400	0.200	0.090	0.300	4.000	2.000	0.900	3.000
6500.	0.400	0.200	0.090	0.300	4.000	2.000	0.900	3.000
7000.	0.400	0.200	0.100	0.310	4.000	2.000	1.000	3.100
7500.	0.400	0.200	0.140	0.330	4.000	2.000	1.400	3.300
8000.	0.400	0.200	0.160	0.380	4.000	2.000	1.600	3.800
10000.	0.400	0.200	0.170	0.340	4.000	2.000	1.700	3.400
12000.	0.400	0.200	0.200	0.300	4.000	2.000	2.000	3.000

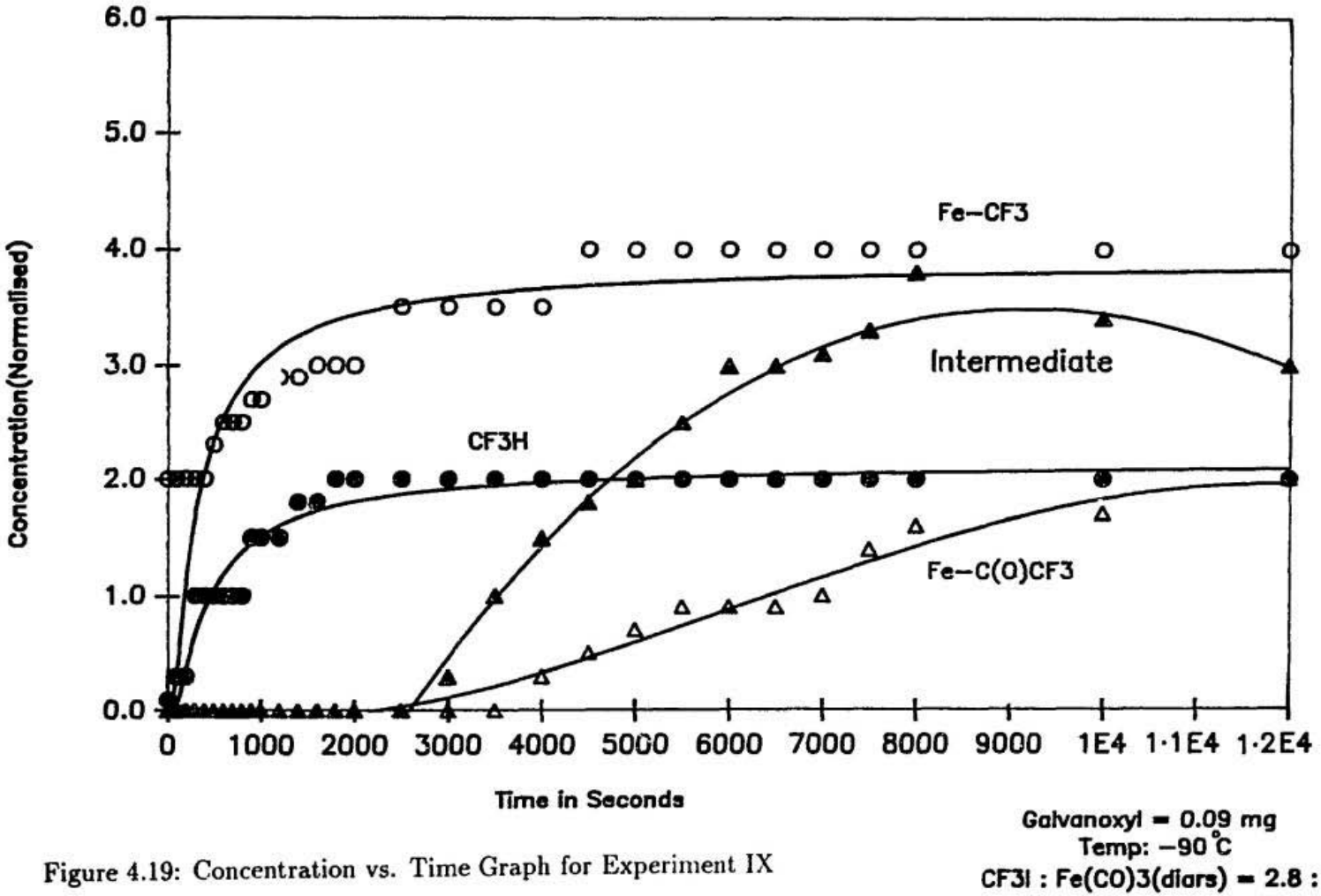

Figure 4.19: Concentration vs. Time Graph for Experiment IX

Table 4.13: Concentration vs. Time Data for Experiment X

$[CF_3I]$ = a = 0.268 mol/L
.$[Fe(CO)_3(diars)]$ = b = 1.13×10^{-1} mol/L
Ratio a:b = 2.4:1

Temperature : -90 °C

Time	Raw Data				Normalised Data			
(s)	$Fe\text{-}CF_3$	CF_3H	$Fe\text{-}C(O)CF_3$	Interm.	$Fe\text{-}CF_3$	CF_3H	$Fe\text{-}C(O)CF_3$	Interm.
10.	0.000	0.100	0.000	0.000	0.000	1.000	0.000	0.000
100.	0.000	0.100	0.000	0.000	0.000	1.000	0.000	0.000
200.	0.000	0.100	0.000	0.000	0.000	1.000	0.000	0.000
300.	0.000	0.110	0.000	0.000	0.000	1.100	0.000	0.000
400.	0.060	0.150	0.000	0.000	0.600	1.500	0.000	0.000
500.	0.060	0.190	0.000	0.000	0.600	1.900	0.000	0.000
600.	0.080	0.200	0.000	0.000	0.800	2.000	0.000	0.000
700.	0.080	0.200	0.000	0.000	0.800	2.000	0.000	0.000
800.	0.080	0.210	0.000	0.000	0.800	2.100	0.000	0.000
900.	0.080	0.230	0.000	0.000	0.800	2.300	0.000	0.000
1000.	0.080	0.250	0.000	0.000	0.800	2.500	0.000	0.000
1200.	0.090	0.290	0.000	0.000	0.900	2.900	0.000	0.000
1400.	0.100	0.300	0.000	0.030	1.000	3.000	0.000	0.300
1600.	0.110	0.300	0.000	0.050	1.100	3.000	0.000	0.500
1800.	0.110	0.300	0.000	0.100	1.100	3.000	0.000	1.000
2000.	0.110	0.300	0.000	0.120	1.100	3.000	0.000	1.200
2500.	0.110	0.300	0.000	0.250	1.100	3.000	0.000	2.500
3000.	0.110	0.300	0.010	0.400	1.100	3.000	0.100	4.000
3500.	0.110	0.300	0.030	0.450	1.100	3.000	0.300	4.500
4000.	0.110	0.300	0.050	0.500	1.100	3.000	0.500	5.000
4500.	0.110	0.300	0.100	0.550	1.100	3.000	1.000	5.500
5000.	0.110	0.300	0.100	0.600	1.100	3.000	1.000	6.000
5500.	0.110	0.300	0.100	0.650	1.100	3.000	1.000	6.500
6000.	0.110	0.300	0.130	0.650	1.100	3.000	1.300	6.500
6500.	0.110	0.300	0.180	0.650	1.100	3.000	1.800	6.500
7000.	0.110	0.300	0.200	0.650	1.100	3.000	2.000	6.500
7500.	0.110	0.300	0.250	0.650	1.100	3.000	2.500	6.500
8000.	0.110	0.300	0.300	0.650	1.100	3.000	3.000	6.500
10000.	0.110	0.300	0.350	0.550	1.100	3.000	3.500	5.500
12000.	0.110	0.300	0.500	0.500	1.100	3.000	5.000	5.000

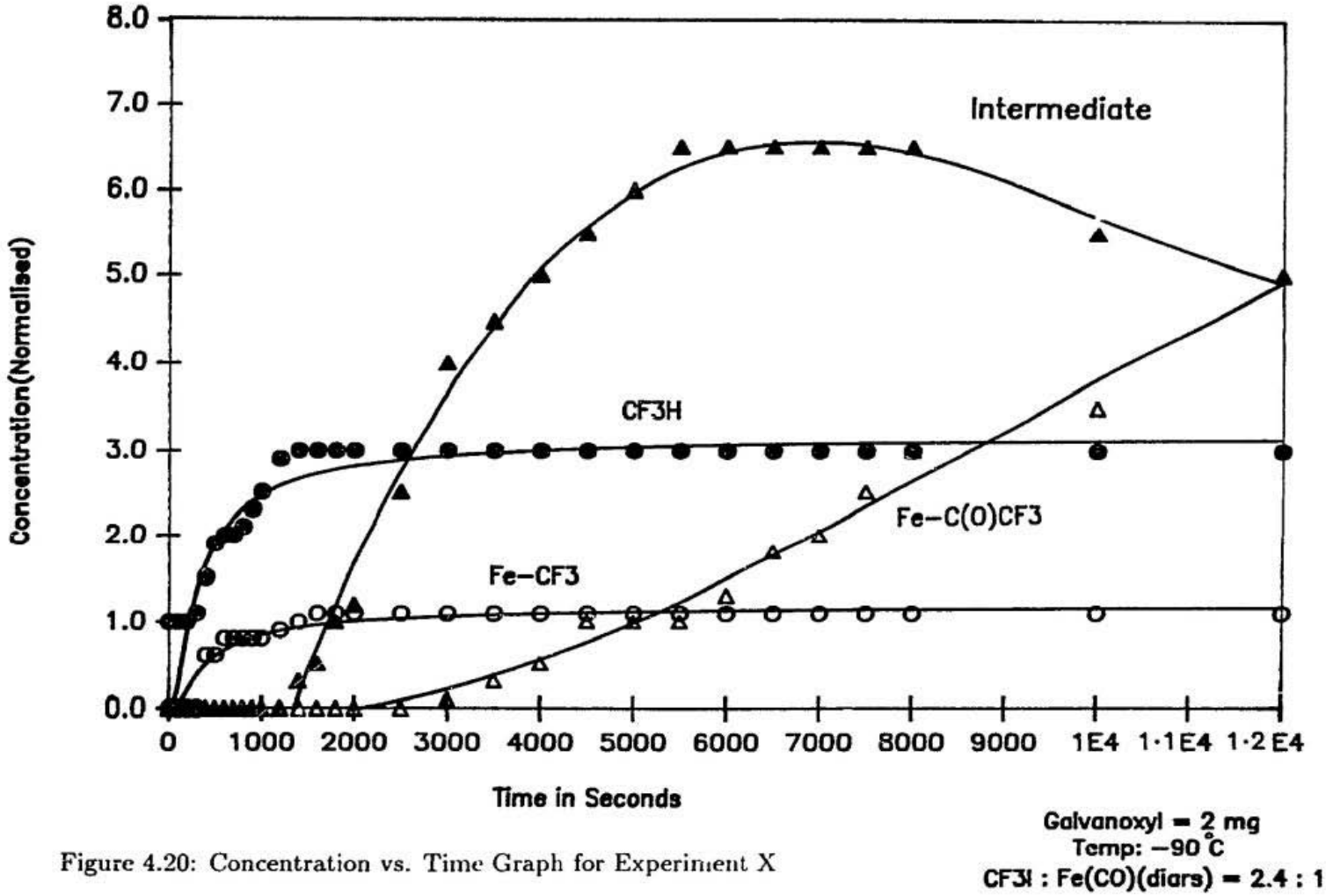

Figure 4.20: Concentration vs. Time Graph for Experiment X

Table 4.14: Concentration vs. Time Data for Experiment XI

$[CF_3I] = a = 0.268$ mol/L
$[Fe(CO)_3(diars)] = b = 9.39 \times 10^{-2}$ mol/L
Ratio a:b = 2.9:1

Temperature : -90 °C

Time	Raw Data				Normalised Data			
(s)	$Fe\text{-}CF_3$	CF_3H	$Fe\text{-}C(O)CF_3$	Interm.	$Fe\text{-}CF_3$	CF_3H	$Fe\text{-}C(O)CF_3$	Interm.
10.	0.030	0.050	0.000	0.000	0.150	0.250	0.000	0.000
100.	0.030	0.090	0.000	0.000	0.150	0.450	0.000	0.000
200.	0.030	0.110	0.000	0.000	0.150	0.550	0.000	0.000
300.	0.030	0.140	0.000	0.000	0.150	0.700	0.000	0.000
400.	0.030	0.160	0.000	0.000	0.150	0.800	0.000	0.000
500.	0.050	0.190	0.000	0.000	0.250	0.950	0.000	0.000
600.	0.050	0.200	0.000	0.000	0.250	1.000	0.000	0.000
700.	0.050	0.200	0.000	0.000	0.250	1.000	0.000	0.000
800.	0.050	0.250	0.000	0.000	0.250	1.250	0.000	0.000
900.	0.070	0.290	0.000	0.000	0.350	1.450	0.000	0.000
1000.	0.070	0.300	0.000	0.000	0.350	1.500	0.000	0.000
1200.	0.070	0.350	0.000	0.000	0.350	1.750	0.000	0.000
1400.	0.070	0.390	0.000	0.000	0.350	1.950	0.000	0.000
1600.	0.070	0.400	0.000	0.000	0.350	2.000	0.000	0.000
1800.	0.070	0.430	0.000	0.000	0.350	2.150	0.000	0.000
2000.	0.070	0.500	0.000	0.000	0.350	2.500	0.000	0.000
2500.	0.070	0.550	0.000	0.000	0.350	2.750	0.000	0 000
3000.	0.070	0.600	0.000	0.000	0.350	3.000	0.000	0 000
3500.	0.070	0.680	0.000	0.000	0.350	3.400	0.000	0.000
4000.	0.070	0.730	0.000	0.000	0.350	3.650	0.000	0.000
4500.	0.070	0.760	0.000	0.000	0.350	3.800	0.000	0.000
5000.	0.070	0.800	0.000	0.000	0.350	4.000	0.000	0.000
5500.	0.070	0.830	0.000	0.000	0.350	4.150	0.000	0.000
6000.	0.070	0.880	0.000	0.000	0.350	4.400	0.000	0.000
6500.	0.070	0.900	0.000	0.000	0.350	4.500	0.000	0.000
7000.	0.070	0.900	0.000	0.050	0.350	4.500	0.000	0.250
7500.	0.070	0.900	0.000	0.100	0.350	4.500	0.000	0.500
8000.	0.070	0.900	0.030	0.200	0.350	4.500	0.150	1.000
10000.	0.070	0.900	0.100	0.290	0.350	4.500	0.500	1.450
12000.	0.070	0.900	0.150	0.280	0.350	4.500	0.750	1.400

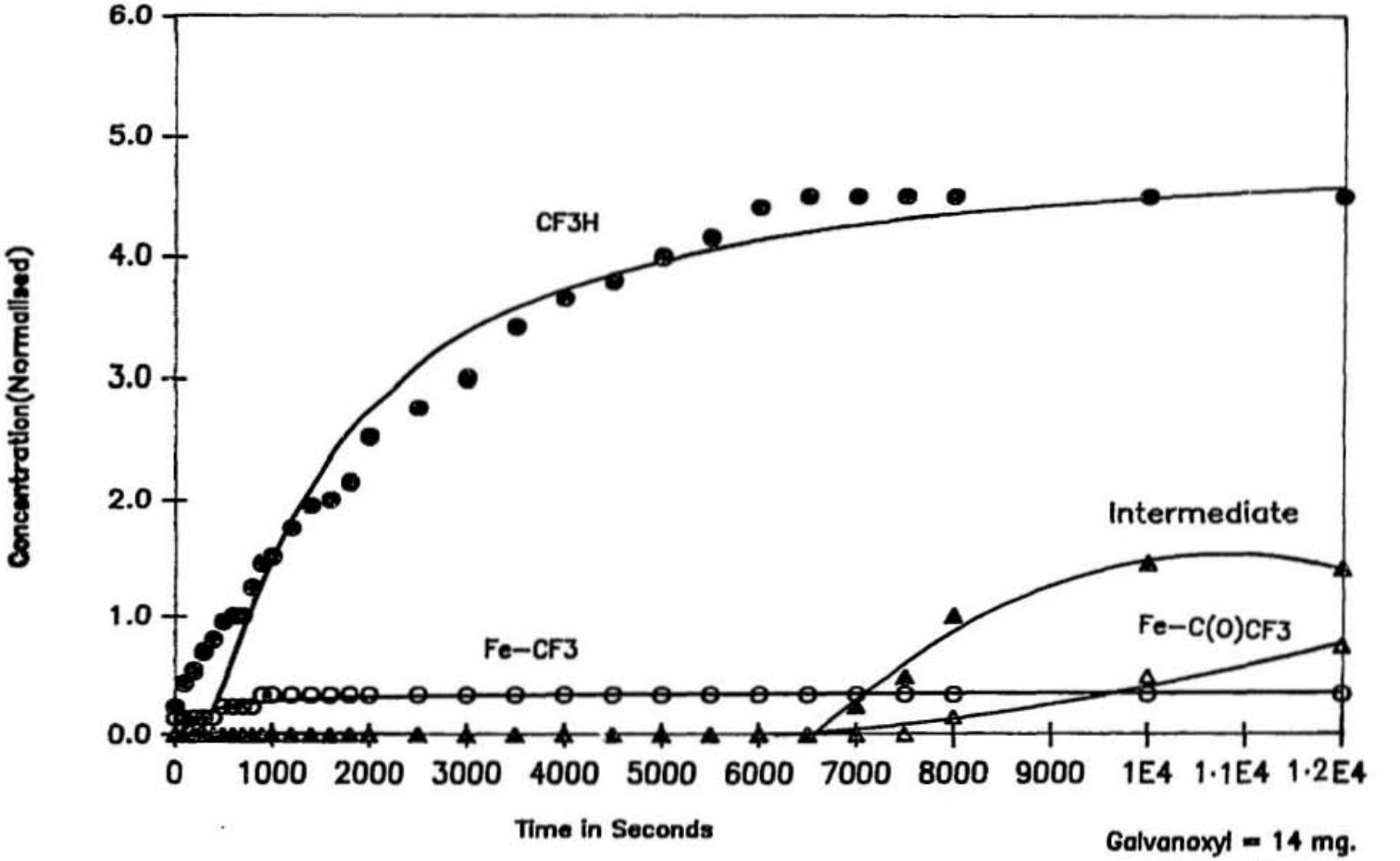

Figure 4.21: Concentration vs. Time Graph for Experiment XI

Table 4.15: Concentration vs.Time Data for Experiment XII

$[CF_3I] = a = 0.268$ mol/L
.$[Fe(CO)_3(diars)] = b = 8.26 \times 10^{-2}$ mol/L
Ratio a:b = 3.2:1

Temperature : -90 °C

Time	Raw Data				Normalised Data			
(s)	$Fe\text{-}CF_3$	CF_3H	$Fe\text{-}C(O)CF_3$	Interm.	$Fe\text{-}CF_3$	CF_3H	$Fe\text{-}C(O)CF_3$	Interm.
10.	0.050	0.000	0.000	0.000	0.714	0.000	0.000	0.000
100.	0.050	0.000	0.000	0.000	0.714	0.000	0.000	0.000
200.	0.060	0.030	0.000	0.000	0.857	0.429	0.000	0.000
300.	0.070	0.060	0.000	0.000	1.000	0.857	0.000	0.000
400.	0.080	0.070	0.000	0.000	1.143	1.000	0.000	0.000
500.	0.090	0.080	0.000	0.000	1.286	1.143	0.000	0.000
600.	0.100	0.090	0.000	0.000	1.429	1.286	0.000	0.000
700.	0.130	0.090	0.000	0.000	1.857	1.286	0.000	0.000
800.	0.180	0.090	0.000	0.000	2.571	1.286	0.000	0.000
900.	0.180	0.100	0.000	0.000	2.571	1.429	0.000	0.000
1000.	0.180	0.100	0.000	0.000	2.571	1.429	0.000	0.000
1200.	0.180	0.120	0.000	0.030	2.571	1.714	0.000	0.429
1400.	0.180	0.130	0.000	0.060	2.571	1.857	0.000	0.857
1600.	0.180	0.140	0.000	0.100	2.571	2.000	0.000	1.429
1800.	0.180	0.150	0.000	0.140	2.571	2.143	0.000	2.000
2000.	0.180	0.150	0.000	0.180	2.571	2.143	0.000	2.571
2500.	0.180	0.150	0.000	0.200	2.571	2.143	0.000	2.857
3000.	0.180	0.150	0.000	0.220	2.571	2.143	0.000	3.143
3500.	0.180	0.150	0.030	0.250	2.571	2.143	0.429	3.571
4000.	0.180	0.150	0.050	0.300	2.571	2.143	0.714	4.286
4500.	0.180	0.150	0.070	0.300	2.571	2.143	1.000	4.286
5000.	0.180	0.150	0.090	0.300	2.571	2.143	1.286	4.286
5500.	0.180	0.150	0.110	0.300	2.571	2.143	1.571	4.286
6000.	0.180	0.150	0.130	0.300	2.571	2.143	1.857	4.286
6500.	0.180	0.150	0.150	0.300	2.571	2.143	2.143	4.286
7000.	0.180	0.150	0.150	0.300	2.571	2.143	2.143	4.286
7500.	0.180	0.150	0.170	0.300	2.571	2.143	2.429	4.286
8000.	0.180	0.150	0.230	0.270	2.571	2.143	3.286	3.857
10000.	0.180	0.150	0.310	0.190	2.571	2.143	4.429	2.714
12000.	0.180	0.150	0.400	0.180	2.571	2.143	5.714	2.571

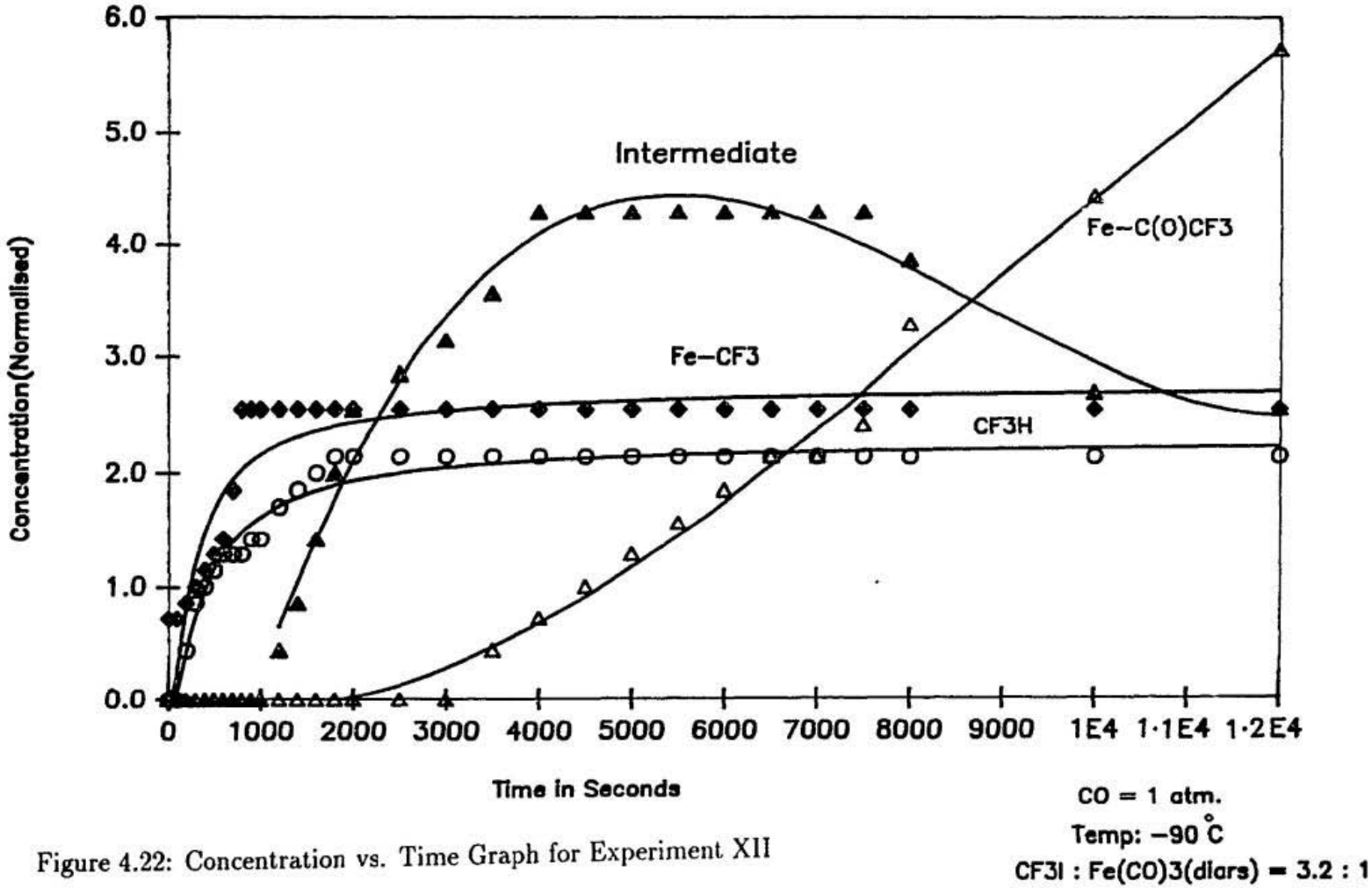

Figure 4.22: Concentration vs. Time Graph for Experiment XII

Table 4.16: Concentration vs. Time Data for Experiment XIII

$[\ CF_3I\ ] = a = 0.268$ mol/L
$[Fe(CO)_3(diars)] = b = 9.39 \times 10^{-2}$ mol/L
Ratio a:b = 3:1

Temperature : -90 °C

Time	Raw Data						Normalised Data					
(s)	$Fe\text{-}CF_3$	CF_3H	$Fe\text{-}C(O)CF_3$	Interm	Ref	BF_4^-	$Fe\text{-}CF_3$	CF_3H	$Fe\text{-}C(O)CF_3$	Interm	Ref	BF_4^-
0.	0.750	0.400	0.100	0.730	0.150	0.000	5.000	2.670	0.670	4.870	1.000	0.000
3600.	1.000	1.500	0.300	0.050	0.200	0.550	5.000	7.500	1.500	0.250	1.000	2.750
7200.	1.000	1.600	0.300	0.100	0.200	0.550	5.000	8.000	1.500	0.500	1.000	2.750
10800.	1.000	1.700	0.300	0.200	0.200	0.550	5.000	8.500	1.500	1.000	1.000	2.750

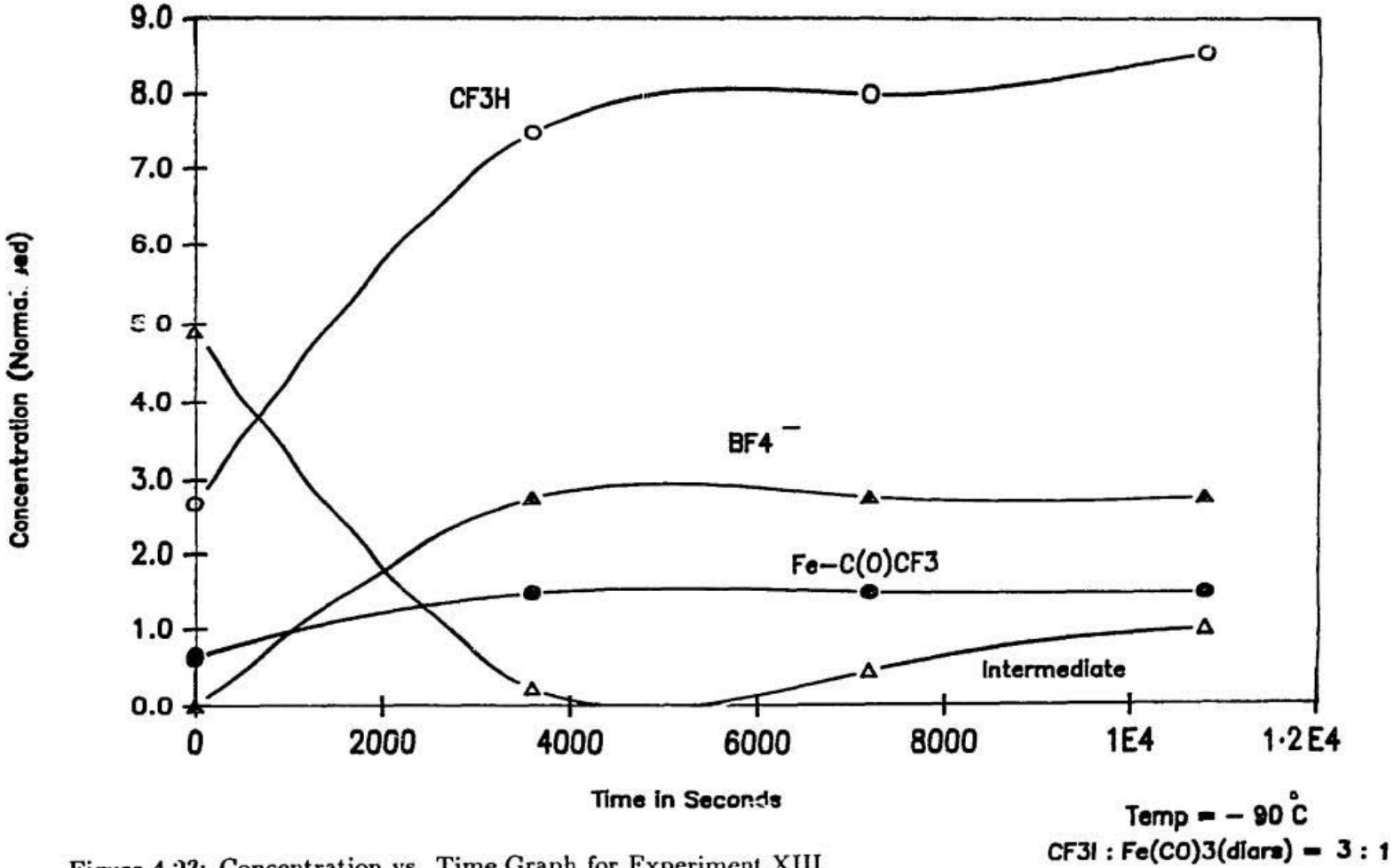

Figure 4.23: Concentration vs. Time Graph for Experiment XIII

Chapter 5

Conclusion and Recommendation

Carbonyl insertion into M-CF_3 bonds (M= Transition metal) has not been observed experimentally. As discussed in Chapter 1, this is in agreement with the theoretical predictions. The apparent CO insertion into the Fe-CF_3 bond reported in 1981, was therefore in open conflict with both experimental and theoretical results. An investigation of the above report was presented in this thesis.

Fe(diars)$(CO)_3$ was treated with excess CF_3I gas at -78°C and as reported, two perfluoroacyl isomers were isolated as major products. Along with this, two other isomers were also isolated, and the X-ray structure of cis,cis-Fe(diars)$(CO)_2(C(O)CF_3)I$ was determined. Under certain conditions, no perfluoroacyl product was obtained and instead the perfluoroalkyl Fe(diars)$(CO)_2(CF_3)I$ compound was obtained. The cis,cis perfluoroalkyl isomer was the major product. Its structure was confirmed by spectroscopy and single crystal X-ray diffraction. On prolonged stirring of the crude product the cis,trans isomer was also obtained. The conditions leading to the perfluoroalkyl and the perfluoroacyl products were identified. The mechanisms leading to the two products were studied by following the concentration vs. time curves at different reaction conditions using ^{19}F NMR.

The results indicate that the two products are formed by two separate reaction mechanisms.

The apparent CO insertion into the Fe-CF_3 bond is in fact an intermolecular nucleophilic addition where the external nucleophile, CF_3^-, attacks the coordinated carbonyl ligand forming the perfluoroacyl compound. This result is therefore in agreement with the experimental and theoretical results in the literature thus far, and an intramolecular insertion in M-CF_3 bond is yet to be identified.

The perfluoroalkyl compound appears to be formed by a free radical oxidative addition reaction and further research is required to identify the exact mechanism. The mechanism of oxidative addition of alkyl halides to low valent Group VIII metal complexes has attracted much study and controversy. There is evidence for S_N2 type as well as free radical mechanisms. However, with the perfluoroalkyl halides, no general mechanism has yet been established, even though some evidence for both concerted and free radical mechanisms has been reported. Since the industrial preparation of perfluoroalkyl iodides is reported to involve free radicals, it is possible that in general all perfluoroalkyl iodide oxidative additions involve a free radical mechanism as observed in the present system. It would therefore make an interesting research topic to study the oxidative addition of perfluoroalkyl iodides and other halides to various transition metal systems and establish the mechanism of oxidative addition of perfluoroalkyl halides to transition metals.

The higher analogues of CF_3I, namely, C_2F_5I, n-C_3F_7I, n-$C_6F_{13}I$, n-$C_7F_{15}I$ as well as CF_3CH_2I, yield only the perfluoroalkyl compound, all of which are new compounds. The lack of dual reaction with the higher analogues is attributed to the greater stability of the R_f radical, which enhances the rate of the free radical reaction thus dominating the much slower nucleophilic addition path to the perfluoroacyl compound. No mechanistic work was carried out for these sys

tems. It should be possible to bring about nucleophilic addition with the higher analogues either by further decreasing the reaction temperature, thereby slowing down the free radical reaction or by quenching the reaction with suitable radical traps. Quantitative kinetic data could not be obtained for either the nucleophilic or the oxidative addition reaction of $Fe(diars)(CO)_3$ with CF_3I owing to experimental difficulties.

The problems encountered in this study mentioned in Chapter 2 are not new. Puddephatt [102] has reported that CF_3I reacted with $Au(CH_3)(P(CH_3)_3)$ to yield a variety of products depending on the reaction conditions. The reaction either yielded $Au(CH_3)_2(CF_3)(P(CH_3)_3)$ at room temperature after about one day or proceeded rapidly to yield $Au(CH_3)(CF_3)I(P(CH_3)_3)$ in less than five minutes. Similarly, Haszeldine [88] has reported that CF_3I reacted with magnesium to yield either perfluoromethylmagnesium iodide or CF_3H depending on the reaction conditions. The concentration of CF_3I, a low temperature of -20 °C to -40 °C, the purity of magnesium used, and the basicity of the solvent were found to be crucial factors. Reproducible results were not obtained. Hence, the reactions of CF_3I are yet to be completely understood and rationalized.

References

[1] Abraham, R. J.; Fisher, J.: Loftus, L. *Introduction to NMR Spectroscopy*; John Wiley: New York, 1988; pp 67-68.

[2] Angelici, R. J. *Acc. Chem. Res.* **1972**, 5, 335.

[3] Ashcroft, S. J.; Maddock, A. *J. Chem. Soc. Dalton Trans.* 1974, 462.

[4] Astruc, D. *Chem. Rev.* 1988, 88, 1189.

[5] Attig, T. G.; Wojcicki, A. *J. Organomet. Chem.* 1974, 82, 397.

[6] Atwood, J. D. *Inorganic and Organometallic Reaction Mechanisms* Brooks/Cole: Monterey, CA; 1985.

[7] Axe, F. U.; Marynick, D. S. *Organometallics* **1987**, 6, 572.

[8] Axe, F. U.; Marynick, D. S. *J. Am. Chem. Soc.* 1988, 110, 3728.

[9] Azran, J.; Orchin, M. *Organometallics* 1984, 3, 197.

[10] Baird, M. C. *Chem. Rev.* 1988, 88, 1217.

[11] Baker, P. K.; Connelly, N. G.; Jones, B. M. R.; Maher, J. P.; Somers, K. R. *J. Chem. Soc. Dalton Trans.* 1980, 579.

[12] Banks, R. E. *Fluorocarbons and Their Derivatives*; MacDonald: London, **1970**; p 83.

[13] Banks, R. E., *Fluorocarbons and Their Derivatives*; MacDonald: London, 1970; pp 79-82.

[14] Barnus, J.; Emeleus, H. J.; Haszeldine, R. N. *J. Chem. Soc. (A)* **1951**, 60.

[15] Beagley, B.; Yound, G. G. *J. Mol. Struct.* 1977, 40, 295.

[16] Beck, W.; Hieber, W.; Tengler,H. *Chem. Ber.* **1961**, 94, 862.

[17] Beck, W.; Schloter, K. *Z. Naturforsch; B.* 1978, 33, 1214.

[18] Bellachioma, G.; Cardaci, G.; Reichenbach, G. *J. Organomet. Chem.* 1981, 221, 291.

[19] Bergman, E., *J. Org. Chem.* 1958, 23, 476.

[20] Berke, H.; Hoffman, R. *J. Am. Chem. Soc.* 1978, 100, 7226.

[21] Berke, H. *Chem. Ber.* 1988, 121, 1557.

[22] Bibler, J. P.; Wojcicki, A. *Inorg. Chem.* **1966**, 5, 889.

[23] Bird, C. W. *Chem. Rev.* **1962**, 62, 283.

[24] Birk, R.; Berke, H.; Huttner, G.; Zsolnai, L. *Chem. Ber.* **1988**, 121, 1557.

[25] Birk, R.; Berke, H.; Huttner, G.; Zsolnai, L. *J. Organomet. Chem.* **1986**, 309, C18.

[26] Blake, D. M.; Chung, Y. L.; DeFaller, J.; Winkelman, A. *J. Am. Chem. Soc.* **1974**, 96, 5568.

[27] Blake, D. M.; Winkelman, A.; Chung, Y. L. *Inorg. Chem.* **1975**, 14, 1326.

[28] Blake, D.M.; Shields, S.; Wymann, L. *Inorg. Chem.* **1974**, 13, 1595.

[29] Bock, P. I.; Boschetto, D. J.; Rasmussen, J. R.; Demers, J. P.; Whitesides, G. M. *J. Am. Chem. Soc.* **1974**, 96, 2814.

[30] Boniface, S.M.; Clark, G.R.; Collins, T. J.; Roper, W.R. *J. Organomet. Chem.* **1981**, 206, 109.

[31] Brace, N. O. *J. Org. Chem.* **1963**, 28, 3093.

[32] Brown, D.A.; Fitzpatrick, N.J.; Glass, W.K.; Sayal, P.K. *Organometallics*, **1984**, 3, 1137.

[33] Brunner, H.; Hammer, B.; Bernal, I.; Draux, M. *Organometallics*, **1983**, 2, 1595.

[34] Brunner, H.; Vogt, E. H. *Chem. Ber.* **1981**, 114, 2186.

[35] Burt, R.; Cooke, M.; Green, M. *J. Chem. Soc. (A)* **1970**, 2981.

[36] Burt, R.; Cooke, M.; Green, M. *J. Chem. Soc. (A)* **1969**, 2645.

[37] Butler, I. S.; Basdo, F.;Pearson, R. G. *Inorg. Chem.* **1967**, 6, 2074.

[38] Calderazzo, F. *Angew. Chem. Int. Ed. Eng.* **1977**, 16, 299.

[39] Calderazzo, F.; Cotton, F. A. *Inorg. Chem.* **1962**, 1, 30.

[40] Calderazzo, F.; Cotton, F. A. *7th Int. Conf. Coord. Chem. Stockholm* **1962**, 6H7.

[41] Calderazzo, F.; Noack, K. *Coord. Chem. Rev.* **1966**, 1, 118.

[42] Calderazzo, F.; Cotton, F. A. *Inorg. Chem.* **1962**, 1, 30.

[43] Cardaci, G.; Bellachioma, G.; Zanazzi, P. *Organometallics* **1988**, 7, 172.

[44] Cardaci, G.; Reichenbach, G.; Bellachioma, G. *Inorg. Chem.* **1983**, 23, 2936.

[45] Casey, C. P.; Baltusis, L. M. *J. Am. Chem. Soc.* **1982**, 104, 6347.

[46] Casey, C. P.; Scheck, D. M. *J. Am. Chem. Soc.* **1980**, 102, 2732.

[47] Cawse, J. N.; Fiato, R. A.; Pruett, R. L. *J. Organomet. Chem.* **1979**, 172, 405.

[48] Chiusoli, G. P. *Acc. Chem. Res.* **1973**, 6, 422.

[49] Churchill, M. R. *Inorg. Chem.* **1965**, 4, 1734.

[50] Churchill, M. R. *Inorg. Chem.* **1967**, 6, 185.

[51] Clark, H. C.; Reimer, K. J. *Can. J. Chem.* **1976**, 54, 2073.

[52] Collman, J. P.; Hegedus, L. S. *Principles and Applications of Organotransition Metal Chemistry*; University Science Books: Mill Valley, CA, 1980; pp 298-299.

[53] Collman, J. P.; Hegedus, L. S. *Principles and Applications of Organotransition Metal Chemistry*; University Science Books: Mill Valley, CA, 1980; p 259.

[54] Collman, J. P.; Sears, C. T. *Inorg. Chem.* **1968**, 7, 27.

[55] Connor, J. A.; Zafarani-Moattar, M. T.; Bickerton, J.; El Saied, N. I.; Suradi, S.; Carson, R.; Al Takhin, G.; Skinner, H. A. *Organometallics* **1982**, 1, 1166.

[56] Cotton, F. A.; McCleverty, J. A. *J. Organomet. Chem.* **1965**, 4, 490.

[57] Cotton, F. A. *Proc. Robert A. Welch Foundation Conf. on Chemical Research, IX Organometallic Compounds*, **1965**, Houston, Texas, pp 215-217.

[58] Cotton, F. A.; Wilkinson, G. *Basic Inorganic Chemistry*; 2nd ed.; Wiley: New York, **1987**.

[59] Cotton, J. D.; Markwell, R. D.; *Organometallics* **1985**, 4, 937.

[60] Coulton, K. G.; Fenske, R. F. *Inorg. Chem.* **1968**, 7, 1273.

[61] Crabtree, R. H. *The Organometallic Chemistry of the Transition Metals*; Wiley: New York; 1988.

[62] Craig, P. J.; Green, M. *J. Chem. Soc. (A)* **1969**, 157.

[63] Craig, P. J.; Green, M. *J. Chem. Soc. (A)* **1968**, 1978.

[64] Cram, D. J. *Fundamentals of Carbanion Chemistry*; Academic Press: New York; **1965**.

[65] Davis, S. G.; Watts, O. *J. Organomet. Chem.* **1983**, 243, C51.

[66] Dombek, B. D. *J. Chem. Ed.* **1986**, 63, 210.

[67] Emeleus, H. J. *J. Chem. Soc. (A)* **1954**, 2979.

[68] Falbe, J.; Bahrmann, H. *J. Chem. Ed.* **1984**, 61, 961.

[69] Feder, H. M.; Halpern, J. *J. Am. Chem. Soc.* **1975**, 97, 7187.

[70] Fernandez, J. M.; Gladysz, J. A. *Organometallics* **1989**, 8, 207.

[71] Flood, T. C.; Jenson, J. E.; Statler, J. A. *J. Am. Chem. Soc.* **1981**, 103, 4411.

[72] Flood, T. C.; Campbell, K. D. *J. Am. Chem. Soc.* **1984**, 106, 2853.

[73] Flood, T. C. *Top. Stereochem.* **1981**, 12, 37.

[74] Flood, T. C.; Campbell, K. D.; Downs, H. H.; Nakanishi, S. *Organometallics* **1983**, 2, 1590.

[75] Flood, T. C.; Jensen, J. E.; Statler, J. A. *J. Am. Chem. Soc.* **1981**, 103, 4410.

[76] Forsten, D.; Dekleva, T. W. *J. Chem. Ed.* **1986**, 63, 204.

[77] Frankiss, S. G. *J. Phys. Chem.* **1963**, 67, 752.

[78] Gabe, E. J.; Lee, F. L.; LePage, Y. In *Crystallographic Computing Vol 3*; Sheldrick, G.; Kruger, C.; Goddard, R., Eds.; Clarendon Press: Oxford, **1985**; p 167.

[79] Gardner, S. A.; Rausch, M.D. *Inorg. Chem.* **1974**, 13, 997.

[80] Gaughan, A. P.; Dori, Z. Jr.; Ibers, J. A. *Inorg. Chem.* **1974**, 13, 1657.

[81] Glyde, R. W.; Mawby, R. J. *Inorg. Chim. Acta* **1971**, 5, 317.

[82] Glyde, R. W.; Mawby, R. J. *Inorg. Chem.* **1971**, 10, 854.

[83] Glyde, R. W.; Mawby, R. J. *Inorg. Chim. Acta* **1970**, 4, 331.

[84] Green, M.; Westlake, D. *J. Chem. Soc. (A)* **1971**, 367.

[85] Gregory, B.; Jablonski, C. R.; Wang, Y. P. *J. Organomet. Chem.* **1984**, 269, 75.

[86] Haggins, J. *Chem. Eng. News* **1981**, 59, 22.

[87] Haszeldine, R. N. *J. Chem. Soc. (A)* **1953**, 2622.

[88] Haszeldine, R. N. *J. Chem. Soc.* **1954**, 1273.

[89] Haszeldine, R. N. *J. Chem. Soc.* **1953**, 1764.

[90] Heck, R. F. *Organotransition Metal Chemistry*; Academic: New York, 1974; p 210.

[91] Herlinger, A. W.; Brown, T. L. *J. Am. Chem. Soc.* **1971**, 93, 1790.

[92] Hitchcock, P. B.; Lappert, M. F.; Taylor, R. G. *J. Chem. Soc. Chem. Comm.* **1984**, 1082.

[93] Horwitz, C. P.; Shriver, D. F. *Adv. Organomet. Chem.* **1984**, 23, 219.

[94] International Tables for X-ray Crystallography, Vol. IV; Kynoch: Birmingham, England, 1974; p 99, Table 2.2B.

[95] Jablonski, C. R. *Inorg. Chem.* **1981**, 20, 3940.

[96] Jablonski, C. R.; Jacob, J.; Newlands, M. J. *Proc. of 72nd Can. Chem. Conf.* **1989**, Abstract No. 397.

[97] Jablonski, C. R.; Bellachioma, G.; Cardaci, G.; Reichenbach, G. *J. Am. Chem. Soc:* **1990**, 112, 1632.

[98] Jablonski, C. R.; Wang, Y. P. *J. Organomet. Chem.* **1986**, 301, C49.

[99] Jablonski, C. R.; Wang, Y. *Inorg. Chim. Acta* **1985**, 96, L17.

[100] Jablonski, C. R.; Wang, Y. *Inorg. Chim. Acta* **1983**, 69, 147.

[101] John, G. R.; Kane-Maguire, L. A. P.; Kanitz, R. *J. Organomet. Chem.* **1986**, 312, C21.

[102] Johnson, A.; Puddephatt, R. J. *J. Chem. Soc. Dalton Trans.* **1976**, 1360.

[103] Kane-Maguire, L. A. P.; Honig, E. D.; Sweigart, D. A. *Chem. Rev.* **1984**, 84, 525.

[104] Karel, K. J.; Tulip, T. H.; Ittel, S. D. *Organometallics*, **1990**, 9, 1276.

[105] King, R. B.; Birnetti, M. B. *J. Organomet. Chem.* **1964**, 2, 33.

[106] King, R. B.; Kapoor, R. N.; Pannel, K. H. *J. Organomet. Chem.* **1969**, 20, 187.

[107] King, R. B.; Stafford, S. L.; Treichel, P. M.; Stone, F. G. A. *J. Am. Chem. Soc.* **1961**, 83, 3604.

[108] King, R. B.; Efraty, A. *J. Organomet. Chem.* **1971**, 27, 409.

[109] King, R. B.; Kapoor, N. R.; Houk, L. W. *Inorg. Nucl. Chem.* **1969**, 31, 2179.

[110] King, R. B.; Treichel, P. M.; Stone, F. G. A. *J. Am. Chem. Soc.* **1961**, 83, 3593.

[111] Kramer, A. V.; Labinger, J. A.; Bradley, J. S.; Osborn, J. A. *J. Am. Chem. Soc.* **1974**, 96, 7145.

[112] Kramer, A. V.; Osborn, J. A. *J. Am. Chem. Soc.* **1974**, 96, 7832.

[113] Krueger, C.; Barnett, B. L.; Brauer, D.; Koerner Von Gustorf E. A. and Grevels, F. W. (Eds.) *The Organic Chemistry of Iron*; AcaJemic: New York, **1978**; Vol I; p 1.

[114] Kubota, M.; Blake, D. M.; Smith, S. A. *Inorg. Chem.* **1971**, 10, 1430.

[115] Labinger, J. A.; Osborn, J. A.; Coville, N. J. *Inorg. Chem.* **1980**, 19, 3236.

[116] Lagowski, J. J., *Quart. Revs. Chem. Soc.* **1959**, 13, 233.

[117] Lappert, M. F.; Prokai, B. *Adv. Organomet. Chem.* **1967**, 5,225.

[118] Lappert, M. F.; Lednor, P. W. *Adv. Organomet. Chem.* **1976**, 14, 345.

[119] Lappert, M. F.; Lednor, P. W. *J. Chem. Soc. Chem. Comm.* **1973**, 948.

[120] Lappert, M. F.; Lednor, P. W. *J. Chem. Soc. Dalton Trans.* **1980**, 1448.

[121] Litzow, M. R.; Spalding, T. R. *Mass Spectrometry of Inorganic and Organometallic Compounds*; Elsevier: Amsterdam, **1973**; pp 471-548.

[122] Manuel, T. A.; Stafford, P. N.; Stone, F. G. A. *J. Am. Chem. Soc.* **1961**, 83, 249.

[123] Manuel, T. A. *Inorg. Chem.* **1963**, 2, 854.

[124] Manuel, T. A.; Stafford, P. N.; Treichel, P. M.; Stone, F. G. A. *J. Am. Chem. Soc.* **1961**, 3604.

[125] Martley, F. R.; Patai, S. *The Chemistry of the Metal-Carbon Bond*; John Wiley: Toronto, **1982**; Vol. 2; pp 219-400.

[126] Mason, R.; Russell, D. R. *J. Chem. Soc. Chem. Comm.* **1965**, 182.

[127] Masters, A. P.; Sorensen, T. S.; Ziegler, T. *Organometallics* **1989**, 8, 1088.

[128] Mawby, R. J.; Basolo, F.; Pearson, R. G. *J. Am. Chem. Soc.* **1964**, 86, 3994.

[129] McHugh, T. M.; Rest, A. J. *J. Chem. Soc. Dalton Trans.* **1980**, 2323.

[130] Accleverty, J. A.; Wilkerson, G. *J. Chem. Soc.* **1964**, 4200.

[131] Miller, I. T.; Heaney, H.; Heinekey, D. M.; Fernelius, W. C. *Inorg. Synth.* **1960**, 6, 116.

[132] Miller, W. T.; Bergman, E.; Fainberg, A. H. *J. Am. Chem. Soc.* **1957**, 79, 4159.

[133] Morrison, J. A. *Adv. Inorg. Chem. Radiochem.* **1983**, 27, 293.

[134] Nicholas, K.; Raghu, S.; Rosenblum, M. *J. Organomet. Chem* **1974**, 78, 133.

[135] Nigam, H.; Nyholm, R. S.; Ramana Rao, D. V. *J. Chem. Soc.* **1959**, 1397.

[136] Noack, K.; Ruch, M.; Calderazzo, F. *Inorg. Chem.* **1968**, 7, 345.

[137] Noack, K.; Calderazzo, F. *J. Organomet. Chem.* **1967**, 10, 101.

[138] Nolan, S. P.; Lopez de la Vega, R.; Mukerjee, S. L.; Hoff, C. D. *Inorg. Chem.* **1986**, 25, 1160.

[139] Nyholm, R. S.; Kasenally, A.; Feltham, R. D. *J. Organomet. Chem.* **1967**, 7, 285.

[140] Pankowski, M.; Bigorgne, M. *J. Organomet. Chem.* **1977**, 125, 231.

[141] Pankowski, M.; Bigorgne, M. *J. Organomet. Chem.* **1983**, 251, 333.

[142] Pankowski, M.; Chodkiewicz, W.; Simonnin, M. P. *Inorg. Chem.* **1985**, 24, 533.

[143] Pankowski, M.; Bigorgne, M. *J. Organomet. Chem.* **1971**, 30, 229

[144] Pankowski, M.; Bigorgne, M. *J. Organomet. Chem.* **1971**, 30, 227.

[145] Park, J. D.; Rogers, F. E.; Lacher, J. R. *J. Org. Chem.* **1961**, 24, 2089.

[146] Pino, P.; Braca, G.; Sabrana, G.; Cuccuru, A. *Chem. Ind. (London)* **1968**, 1732.

[147] Pitcher, E.; Buckingham, A. D.; Stone, F. G. A. *J. Chem. Phys.* **1962**, 36, 124.

[148] Pitcher, E.; Stone, F. G. A. *Spectrochim. Acta* **1962**, 18, 585.

[149] Pruett, R. L. *J. Chem. Ed.* **1986**, 63, 196.

[150] Rathke, J. W.; Feder, H. M. *J. Am. Chem. Soc.* **1978**, 100, 3623.

[151] Reich-Rohrwig, P.; Wojcicki, A. *Inorg. Chem.* **1974**, 13, 2457.

[152] Ruiz, M. E.; Flores-Riveros, A.; Novaro, O. *J. Catalysis* **1980**, 64, 1.

[153] Saddei, I. D.; Freund, H. J.; Hohlneicher, G. *J.Organomet. Chem.* **1980**, 186, 63.

[154] Saraki, S.; Kitaura, K.; Morokuma, K.; Onkubo, K. *J. Am. Chem. Soc.* **1983**, 105, 2280.

[155] Shaver, A.; Quin, S. *J. Am. Chem. Soc.* **1984**, 106, 2853.

[156] Sheppard, W. A.; Sharts, C. M. *Organic Fluorine Chemistry*; Benjamin: New York, **1969**; pp 185-208.

[157] Shriver, D. F. *The Manipulation of Air Sensitive Compounds*; McGraw-Hill: New York, **1969**.

[158] Sunkel, K.; Ernst, H.; Beck, W. *Z. Naturforsch; B.* **1981**, 3613, 474.

[159] Sunkel, K.; Nagel, U.; Beck, W. *J. Organomet. Chem.* **1983**, 251, 227.

[160] Sunkel, K.; Urban, G.; Beck, W. *J. Organomet. Chem.* **1983**, 252, 187.

[161] Sweany, R. C.; Halpern, J. *J. Am. Chem. Soc.* **1977**, 99, 8335.

[162] Sweany, R. C. *Organometallics* **1988**, 8, 175.

[163] Therien, M. J.; Trogler, W. C. *J. Am. Chem. Soc.* **1987**, 109, 5127.

[164] Thomas, R. R.; Chebolu, V.; Sen, A. *J. Am. Chem. Soc.* **1986**, 108, 4096

[165] Wax, M. J.; Bergman, R. G. *J. Am. Chem. Soc.* **1981**, 103, 7028.

[166] Webb, S. C.; Giandomenico, C. M.; Halpern, J. *J. Am. Chem. Soc.* **1986**, 108, 345.

[167] Wright, S. C.; Baird, M. C. *J. Am. Chem. Soc.* **1985**, 107, 6899.

[168] Ziegler, T.; Versuis, L.; Tschinke, V. *J. Am. Chem. Soc.* **1986**, 108, 612.

Appendix A

Calculation of ^{19}F Shifts for AB Systems

A.1 Compound : $Fe(CO)_2(diars)(C_2F_5)I$

$F_1 = 5300.81$ Hz

$F_2 = 5038.2$ Hz

$F_3 = 4868.0$ Hz

$F_4 = 4605.4$ Hz

$$J = F_1 - F_2 = 262.0Hz$$
$$J = F_3 - F_4 = 262.0Hz$$

$$J_{F_AF_B} = 262.0Hz$$

$$dv = \sqrt{(F_1 - F_4)(F_2 - F_3)} = 4.4$$

$\frac{1}{2}(v_A + v_B)$ = Center of AB spectrum = 65.7 ppm

dv = 4.4 ppm = $v_A - v_B$

v_A = 4.4 + v_B

$(v_A + v_B)$ = 65.7 x 2

v_B = 131.4 - v_A

= 131.4 - (4.4 + v_B)

$2v_B$ = 127.0

v_B = 63.5 ppm

v_A = 4.4 + v_B

= 67.9 ppm

A.2 Compound : $Fe(CO)_2(diars)(C_3F_7)I$

F_1 = 17046.7 Hz	or	60.18 ppm
F_2 = 17314.6 Hz	or	61.32 ppm
F_3 = 18088.3 Hz	or	64.06 ppm
F_4 = 18356.2 Hz	or	65.01 ppm

$$J = F_1 - F_2 = 267.9Hz$$
$$J = F_3 - F_4 = 267.9Hz$$

$$J_{F_AF_B} = 267.9Hz$$

$$dv = \sqrt{(F_1 - F_4)(F_2 - F_3)} = 3.64$$

$\frac{1}{2}(v_A + v_B)$ = Center of AB spectrum = 62.69 ppm

dv = 3.64 ppm = $v_A - v_B$

v_A = 3.64 + v_B

$(v_A + v_B)$ = 62.69 x 2

v_B = 125.38 - v_A

= 125.38 - (3.64 + v_B)

$2v_B$ = 125.38 - 3.64

$= 121.74$

$v_B = 60.87$ ppm

$v_A = 3.64 + v_B$

$= 64.51$ ppm

A.3 Compound : $Fe(CO)_2(diars)(C_6F_{13})I$

$F_1 = 16813.4$ Hz	or	59.5 ppm
$F_2 = 17084.3$ Hz	or	60.4 ppm
$F_3 = 17711.2$ Hz	or	62.8 ppm
$F_4 = 17975.3$ Hz	or	63.7 ppm

$$J = F_1 - F_2 = 264.9Hz$$
$$J = F_3 - F_4 = 264.1Hz$$

$$J_{F_AF_B} = 264.5Hz$$

$$dv = \sqrt{(F_1 - F_4)(F_2 - F_3)}$$
$$= \sqrt{(63.7 - 59.5)(62.8 - 60.4)}$$
$$= 3.17$$

$\frac{1}{2}(v_A + v_B)$ = Center of AB spectrum = 61.6 ppm

$dv = 3.17$ ppm $= v_A - v_B$

$v_A = 3.17 + v_B$

$(v_A + v_B) = 61.6 \times 2$

$v_B = 123.2 - v_A$

$= 123.2 - (3.17 + v_B)$

$2v_B = 123.2 - 3.17$

$= 120.03$

v_B = 60.015 ppm

v_A = 3.17 + v_B

= 63.18 ppm

A.4 Compound : $Fe(CO)_2(diars)(CH_2CF_3)I$

.

F_1 = 746.7 Hz

F_2 = 733.8 Hz

F_3 = 586.4 Hz

F_4 = 573.5 Hz

$$J = F_1 - F_2 = 12.9Hz$$
$$J = F_3 - F_4 = 12.9Hz$$

$$J_{F_AF_B} = 12.9Hz$$

$$dv = \sqrt{(F_1 - F_4)(F_2 - F_3)} = 0.53ppm$$

$\frac{1}{2}(v_A + v_B)$ = Center of AB spectrum = 2.21 ppm

dv = 0.53 ppm = $v_A - v_B$

v_A = 0.53 + v_B

$(v_A + v_B)$ = 2.21 x 2

v_B = 4.42 - v_A

= 4.42 - (0.53 + v_B)

$2v_B$ = 3.89

v_B = 1.95 ppm

v_A = 0.53 + v_B

= 2.48 ppm

Appendix B

^{19}F Chemical Shift Temperature Gradient Data

Compound	Chemical Shift *		
	-90°C	-80°C	20°C
Fe-CF_3	13.1	12.3	10.7
Intermediate	-38.2	-38.9	-
Fe-C(O)CF_3	-76.1	-76.9 -77.1	-78.5 -79.3
CF_3H	-74.84 -75.9	-75.7 76.8	-79.0 -77.9
CF_3I	-5.5	-5.5	-5.6

* = relative to internal $CFCl_3$ in ppm

Appendix C

Crystallographic Data

Table C.1: Positional and Thermal Parameters and Equivalent Isotropic Temperature Factors for **17**

	x	y	z	Biso, Å^2
I	0.7485(4)	0.91505( )	0.42869(23)	6.62(16)
As 1	0.5265(3)	1.0556 (5)	0.17154(24)	2.90(12)
As 2	0.7146(4)	1.2978 (5)	0.3344 (3)	3.66(15)
Fe	0.7797(5)	1.0744 (6)	0.2527 (4)	3.05(18)
F 1	1.027 (3)	0.925 (4)	0.114 (3)	9.3 (18)
F 2	1.0417(24)	0.804 (3)	0.2624 (19)	7.5 (13)
F 3	0.953 (3)	0.704 (3)	0.1100 (24)	8.0 (15)
O 1	1.080 (3)	1.120 (3)	0.359 (3)	6.6 (17)
O 2	0.8263(23)	1.2165 (24)	0.0687 (18)	2.6 (4)
O 3	0.7063(25)	0.804 (3)	0.1421 (18)	4.9 (5)
C 1	0.964 (4)	1.099 (3)	0.312 (3)	4.1 (17)
C 2	0.809 (5)	1.197 (5)	0.114 (4)	5.0 (9)
C 3	0.816 (3)	0.877 (4)	0.1769 (24)	3.4 (6)
C 4	0.940 (4)	0.835 (4)	0.170 (3)	3.9 (7)
C 5	0.430 (3)	1.243 (3)	0.2024 (23)	2.6 (6)
C 6	0.283 (3)	1.268 (4)	0.1466 (24)	3.2 (6)
C 7	0.213 (4)	1.398 (5)	0.171 (3)	5.1 (8)
C 8	0.305 (5)	1.509 (5)	0.249 (3)	6.3 (10)
C 9	0.439 (4)	1.483 (4)	0.298 (3)	3.9 (7)
C 10	0.509 (3)	1.342 (4)	0.268 (3)	3.5 (6)
C 11	0.473 (4)	1.039 (4)	0.016 (3)	4.5 (7)
C 12	0.411 (5)	0.904 (6)	0.228 (3)	7.1 (11)
C 13	0.826 (4)	1.476 (5)	0.308 (3)	5.5 (9)
C 14	0.716 (5)	1.319 (5)	0.497 (3)	6.6 (10)

Table C.2: Positional and Thermal Parameters and Equivalent Isotropic Temperature Factors for **21**

	x	y	z	Biso
I	0.11894(11)	0.25107(10)	0.23928(7)	5.25(8)
As 1	0.06013(16)	0.06181(12)	0.32557(10)	2.89(11)
As 2	0.00833(17)	0.22658(11)	0.41863(10)	3.24(11)
Fe	-0.03745(23)	0.17717(17)	0.29488(16)	2.74(14)
F 1	0.8626 (14)	0.1421 (12)	0.1610 (11)	8.8 (12)
F 2	0.9722 (16)	0.1202 (13)	0.1421 (9)	11.5 (15)
F 3	0.9102 (15)	0.0553 (15)	0.1878 (9)	13.1 (16)
O 1	-0.1345 (12)	0.3330 (9)	0.2597 (12)	7.8 (11)
O 2	-0.2050 (12)	0.1017 (12)	0.3602 (12)	5.8 (11)
C 1	-0.1014 (16)	0.2748 (14)	0.2731 (13)	5.0 (14)
C 2	-0.1346 (23)	0.1313 (17)	0.3329 (15)	7.0 (20)
C 3	0.9203 (20)	0.1219 (14)	0.1821 (12)	0.6 (4)
C 4	0.1375 (15)	0.0890 (12)	0.4164 (10)	2.9 (10)
C 5	0.2159 (17)	0.0387 (12)	0.4413 (12)	3.9 (12)
C 6	0.2620 (19)	0.0579 (16)	0.5092 (16)	5.7 (16)
C 7	0.2376 (20)	0.1257 (18)	0.5494 (14)	5.7 (16)
C 8	0.1683 (17)	0.1792 (12)	0.5257 (11)	3.8 (12)
C 9	0.1152 (15)	0.1616 (11)	0.4565 (10)	3.1 (11)
C 10	0.1473 (16)	0.0211 (11)	0.2496 (14)	6.9 (14)
C 11	-0.0064 (14)	-0.0359 (10)	0.3625 (11)	4.5 (12)
C 12	0.0494 (17)	0.3379 (10)	0.4313 (11)	5.9 (13)
C 13	-0.0844 (16)	0.2134 (12)	0.4990 (11)	5.8 (12)